

# Ultimate Strength of the Local Zone in Load Transfer Tests

by

Rodolfo Arturo Bonetti

Thesis submitted to the Faculty of the  
Virginia Polytechnic Institute and State University  
in partial fulfillment of the requirements for the degree of

Master of Science

In

Civil Engineering

Approvals

---

Carin L. Roberts-Wollmann  
Committee Chair

---

Thomas E. Cousins  
Committee Member

---

Finley A. Charney  
Committee Member

February 18, 2005  
Blacksburg, VA

Keywords: Bearing, Plain Concrete, Reinforced Concrete, Local Zone, Load Transfer Test,  
Finite Element Analysis, Mohr Failure Criterion

## Ultimate Strength of the Local Zone in Load Transfer Tests

**Rodolfo Arturo Bonetti**

(ABSTRACT)

An improved equation is presented for the prediction of the ultimate strength of the local zone in Load Transfer Tests. The derivation of this new formulation is the result of the investigation of the ultimate bearing strength of plain and reinforced concrete blocks, concentrically loaded. A total of 199 bearing tests were performed on plain and reinforced concrete prisms to evaluate the variables involved in the bearing problem. A finite element analysis of a typical square block loaded with different bearing areas was performed. Two equations, one for plain concrete and the other for reinforced concrete were derived using the Mohr failure criterion.

The performance of the derived equations was evaluated against actual test data. The results of this evaluation showed very good agreement between the predicted ultimate strength and the actual test strength for both plain and reinforced concrete. For plain concrete specimens the ratio  $P_{\text{test}}/P_{\text{pred}}$  was 1.05 with a coefficient of variation of 9 percent. In the case of reinforced concrete blocks the ratio  $P_{\text{test}}/P_{\text{pred}}$  was 1.00 with a coefficient of variation of 14 percent.

## Acknowledgements

This is an opportunity to express my thanks to God and all the wonderful people who made this work possible.

- **My Lord Jesus**, for giving me my life and all the blessings I have receive during this journey.
- **Celeste Hernandez**, for all the sacrifices you have done to make this dream possible. I know God will give you in abundance for your dedication to your children and me.
- **Susana, Carolina and Brian**, for being patient and forgive all the time I took from you to finish this work. I hope this effort becomes a model to follow in your own lives.
- **My mother and father**, for the values I learned from you that made me the person I am. Wherever you are, rejoice with me for this achievement.
- **Dr. Carin L. Roberts-Wollmann**, for the opportunity to work for you and trusting the realization of this research. It has been an honor and a real pleasure to have you as my professor and advisor.
- **Dr. Thomas E. Cousins**, for your support, mentoring and guidance and for all the wonderful lectures in the Prestress Concrete class.
- **Dr. Finley A. Charney**, for your encouragement in a moment of doubt and the concepts I learned in your class.
- **Susana Bonetti, my sister**, for her support to my decision of pursuing graduate studies.
- **My family in law**, for their extraordinary support from the Dominican Republic.
- **Maria de Alles**, for taking care of me during the time I need it most.
- **Petrica and Jose Leon**, for your support and friendship that has been present during this time.
- **Luis Mañan**, for being my friend and teaching me, as a father, how to walk the extra mile.
- **Jose and Esmeralda Madera**, for their true friendship shown during this time.
- **Nancy Lopez, Pachi and Edward**, for being our family in Blacksburg.

- **Omar, Gustavo and Ana Guzman** for their encouragement and support.
- **Roman Medina**, for being an objective counselor.
- **Luis Nieto**, for his advises and good wishes since the beginning of this endeavor.
- **Brett Farmer and Dennis Hoffman**, for teaching me how to use the labs' equipment and provide your expertise when I need it.
- **Charles Newhouse**, for being ready to answer all my questions and provide his help in the concrete pours and testing.
- **David Martin**, for his good sense of humor and help during long hours at the lab.
- **The Big Beam Team:** Devin Harris, Kim Phillips and Jeremy Lucas for the good moments we spent together during the competition.
- **Lindy Cranwell**, for all the help provided while I was finishing this thesis.
- **Dr. Donald Mckeon**, for all the help provided.
- **Zuming Xia and Brian Gallagher from VSL**, for providing some of the pictures and the authorization for their use in this thesis.
- **VSL**, for the financial support that made possible this work.

<b>Table of Contents</b>	<b>Page</b>
<b>List of Tables</b>	<b>vii</b>
<b>List of Figures</b>	<b>viii</b>
<b>Nomenclature</b>	<b>x</b>
<b>Chapter 1. Introduction, Objectives and Thesis Organization</b>	<b>1</b>
1.1 Introduction	1
1.2 Objectives	6
1.3 Thesis Organization	7
<b>Chapter 2. Literature Review</b>	<b>8</b>
2.1 Plain Concrete Bearing Strength (PCBS)	8
2.2 Reinforced Concrete Bearing Strength (RCBS)	11
<b>Chapter 3. Experimental Procedures</b>	<b>15</b>
3.1 General Procedures	15
3.2 Plain Concrete Specimens	16
3.3 Reinforced Specimens	26
<b>Chapter 4: Analysis Procedures</b>	<b>29</b>
4.1 Mohr failure criterion	29
4.2 Linear Elastic Finite Element Analysis of the Bearing Problem in a Square Prism	30
4.3 Development of Equation for Plain Concrete Specimens	34
4.4 Development of Equation for Reinforced Specimens Using Curve Fitting	37
4.5 Development of Equation for Reinforced Specimens Using Mohr's Failure Criterion	37
<b>Chapter 5. Tests results and Discussion</b>	<b>39</b>
5.1 Plain concrete Specimens	39
5.1.1 Test Series 1	39

	Page
5.1.2 Test Series 2	43
5.1.3 Test Series 3	46
5.1.4 Test Series 4	48
5.1.5 Test Series 5 and 6	51
5.1.6 Test Series 7	53
5.1.7 Prediction of the UBS of Plain Concrete Specimens Using Equation Based on the Mohr Criterion	57
5.2 Reinforced Specimens	62
5.3 Comparison of Curve Fit Equation 4.10 with Previous Local Zone Tests	68
5.4 Prediction of the Ultimate Bearing Strength Using the Equivalent Material Approach and the Mohr Failure Criterion	73
<b>Chapter 6. Conclusions and Recommendations</b>	<b>81</b>
6.1 Conclusions	81
6.2 Recommendations	83
<b>References</b>	<b>84</b>





	Page
Fig. 5.10-Failure of Cylinder Block with Aspect Ratio = 3	46
Fig. 5.11-Failure of cylinder block with aspect ratio = 1	47
Fig. 5.12- $f_b/f_c$ vs. AR for $A/A_b=3$ , Cylinder Blocks	48
Fig. 5.13-Failure of Cylinder Block with $A/A_b=8$ (Round Plate)	49
Fig. 5.14-Failure of Cylinder Block with $A/A_b=2$ (Square Plate)	49
Fig. 5.15- $f_b/f_c$ vs. $A/A_b$ Lightweight Concrete Specimens (Test Series 4)	50
Fig. 5.16-Failure of Cylinder Block with $A/A_b=16$ (Round Plate)	51
Fig. 5.17-Failure of Cylinder Block with $A/A_b=1.5$ (Hex Plate)	52
Fig. 5.18- $f_b/f_c$ vs. $A/A_b$ High Strength Concrete Specimens (Test Series 5 and 6)	53
Fig. 5.19-Failure of Cylinder Block with Duct Size of 2.375 in.	54
Fig. 5.20-Failure of Cylinder Block with Duct Size of 3.375 in.	54
Fig. 5.21-Effect of the Duct Size on the Ultimate Bearing Stress	56
Fig. 5.22-Effect of the Duct Size on the Average Compressive Stress	57
Fig. 5.23-Performance of Equation 4.7	62
Fig. 5.24-Typical Failure in the General Zone	63
Fig. 5.25-Typical Failure in the General Zone Showing Plate Indentation	64
Fig. 5.26-Failure in the Base of the Prism	64
Fig. 5.27-Failure Cone in Specimen Failed in the Base	64
Fig. 5.28-Enhancement of the Ultimate Bearing Strength by Steel Reinforcement	67
Fig. 5.29-Performance of Equation 4.8 against Load Transfer Tests Database	73
Fig. 5.30-Performance of Equation 4.10 against Local Transfer Tests Database	78
Fig. 5.31-Performance of Equation 4.10 against Wurm and Daschner Data	78
Fig. 5.32-Comparison of performance of Equation 4.10 against NCHRP 356 Equation	79

## Nomenclature

$A$	= gross sectional area of concrete prism (this research)
$A_1$	= gross plate area (Eq. 2.2)
$A_2$	= gross sectional area of concrete prism (Eq. 2.3)
$A_b$	= gross plate area (this research)
$A_c$	= gross sectional area of concrete prism (Eq. 2.2)
$A_{core}$	= confined concrete area (Eq. 1.1)
$A_{cr}$	= area surrounded by the spiral (Eq. 2.9)
$A_g$	= gross plate area (Eq. 1.1)
$AR$	= aspect ratio of concrete block (height/width)
$A_s$	= reinforcing steel area
$A_y$	= area under assumed uniform state of stress $f_{c\ max}$
$a$	= block side dimension (Eq. 2.1)
$a'$	= plate side dimension (Eq. 2.1)
$b$	= plate side dimension (this research)
$C_1$	= coefficient depending on load condition (Eq. 2.11)
$D$	= spiral diameter
$F_{br}$	= ultimate bearing stress (Eq. 2.7-2.9)
$f_1$	= ultimate compressive strength (Eq. 2.5)
$f_2$	= lateral confining pressure (Eq. 2.5)
$f'_b$	= ultimate bearing stress
$f_c$	= average compressive stress at failure in the base of block with duct
$f_{c\ max}$	= assumed maximum uniform compressive stress at distance $y$ .
$f_{co}$	= average compressive stress at failure in the base of block without duct
$f'_c$	= cylinder compressive strength of concrete
$f'_{cu}$	= cube compressive strength of concrete
$f_{lat}$	= lateral confining pressure
$f_{t\ max}$	= maximum tensile stress at distance $y$ .
$f'_t$	= concrete tensile splitting strength
$f_y$	= reinforcing steel yield strength

- $h$  = block side dimension (this research)  
 $K$  = constant function of the concrete tensile strength and angle of friction (Eq.2.4)  
 $K$  = constant function of the reinforcing steel properties (Eq.2.6)  
 $k$  = factor function of the mechanical reinforcing ratio (Eq. 4.10)  
 $L$  = block height (Fig. 4.8)  
 $L$  = tie side dimension (Fig. 2.2)  
 $m$  = factor function of the bearing reinforcing index,  $q_b$   
 $m$  = compressive and tensile strengths ratio of plain concrete (Eq. 4.7)  
 $m_r$  = compressive and tensile strengths ratio of reinforced concrete (Eq. 4.10)  
 $n$  = normalized ultimate bearing stress  
 $n_{\text{reinf}}$  = normalized ultimate bearing stress of reinforced concrete  
 $n_{\text{plain}}$  = normalized ultimate bearing stress of plain concrete  
 $P$  = ultimate bearing strength of plain concrete  
 $P_{\text{pred}}$  = ultimate load predicted by equation  
 $P_r$  = ultimate bearing strength of reinforced concrete  
 $P_{\text{test}}$  = ultimate load from test  
 $q$  = ultimate bearing stress (Eq. 2.4)  
 $q_b$  = bearing reinforcing index (Eq. 2.10)  
 $q'_c$  = ultimate bearing stress (Eq. 2.11)  
 $R$  =  $A/A_b$  ratio  
 $R^2$  = correlation factor from curve fitting  
 $S$  = scale factor  
 $s$  = spiral pitch or tie spacing  
 $\omega$  = mechanical reinforcing ratio  
 $y$  = position of maximum tensile stress  $f_{t \max} = \sigma_I$   
 $\alpha$  = constant equal to 0.8 for mortar and 0.9 for concrete (Eq. 2.7-2.9)  
 $\alpha$  =  $A/A_y$  ratio  
 $\beta$  = constant equal to 0.55 for mortar and 0.6 for concrete (Eq. 2.7-2.9)  
 $\beta$  = normalized maximum tensile stress  $f_{t \max}/(P/A)$   
 $\sigma_I$  = maximum principal stress  $f_{t \max}$  (tension)  
 $\sigma_3$  = minimum principal stress  $f_{c \max}$  (compression)

## Chapter 1. Introduction and Objectives

### 1.1 Introduction:

In typical post-tensioned construction, the transfer of the prestressing force is achieved by anchoring of the tendons at predetermined locations in the concrete member. The anchorages at the ends of most commonly used multi-strand systems consist of a stiff anchorage head that holds the tendons and bears on an anchorage plate (Fig.1.1). This anchorage plate has the responsibility of effectively transferring the prestress force into the body of the element. Since the area of this plate is usually less than the supporting area, the concrete in contact with the plate is subjected to very high bearing stresses. The magnitude of such stresses, under normal conditions, can be even greater than the cylinder strength of the concrete.



Fig. 1.1 Typical Anchorage Device. Source: VSL

Two well-defined regions characterize the anchorage zone (Fig.1.2). The local zone is the region that extends along the axis of the tendon from the edge of the element for a distance equal to about the plate's smallest side dimension. The general zone is the region that also includes the local zone and extends along the axis of the tendon a length equal to the concrete elements' side dimension. According to Saint Venant's principle, the compressive stress at this point is considered as uniform throughout the entire section.

The behavior of the anchorage zone is governed by a triaxial state of stress comprising the compressive stress flowing in the longitudinal direction of the tendon and the tensile or bursting stresses generated in the transverse directions. The magnitudes of these stresses are determined by the geometry of the anchorage plate and the end block itself.

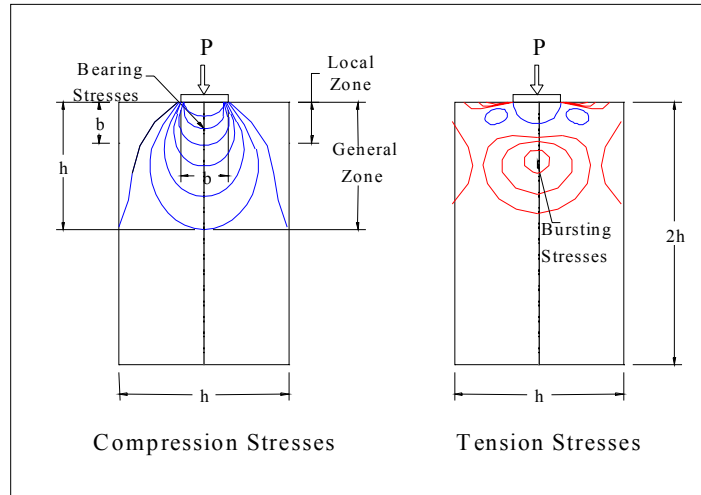


Fig. 1.2 Anchorage Zone Regions and Typical Distribution of Principal Stresses

AASHTO specifications [Standard Specifications for Highway Bridges (2002) and LRFD Specifications for Highway Bridges (2004)], classify the anchorage plates into two main groups. Basic bearing plates, (Fig.1.3a) are regular rectangular plates with sufficient stiffness so that a uniform stress distribution under the plate can be considered. The bearing stresses under these plates are relatively low and the strength of the local zone can be determined by relatively simple calculations. The other group is the Special Bearing plates (Fig.1.3b), which are embedded in the concrete and have a more complex geometry. These plates sometimes include more than one bearing surface and their strength must be determined by load transfer tests.

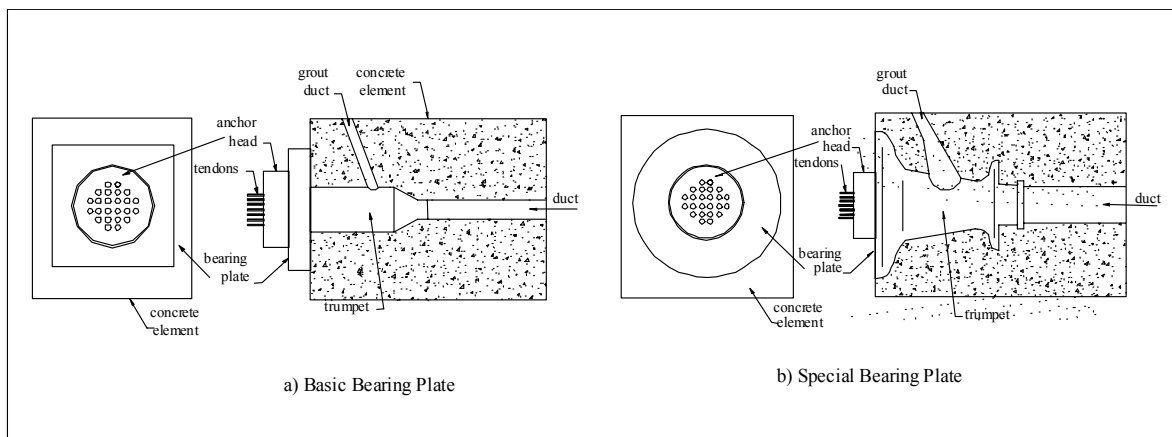


Fig. 1.3 AASHTO classification of anchorage plates

The use of special anchorage devices in post-tensioned structures is allowed provided that each particular anchorage system passes a series of acceptance tests. The purpose of these tests is to guarantee the integrity of the local zone, which is subjected to very high stress concentrations.

The most widely adopted acceptance criterion in the United States is the AASHTO Load Transfer Test. This test consists of a bearing test on a prismatic concrete block in which the compression load is applied directly to the special bearing plate by means of an anchor head (Fig. 1.4a and b). The specimen is a block of rectangular section with side dimensions equal to the smaller of the minimum edge distance or the minimum spacing specified by the anchorage device supplier and must include the proper cover over any reinforcing steel according to the application and environment in which the plate will work. The length of the block is required to be at least two times the larger of the cross section dimensions.



a) Test Setup with Specimen at Failure



b) Condition of Specimen after Testing

Fig. 1.4 Load Transfer Test. Source: VSL.

The prism is reinforced according to the recommendations of the special anchorage devices' supplier (Fig.1.5). The main reinforcement consists most commonly of a spiral or helix, although the use of ties can be convenient in some applications. Secondary reinforcement often called "skin reinforcement" is allowed in the form of ties with a volumetric ratio no greater than 1 %. These ties emulate actual conditions in a beam or slab where extra reinforcement is present.



Fig. 1.5 Typical AASHTO Load Transfer Test Reinforcing. Source: VSL.  
(Specimen shown upside down)

The prism is loaded in one of three regimes: cyclic, sustained or monotonic. Each one of these tests has its own acceptance criterion in terms of cracking and ultimate load value expressed in terms of the Guaranteed Ultimate Tensile Strength (G.U.T.S). The most popular is the cyclic test because of its time-wise convenience. In the cyclic loading test (Fig.1.5) the load is increased from 0 to 80 percent of the Guaranteed Ultimate Tensile Load ( $F_{pu}$ ). Then the load is cycled between  $0.1 F_{pu}$  and  $0.8 F_{pu}$ , for not less than 10 cycles, until the cracks stabilized. Cracks are considered stabilized if they don't grow more than 0.001 in. over the last three cycles. After cycling, the specimen must be loaded to at least  $1.1 F_{pu}$ , to consider it passing the test. Crack widths and patterns are recorded at the initial load of  $0.8 F_{pu}$ , at least three times in the last consecutive cycles and at  $0.9 F_{pu}$

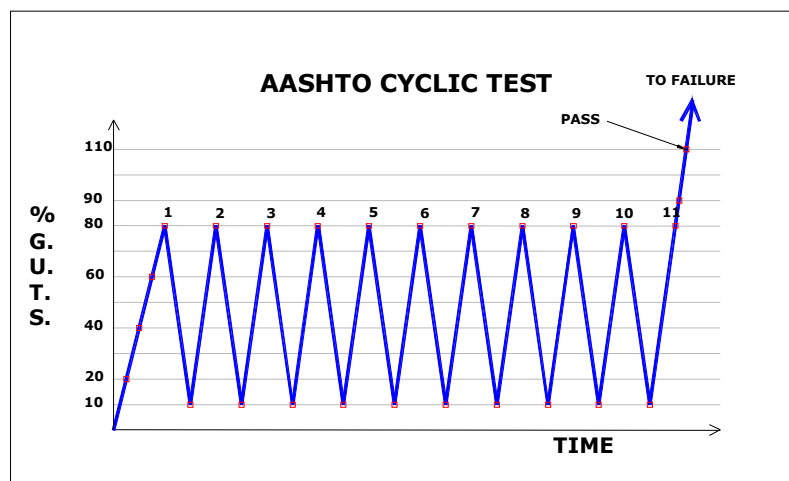


Fig. 1.6 AASHTO Cyclic Test

The basis for the AASHTO test specifications is the recommendations provided by the NCHRP Report 356, Breen et al. (1994), which was the product of the investigations conducted by Breen and Roberts-Wollmann at the University of Texas at Austin. The investigation focused on the main variables involved in the local zone behavior: the ratio between the gross supporting area and the plate area ( $A/A_b$  ratio), the lateral confining pressure ( $f_{lat}$ ), provided by the spiral or stirrups and the area of the confined core ( $A_{core}$ ).

The significant outcome of that investigation was the establishment of acceptance criteria for Special Anchorage Devices and the proposal of an equation for the estimation of the ultimate strength of the local zone. The latter is of capital importance for the manufacturer who is responsible for providing the proper reinforcement for the local zone of each proprietary device.

The proposed equation based on the NCHRP 356 Report to determine the ultimate strength of the local zone for Special Anchorage Devices is:

$$P_u = 0.8f'_c \sqrt{\frac{A}{A_g}} A_b + 4f_{lat} \left(1 - \frac{s}{D}\right)^2 A_{core} \quad (\text{Eq. 1.1})$$

In equation 1.1,  $P_u$  is the ultimate load,  $f'_c$  is the concrete compressive strength,  $A$  is the gross area of the prism,  $A_g$  is the gross area of the plate,  $f_{lat}$  is the lateral confining pressure provided by the reinforcing steel,  $s$  is the pitch of the spiral or spacing of the ties used as lateral reinforcement and  $D$  is the diameter of the spiral or side dimension of the ties.

This equation can be divided in two isolated terms. The first term is the plain concrete bearing strength, and the second term is the enhancement of bearing strength provided by the reinforcing steel.

The Post-Tensioning Institute (Wollmann and Roberts-Wollmann 2000) adopted the equation for the extrapolation of Special Bearing Plate Acceptance Test Results with slight modifications. These modifications include the use of a factor of 4.1 instead of 4 in the second term of the equation, the introduction of a calibration factor ( $\eta$ ) and establishing limits for the plain concrete bearing strength and the nominal or total local zone strength.

In general, the NCHRP 356 equation has performed very well for predicting the ultimate strength of the local zone and this can be proven by the good performance of local zones designed by this method through the years since its appearance. Nevertheless, when the formula is compared against the results from tests of the NCHRP study and other authors (Wurm and Daschner 1977) (Niyogi 1975), the average of the ultimate strength from the test over the predicted strength is 0.89 with a coefficient of variation of 21 percent (Fig.1.7).

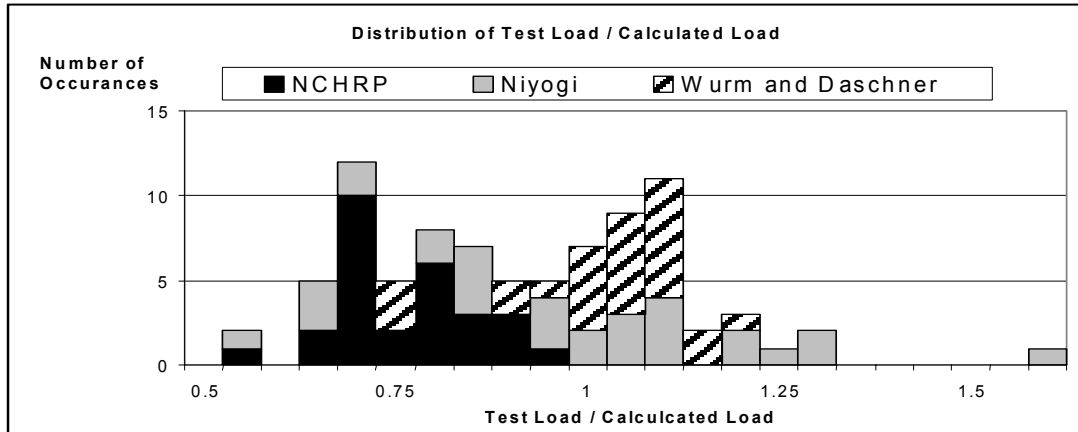


Fig.1.7 Performance of Equation 1.1 versus Experimental Data.

Source: Roberts-Wollmann (2000)

## 1.2 Objectives

The primary objective of this work is to present an expression for the ultimate strength of the local zone with an improved performance in comparison with test results and a smaller coefficient of variation. To achieve these goals the investigation is divided into two main aspects: the bearing strength of plain concrete blocks under concentric loading and the bearing strength of reinforced concrete blocks.

In the first part of this investigation, the bearing strength of plain concrete blocks is revisited. The main variables considered to affect the bearing strength are: the shape of the plate, the ratio between the supporting area and the plate area, the aspect ratio (length/width), the concrete strength and the effect of the duct size. Tests results for each of these variables are presented and a finite element model of a plain concrete block is included in which the effect of the size of the loaded area is investigated.

In the second part of this work the enhancement of the bearing strength provided by the confining steel is investigated. Tests series results for blocks with spiral reinforcement, ties and a combination of spiral and ties are presented.

The analysis of this new data along with the data of previous investigators is the basis for the derivation of a new expression for the local anchorage zone strength.

### **1.3 Thesis Organization**

After this introductory chapter a review of the existing literature on the bearing strength of plain and reinforced concrete is presented in Chapter 2. Chapter 3 covers the test procedures utilized for the evaluation of the plain and reinforced concrete bearing strength, including the different test series in which the experiments were subdivided to study the variables of importance in this research. Chapter 4 presents the theoretical basis for the derivation of the equations for plain and reinforced specimens, results from a finite element analysis of a concrete block is also presented in this chapter. The results from all tests, a description of the different failure modes, and a comparison of the tests result with the induced equations and a discussion of the results is covered in Chapter 5. Chapter 6 presents the conclusions arrived at the end of the study.

## Chapter 2. Literature Review

### 2.1 Plain Concrete Bearing Strength (PCBS).

The ultimate bearing strength (UBS) of plain concrete blocks and rock under concentric loading has been a topic of investigation by several authors since the later 1800's. The main variable of study has been the influence of the ratio  $A/A_b$ , where  $A$  is the supporting area and  $A_b$ , the plate area. The majority of these authors arrived at empirical formulas, mostly based on curve fitting.

Bauschinger (1876) was the first in proposing a cubic root formula as result of his experiments in sandstone. In the 1950's Komendant (1952) proposed the square root formula, which is still in use by ACI today with some modifications. Middendorf (1960) found a very good correlation of the square root formula with his bearing tests on 6 in. x 12 in. cylinders.

The most prolific investigator, Niyogi (1974), performed 1,422 tests on plain and reinforced concrete blocks. The variables of his study included the geometry of the plates, the nature of the supporting bed (rigid and elastic), mix proportions and the size of the specimen. Some of the most interesting conclusions were that the ratio  $f_b/f'_c$  decreases as  $f'_c$  increases, where  $f_b$  is the ultimate bearing stress. Also that specimens tested over compressible beds exhibit lower  $n$  values than those tested over a steel platform, however supporting conditions for specimens with aspect ratios (length / width) greater than 2, appeared to not affect the ultimate bearing strength.

Another important conclusion was the size effect. Apparently a proportional size increase of the specimen decreases the ultimate bearing strength. Niyogi conducted an exhaustive investigation of the variable  $R$  ( $A/A_b$  ratio) and proposed the following equation for the ultimate bearing strength for blocks concentrically loaded thru square plates:

$$n = 0.84\left(\frac{a}{a'}\right) + 0.23 \quad (\text{Eq. 2.1})$$

Where:  $n$ , is the ultimate bearing stress over  $f'_c$ ,  $a$  is the block side dimension and  $a'$  is the plate side dimension.

Suzuki and Nakatsuka (1982) conducted several tests on cylinders. According to their studies the ultimate bearing strength of plain concrete can be determined by the expression:

$$Pu = \alpha \left( \frac{A_c}{A_1} \right)^\beta f'_c A_1 \quad (\text{Eq. 2.2})$$

Where:  $\alpha$  and  $\beta$  are constants equal to 0.80, 0.55 for mortar and 0.9, 0.60 for concrete,  $A_c$  is the specimen gross area,  $A_1$  is the plate area, and  $f'_c$  is the cylinder strength.

Figure 2.1 presents a plot of the results from several investigators (Au 1960, Hawkins 1968 and Niyogi 1973) and 26 tests on 6 in. by 12 in. cylinders conducted by Roberts-Wollmann and Banta at VPI&SU (not published yet). The results are compared against the ACI square root formula and limit, which are as follows:

$$Pu \leq \phi 0.85 f'_c A_1 \sqrt{\frac{A_2}{A_1}} \leq \phi 1.7 f'_c A_1 \quad (\text{Eq. 2.3})$$

Where  $A_1$  is the plate area and  $A_2$  is the block gross area.

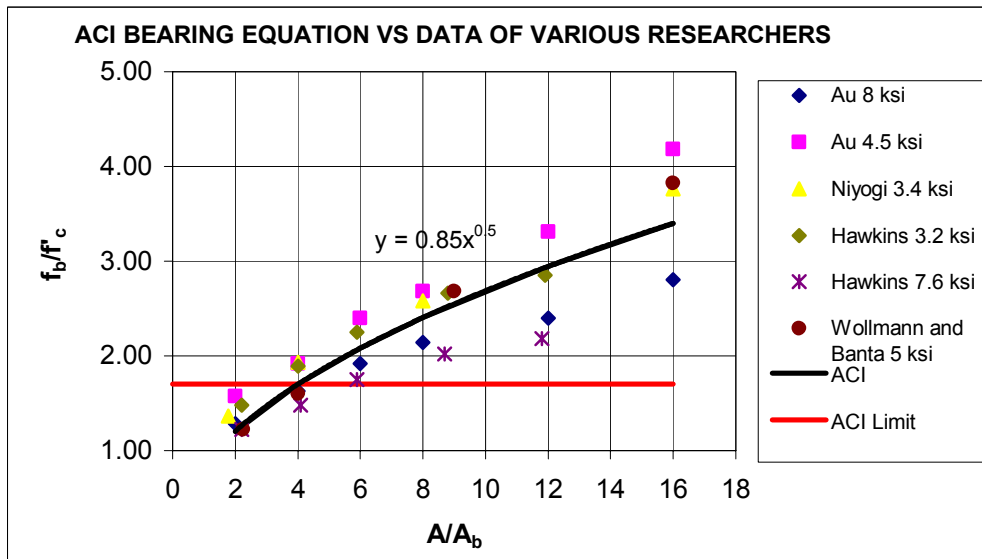


Fig. 2.1 ACI Equation versus Results from Various Investigators

Meyerhof (1953) performed several tests of footing-like blocks with large  $A/A_b$  ratios. In strip-loaded specimens, he observed the formation of a splitting wedge and the characteristic failure cone that preceded the splitting failure of concrete blocks loaded thru circular plates.

His conclusions were that the material fails in a combination of shearing and splitting stresses. Using results from the triaxial tests conducted by Richart and Brandtzaeg (1928), he arrived at an expression for bearing strength in footings that includes the cohesion and the angle of friction of the concrete material.

In a similar manner Hawkins (1968) presented a bearing strength equation based on the dual failure criterion of Cowan (1953). According to this approach a series of stacking slices surround the loading area. On the inside of these slices lies the failure cone, which is pushing down into the block. In order to have a failure, a critical shear stress ( $s$ ) develops on the surface of the cone and its magnitude depends on the magnitude of the hoop stress generated in the uppermost slice. The general expression for the ultimate bearing strength (UBS) for concentrically loaded specimens is:

$$\frac{q}{f'c} = 1 + \frac{K}{\sqrt{f'c}}(\sqrt{R} - 1) \quad (\text{Eq. 2.4})$$

Where  $q$  is the ultimate bearing strength,  $R$  is the  $A/A_b$  ratio and  $K$  is a coefficient that depends on the concrete tensile strength and the angle of friction, both determined experimentally. Hawkins suggested a value of  $K=50$  for design purposes. A good correlation between the UBS calculated by this equation and the experimental results was attained for  $R$  values less than or equal to 40.

The biggest problem associated with this type of model is the difficulty in determining the angle of internal friction of the concrete material, which seems to depend on the maximum aggregate size, the proportions of the mix and the amount of confining pressure provided by the surrounding concrete as well.

Several conclusions can be inferred from this review. The first one is that the empirical formulas show a trend in the behavior of plain concrete under bearing stresses. The correlation ( $R^2$ ) achieved for every particular test is very close to 1. The second one is that the failure mechanism is constant through all the different investigations. The formation of a failure cone or pyramid that precedes the splitting of the blocks loaded concentrically is the

common case. These observations lead to the assumption that the UBS of plain concrete can be modeled by a failure criterion defined with the concepts of mechanics of materials.

Liu, Guan and Wang (1985) presented a formula for estimating the bearing strength of concrete based on the Mohr-Coulomb hypothesis for shear failure. The fact that the triaxial state of stress in the block is governed essentially by compression in one direction and tension in the other two perpendicular directions, make this approach suitable for application to the bearing problem. In Chapter 4, an expression for the UBS based on the Mohr-Coulomb criterion with some assumptions and modifications is derived.

## **2.2 Reinforced Concrete Bearing Strength (RCBS).**

The effect of confining reinforcement on the ultimate strength of concrete columns is widely known. Tests conducted by Richart and Brandtzaeg at the University of Illinois (1928), are the basis for all the theories in this matter. The basic series of tests consisted of the investigation of plain concrete under triaxial states of stress. A confining pressure was applied to concrete cylinders in compression. The results of these tests indicated that an increase of the confining pressure produces an increase in the ultimate compressive stress, governed by the relation:

$$f_1 = f'_c + 4.1f_2 \quad (\text{Eq. 2.5})$$

Where  $f_1$  is the ultimate compressive strength and  $f_2$  is the lateral confining pressure (also known as  $f_{lat}$ ). Results from the same investigators on tests of spirally reinforced columns agreed very well with the above-mentioned expression, hence the adoption of the theory in the NCHRP 356 Report is well justified.

Several authors have studied the effect of lateral reinforcement on the bearing strength of concrete blocks. The case of most interest in this review is the effect on concentrically loaded specimens.

Niyogi (1975) presented results from testing of 154-8 in. concrete cubes, reinforced in the majority with spirals. The main variables investigated were the effect of the reinforcement ratio and the effect of the diameter and extent of the spiral. The conclusions from this work is

that the lateral reinforcement significantly increases the ultimate bearing strength, the use of large diameter spirals provide higher UBS than smaller ones and the reinforcement provides a good resistance against initial cracking. The expression proposed for the UBS according to the investigation is:

$$\frac{n_{rein}}{n_{plain}} = 1 + Kp \quad (\text{Eq. 2.6})$$

Where  $n_{rein}$  and  $n_{plain}$  are the ratio of the UBS of reinforced and plain concrete specimens over the cube compressive strength, respectively,  $K$  is a factor that depends on the size of the spiral, the manner in which the steel percentage is determined and the type and grade of the steel,  $p$  is the steel percentage by volume. Niyogi recommended  $K=55$  for practical purposes. A simple interpretation of this formula is that the UBS of reinforced specimens varies linearly with the volumetric reinforcing ratio.

Suzuki and Nakatsuka (1982) reported results from their test on 6 in. x 12 in. and 8 in. x 20 in. cylinders. In these experiments the reinforcement ratio was the variable of main importance. Three different failure modes were found during their testing. The first one, for lightly reinforced specimens, was the splitting of the cylinder in the same way of the unreinforced ones (failure type Ia). The second mode of failure was a complete deterioration of the local zone or the concrete confined by the spiral (Ib). This can be defined as the ideal bearing failure. The third one was the failure of the concrete beneath the spiral with the formation of a concrete cone that produces the splitting of the concrete below (II). Accordingly they derived expressions defining each UBS limit state, these are:

$$(Ia) F_{br} = \alpha \left( \frac{A_c}{A_1} \right)^\beta f'_c \quad (\text{Eq. 2.7})$$

$$(Ib) F_{br} = m \alpha \left( \frac{A_c}{A_1} \right)^\beta f'_c \quad (\text{Eq. 2.8})$$

$$m = 2.4q_b^{0.4} + 1$$

$$(II) F_{br} = \alpha \left( \frac{A_c}{A_{cr}} \right)^\beta \left( \frac{A_{cr}}{A_1} \right) f'_c \quad (\text{Eq. 2.9})$$

Where  $\alpha$  and  $\beta$  are constants equal to 0.80, 0.55 for mortar and 0.9, 0.60 for concrete,  $A_c$  is the gross area of the prism,  $A_l$  is the area of the bearing plate,  $A_{cr}$  is the area surrounded by the spiral,  $F_{br}$  is the bearing strength,  $f'_c$  is the cylinder strength and  $m$  is a factor that depends on the bearing reinforcing index,  $q_b$ , which is half of the mechanical reinforcement ratio (known as  $\omega$  in the ACI Code),

$$q_b = \frac{\omega}{2} = \frac{\rho}{2} \left( \frac{f_y}{f'_c} \right) = \frac{2A_s f_y}{sDf'_c} = \frac{f_{lat}}{f'_c} \quad (\text{Eq. 2.10})$$

Again,  $f_{lat}$  is the confining pressure (Fig. 2.2),  $s$  is the pitch of the spiral or the ties spacing and  $D$  is the diameter of the spiral or side dimension of ties. The criterion is then applied as follow: when (Ia)  $F_{br} > (Ib) F_{br}$ , equation 2.7 governs, when (Ib)  $F_{br} > (II) F_{br}$ , equation 2.8 determines the bearing strength and in the case that (Ia)  $F_{br} < (Ib) F_{br}$  and (Ib)  $F_{br} > (II) F_{br}$ , the bearing strength is calculated with equation 2.9.

An evaluation of the prediction of the UBS by these equations against their experimental results and test data from another research (Wurm and Daschner 1977) was distributed within the range  $-10\%$ ,  $+20\%$  of deviation from the line representing a perfect correlation between the test and the prediction.

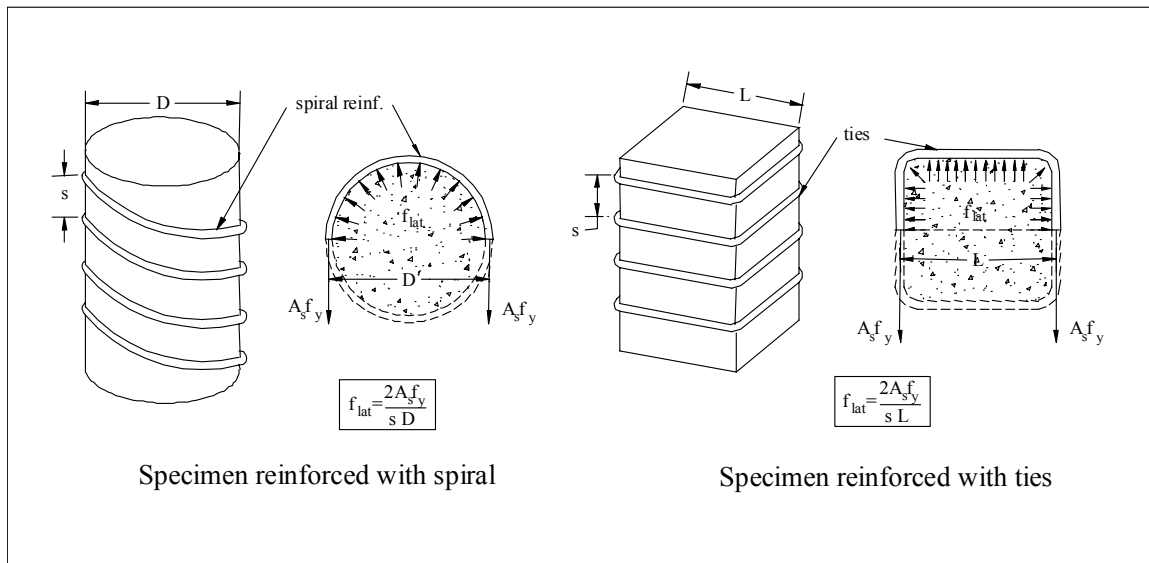


Fig. 2.2 Definition of Confining Pressure  $f_{lat}$ .

Wurm and Daschner (1977) presented the results of 130 tests primarily on reinforced specimens. In those tests they studied the influence of the quantity and type of lateral reinforcement. The typical specimen consisted of a 300 mm. x 600 mm. block reinforced in the majority of tests with a spiral and loaded with an  $A/A_b$  ratio of 4. The most remarkable finding of this work was that an increase of the reinforcing ratio produced an increase of the UBS up to a point of saturation where an increase of reinforcing steel didn't increase the UBS any more.

In more recent years, Ahmed et al. (1998), tested 39 plain and reinforced specimens under several loading regimes. Two test series, one of small blocks (200mm by 300mm) and the other in large blocks (400mm by 600mm) were done in unreinforced and reinforced specimens. The reinforcing in the blocks consisted of three-dimensional and two-dimensional grids. The variables investigated were the reinforcing ratio and the size effect. The proposed formula fitting the tests result was:

$$q'_c = f_{cu} \left[ 3 \left( \frac{\text{Area.of.lateral.steel}}{\text{Area.of.concrete}} \right) \left( \frac{A}{A'} \right) + C_1 \right] \quad (\text{Eq. 2.11})$$

Where  $q'_c$  is the ultimate bearing strength,  $f_{cu}$  is the cube strength,  $A$  is the block area and  $A'$  is the area of the plate.  $C_1$  is a coefficient depending on the loading condition and the percentage of steel.

In terms of the size effects the investigation concluded that a size effect adjustment in the UBS could be approached with the use of a factor equal to  $1/S^{0.25}$ , where  $S$  is the scale factor between the small and large blocks.

It is more evident that the different equations, which were developed by the different investigators, are primarily the result of fitting of test data. A uniform criterion for the evaluation of the ultimate bearing strength of reinforced concrete blocks is still pending and is one of the objectives of this research.

## Chapter 3. Experimental Procedures

In order to have a better understanding of the variables governing the behavior of concrete blocks under bearing stresses a comprehensive test program was proposed. The test program was divided into two main categories. The first one for the investigation of the ultimate bearing of plain concrete blocks and the second one for the investigation of reinforced concrete blocks.

For the investigation of the UBS of plain concrete specimens the test program was divided into seven test series covering the effects of the  $A/A_b$  ratio, the shape of the bearing plate, the concrete weight and strength, the aspect ratio and the duct size. For the reinforced concrete specimens the test program was focused on the effect of the variation of the reinforcing ratio on the ultimate bearing strength.

### 3.1 General Procedures

The first step in the determination of a test matrix was the selection of the variables of main significance and the shape of the blocks. The variables selection was determined by revisiting the results of previous investigations most of which were presented in Chapter 2. The size of the blocks was selected based on the availability and capacity of the test equipment. It was determined that square prisms 8 in. x 8 in. x 16 in. and 6 in. x 12 in. cylinders were the most suitable shapes to use. The equipment used for testing was a standard compression machine (FORNEY) with a capacity of 400 kips and a SATEC machine with a maximum load of 300 kips. The latter was coupled to a load data acquisition system.

The square blocks were cast in plywood formwork and covered with plastic sheathing until the concrete reached a compressive strength of at least 2,000 psi. At that point the forms were stripped and the specimens stored at room temperature. In the first series of specimens the top surface of the blocks was hand tooled finished after casting. Later, it was determined that more consistent results could be achieved by the use of a thin layer of low viscosity epoxy on the top surface. This provided an almost perfectly leveled surface. In this case the actual

conditions of a regular AASHTO (2002, 2004) acceptance test are also achieved, because in most cases a layer of epoxy is used to level the surface in contact with the steel platform. The cylinder specimens were cast in standard 6 in. x 12 in. plastic molds and the finishing after casting was performed with hand tools. The specimens were stored and covered at room temperature (+/- 75 F) up to the moment of testing.

Several 4 in. x 8 in. cylinders were cast with concrete from each pour for the determination of the concrete compressive strength and the tensile (splitting) strength. At least two tests were performed for each material property. These values were recorded at the beginning of each test series.

### **3.2 Plain Concrete Specimens**

In test series 1 the variables of investigation were the effect of the shape of the plate in relation to the shape of the block and the effect of the ratio of supporting area over the plate area ( $R=A/A_b$ ) on the ultimate bearing strength. A typical VDOT A-4 concrete mix was selected with a characteristic compressive strength of  $f'_c=4,000$  psi at 28 days and a maximum aggregate size of  $\frac{3}{4}$  in. In terms of this research's strength classification, this value corresponds to the low strength specimens.

The series was divided into four groups: Square prism loaded with square plate (SS), square prism loaded through circular plate (RS), cylinder loaded with square plate (SC) and cylinder loaded through circular plate (RC). The  $A/A_b$  ratios tested for each group were 2, 4, 6, 8, 12 and 16 respectively. At least two specimens were tested for each  $A/A_b$  ratio.

When a very high discrepancy existed between similar tests, a third specimen was tested in order to have a better idea of the actual bearing strength of a particular data point. A total of 50 specimens were tested in this series. A test matrix for this series is presented in Table 3.1.

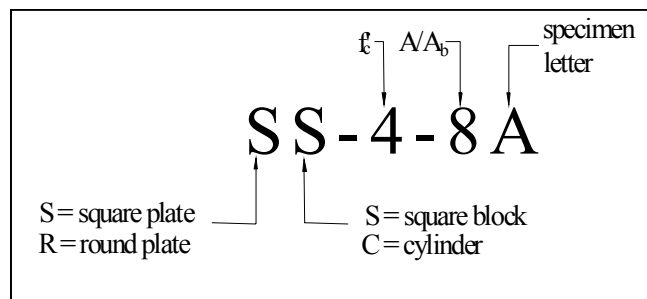
Table 3.1 Matrix of Test Series 1

Specimen	Block Size				Plate Size		Block Area (in <sup>2</sup> )	R A/A <sub>b</sub>	f <sub>c</sub> target (ksi)
	Cylinder		Square Block		Round	Square			
	h	L	h	L	b	b			
	(in)	(in)	(in)	(in)	(in)	(in)			
SS-4-2A			8.00	16.00		5.66	64.00	2	4.00
SS-4-2B			8.00	16.00		5.66	64.00	2	4.00
SS-4-4A			8.00	16.00		4.00	64.00	4	4.00
SS-4-4B			8.00	16.00		4.00	64.00	4	4.00
SS-4-6A			8.00	16.00		3.27	64.00	6	4.00
SS-4-6B			8.00	16.00		3.27	64.00	6	4.00
SS-4-8A			8.00	16.00		2.83	64.00	8	4.00
SS-4-8B			8.00	16.00		2.83	64.00	8	4.00
SS-4-12A			8.00	16.00		2.31	64.00	12	4.00
SS-4-12B			8.00	16.00		2.31	64.00	12	4.00
SS-4-16A			8.00	16.00		2.00	64.00	16	4.00
SS-4-16A			8.00	16.00		2.00	64.00	16	4.00
RS-4-2A			8.00	16.00	6.38		64.00	2	4.00
RS-4-2B			8.00	16.00	6.38		64.00	2	4.00
RS-4-4A			8.00	16.00	4.51		64.00	4	4.00
RS-4-4B			8.00	16.00	4.51		64.00	4	4.00
RS-4-6A			8.00	16.00	3.69		64.00	6	4.00
RS-4-6B			8.00	16.00	3.69		64.00	6	4.00
RS-4-8A			8.00	16.00	3.19		64.00	8	4.00
RS-4-8B			8.00	16.00	3.19		64.00	8	4.00
RS-4-12A			8.00	16.00	2.61		64.00	12	4.00
RS-4-12B			8.00	16.00	2.61		64.00	12	4.00
RS-4-16A			8.00	16.00	2.26		64.00	16	4.00

Table 3.1 (Cont.) Matrix of Test Series 1

Specimen	Block Size				Plate Size		Block Area (in <sup>2</sup> )	R A/A <sub>b</sub>	f <sub>c</sub> target (ksi)
	Cylinder		Square Block		Round	Square			
	h (in)	L (in)	h (in)	L (in)	b (in)	b (in)			
RC-4-2A	6.00	12.00			4.24		28.27	2	4.00
RC-4-2B	6.00	12.00			4.24		28.27	2	4.00
RC-4-4A	6.00	12.00			3.00		28.27	4	4.00
RC-4-4B	6.00	12.00			3.00		28.27	4	4.00
RC-4-6A	6.00	12.00			2.45		28.27	6	4.00
RC-4-6B	6.00	12.00			2.45		28.27	6	4.00
RC-4-8A	6.00	12.00			2.12		28.27	8	4.00
RC-4-8B	6.00	12.00			2.12		28.27	8	4.00
RC-4-12A	6.00	12.00			1.73		28.27	12	4.00
RC-4-12B	6.00	12.00			1.73		28.27	12	4.00
RC-4-16A	6.00	12.00			1.50		28.27	16	4.00
RC-4-16A	6.00	12.00			1.50		28.27	16	4.00
SC-4-2A	6.00	12.00				3.76	28.27	2	4.00
SC-4-2B	6.00	12.00				3.76	28.27	2	4.00
SC-4-4A	6.00	12.00				2.66	28.27	4	4.00
SC-4-4B	6.00	12.00				2.66	28.27	4	4.00
SC-4-6A	6.00	12.00				2.17	28.27	6	4.00
SC-4-6B	6.00	12.00				2.17	28.27	6	4.00
SC-4-8A	6.00	12.00				1.88	28.27	8	4.00
SC-4-8B	6.00	12.00				1.88	28.27	8	4.00
SC-4-12A	6.00	12.00				1.53	28.27	12	4.00
SC-4-12B	6.00	12.00				1.53	28.27	12	4.00
SC-4-16A	6.00	12.00				1.33	28.27	16	4.00
SC-4-16B	6.00	12.00				1.33	28.27	16	4.00

Legend



Test Series 1

The test procedure was as follows: For the square prisms the hand-finished surface served as the bearing area. To minimize the effect of an uneven surface and secure a uniform load application a 1/8 in. thick rubber pad was placed between the bearing plate and the concrete surface. The bearing plates consisted in 1/2 in. A-36 steel plates, cut to the proper dimensions, corresponding to each  $A/A_b$  ratio. At the bottom of the specimen, another 1/8 in. bearing pad was placed between the formed surface and the compression machine steel platform. In the case of the cylinders a typical bearing pad for compression tests was used at the bottom.

For each  $A/A_b$  ratio, the steel plate was centered on the specimen with the help of previously drawn aligning marks. Then the specimen was aligned and centered properly with respect to the compression machine's upper head in order to guarantee a concentric application of loading. Figure 3.1 presents a typical setup for the testing of a square prism. The rate of application of loading was on the order of 12,000 lbs/min for the high  $A/A_b$  ratios ( $R > 6$ ) and 20,000 lbs/min for  $R = 6$  or less. Each specimen was tested to failure and the maximum load achieved was recorded. A complete description of the failure modes and a discussion of these test results are presented in Chapter 5.



Fig. 3.1 Test Setup for a Square Prism

After the analysis of the test series 1 it was determined that the target range of  $A/A_b$  ratios to be more closely investigated was the  $1.5 \leq R \leq 6$  range. This covers the most likely  $R$ -values in the AASHTO acceptance test. Also it was determined that the shape of the plate does not significantly affect the UBS for the same  $A/A_b$  ratio; therefore for the next test series only square plates were utilized.

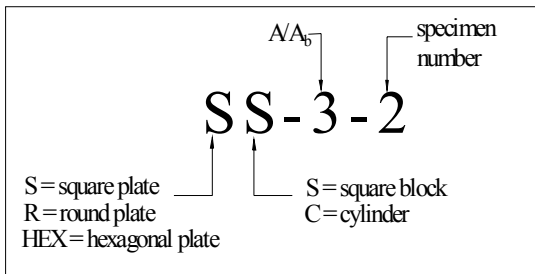
In test series 2, square blocks and cylinders were tested in the  $1.5 \leq R \leq 6$  range, using the same concrete mix and testing procedure explained for test series 1. A thin layer of epoxy was applied to bottom of the square blocks to guarantee a uniform pressure distribution on the opposite end of the specimen. For the cylinder specimens, a hexagonal plate was used for  $R=1.5$ , for the other  $R$ -values the bearing plate was square. A total of 28 specimens were tested to failure and the ultimate load was recorded. Specimen parameters are presented in Table 3.2.

Test series 3 consisted of the investigation of the influence of the aspect ratio ( $AR$ =length/width) on the bearing strength. The specimens were cylinders 6 in. in diameter and 3, 4, 6, 8, 9, 12 and 18 in. in height, corresponding to aspect ratios of 0.5, 0.66, 1, 1.33, 1.5, 2 and 3 respectively. The specimens were cast in plastic molds and tested when the compressive strength was about 4,000 psi. The concrete mix and the testing procedure used were the same as for test series 1 and 2. The test consisted of loading the specimens thru a bearing plate with an  $A/A_b$  ratio of 4. Two specimens for each aspect ratio were tested to failure and the ultimate loads recorded. Specimen parameters are presented in Table 3.3.

Table 3.2 Matrix of Test Series 2

Specimen	Block Size				Plate Size		Block Area (in <sup>2</sup> )	R A/A <sub>b</sub>	f <sub>c</sub> target (ksi)
	Cylinder		Square Block		Round	Square			
	h (in)	L (in)	h (in)	L (in)	b (in)	b (in)			
SS-1.5-1			8.00	16.00		6.53	64.00	1.5	4.00
SS-1.5-2			8.00	16.00		6.53	64.00	1.5	4.00
SS-2-1			8.00	16.00		5.66	64.00	2.0	4.00
SS-2-2			8.00	16.00		5.66	64.00	2.0	4.00
SS-2.5-1			8.00	16.00		5.06	64.00	2.5	4.00
SS-2.5-2			8.00	16.00		5.06	64.00	2.5	4.00
SS-3-1			8.00	16.00		4.62	64.00	3.0	4.00
SS-3-2			8.00	16.00		4.62	64.00	3.0	4.00
SS-4-1			8.00	16.00		4.00	64.00	4.0	4.00
SS-4-2			8.00	16.00		4.00	64.00	4.0	4.00
SS-6-1			8.00	16.00		3.27	64.00	6.0	4.00
SS-6-2			8.00	16.00		3.27	64.00	6.0	4.00
HEXC-1.5-1	6.00	12.00				4.34	28.27	1.5	4.00
HEXC-1.5-2	6.00	12.00				4.34	28.27	1.5	4.00
SC-2-1	6.00	12.00				3.76	28.27	2.0	4.00
SC-2-2	6.00	12.00				3.76	28.27	2.0	4.00
SC-2.5-1	6.00	12.00				3.36	28.27	2.5	4.00
SC-2.5-2	6.00	12.00				3.36	28.27	2.5	4.00
SC-3-1	6.00	12.00				3.07	28.27	3.0	4.00
SC-3-2	6.00	12.00				3.07	28.27	3.0	4.00
SC-4-1	6.00	12.00				2.66	28.27	4.0	4.00
SC-4-2	6.00	12.00				2.66	28.27	4.0	4.00
SC-6-1	6.00	12.00				2.17	28.27	6.0	4.00
SC-6-2	6.00	12.00				2.17	28.27	6.0	4.00

Legend

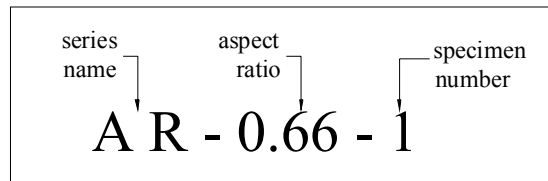


Test Series 2

Table 3.3 Matrix of Test Series 3

Specimen	Block Size		Plate	Block Area (in <sup>2</sup> )	Aspect Ratio L/h	R A/A <sub>b</sub>	f <sub>c</sub> target (ksi)
	Cylinder		Square				
	h (in)	L (in)	b (in)				
AR-0.5-1	6.00	3.00	3.07	28.27	0.50	3.0	4.00
AR-0.5-2	6.00	3.00	3.07	28.27	0.50	3.0	4.00
AR-0.66-1	6.00	4.00	3.07	28.27	0.66	3.0	4.00
AR-0.66-2	6.00	4.00	3.07	28.27	0.66	3.0	4.00
AR-1-1	6.00	6.00	3.07	28.27	1.00	3.0	4.00
AR-1-2	6.00	6.00	3.07	28.27	1.00	3.0	4.00
AR-1.33-1	6.00	8.00	3.07	28.27	1.33	3.0	4.00
AR-1.33-2	6.00	8.00	3.07	28.27	1.33	3.0	4.00
AR-1.5-1	6.00	9.00	3.07	28.27	1.50	3.0	4.00
AR-1.5-2	6.00	9.00	3.07	28.27	1.50	3.0	4.00
AR-2-1	6.00	12.00	3.07	28.27	2.00	3.0	4.00
AR-2-2	6.00	12.00	3.07	28.27	2.00	3.0	4.00
AR-3-1	6.00	18.00	3.07	28.27	3.00	3.0	4.00
AR-3-2	6.00	18.00	3.07	28.27	3.00	3.0	4.00

Legend

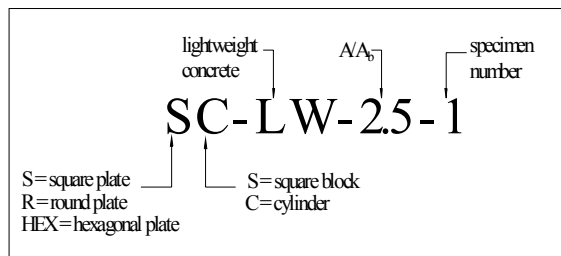


In test series 4 the effect of the use of a lightweight concrete mix on the bearing strength was investigated. The specimens were 6 in. by 12 in. cylinders and the characteristic concrete strength was 8,000 psi. The concrete was 22 months old at the time of testing. The  $A/A_b$  ratio was varied from 1.5 to 16. The plate shape was also varied in this series: hexagonal for  $R=1.5$ , square plates for  $R=2, 2.5, 3, 4, 6$  and circular for  $R=8, 12, 16$ . At least two specimens for each  $R$ -value were tested for a total of 20 specimens. Table 3.4 presents the parameters for this series.

Table 3.4 Matrix of Test Series 4

Specimen	Block Size		Plate Size		Block Area (in <sup>2</sup> )	R A/A <sub>b</sub>	f <sub>c</sub> target (ksi)
	Cylinder		Round	Square			
	h (in)	L (in)	b (in)	b (in)			
HEXC-LW-1.5-1	6.00	12.00		4.34	28.27	1.5	8.00
HEXC-LW-1.5-2	6.00	12.00		4.34	28.27	1.5	8.00
SC-LW-2-1	6.00	12.00		3.76	28.27	2.0	8.00
SC-LW-2-2	6.00	12.00		3.76	28.27	2.0	8.00
SC-LW-2.5-1	6.00	12.00		3.36	28.27	2.5	8.00
SC-LW-2.5-2	6.00	12.00		3.36	28.27	2.5	8.00
SC-LW-3-1	6.00	12.00		3.07	28.27	3.0	8.00
SC-LW-3-2	6.00	12.00		3.07	28.27	3.0	8.00
SC-LW-4-1	6.00	12.00		2.66	28.27	4.0	8.00
SC-LW-4-2	6.00	12.00		2.66	28.27	4.0	8.00
SC-LW-6-1	6.00	12.00		2.17	28.27	6.0	8.00
SC-LW-6-2	6.00	12.00		2.17	28.27	6.0	8.00
RC-LW-8-1	6.00	12.00	2.12		28.27	8.0	8.00
RC-LW-8-2	6.00	12.00	2.12		28.27	8.0	8.00
RC-LW-12-1	6.00	12.00	1.73		28.27	12.0	8.00
RC-LW-12-2	6.00	12.00	1.73		28.27	12.0	8.00
RC-LW-16-1	6.00	12.00	1.50		28.27	16.0	8.00
RC-LW-16-2	6.00	12.00	1.50		28.27	16.0	8.00

Legend

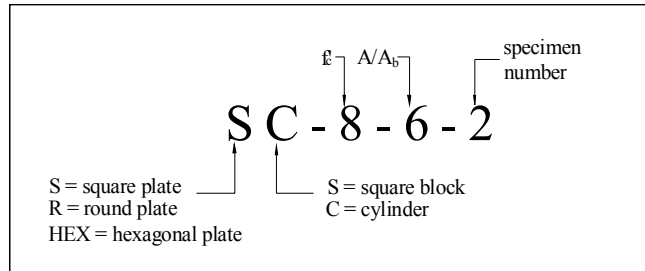


Series 5 and 6 studied the effect of high strength concrete on the bearing strength. The characteristic concrete strengths were 8,000 psi and 11,000 psi, respectively. All the specimens were 6 in. by 12 in. cylinders and the  $A/A_b$  ratio varied from 1.5 to 16. In series 6, moist-cured specimens were used with a concrete age of about 22 months at the time of testing. A total of 19 specimens were tested in series 5 and 15 in series 6. (See Table 3.5)

Table 3.5 Matrix of Test Series 5 and 6

Specimen	Block Size		Plate Size		Block Area (in <sup>2</sup> )	R A/A <sub>b</sub>	f <sub>c</sub> target (ksi)
	Cylinder		Round	Square			
	h (in)	L (in)	b (in)	b (in)			
SC-8-1.5-1	6.00	12.00		4.34	28.27	1.5	8.00
SC-8-1.5-2	6.00	12.00		4.34	28.27	1.5	8.00
SC-8-2-1	6.00	12.00		3.76	28.27	2.0	8.00
SC-8-2-2	6.00	12.00		3.76	28.27	2.0	8.00
SC-8-2.5-1	6.00	12.00		3.36	28.27	2.5	8.00
SC-8-2.5-2	6.00	12.00		3.36	28.27	2.5	8.00
SC-8-3-1	6.00	12.00		3.07	28.27	3.0	8.00
SC-8-3-2	6.00	12.00		3.07	28.27	3.0	8.00
SC-8-4-1	6.00	12.00		2.66	28.27	4.0	8.00
SC-8-4-2	6.00	12.00		2.66	28.27	4.0	8.00
SC-8-6-1	6.00	12.00		2.17	28.27	6.0	8.00
SC-8-6-2	6.00	12.00		2.17	28.27	6.0	8.00
RC-8-8-1	6.00	12.00	2.12		28.27	8.0	8.00
RC-8-8-2	6.00	12.00	2.12		28.27	8.0	8.00
RC-8-12-1	6.00	12.00	1.73		28.27	12.0	8.00
RC-8-12-2	6.00	12.00	1.73		28.27	12.0	8.00
RC-8-16-1	6.00	12.00	1.50		28.27	16.0	8.00
RC-8-16-2	6.00	12.00	1.50		28.27	16.0	8.00
SC-12-1.5-1	6.00	12.00		4.34	28.27	1.5	11.00
SC-12-1.5-2	6.00	12.00		4.34	28.27	1.5	11.00
SC-12-2-1	6.00	12.00		3.76	28.27	2.0	11.00
SC-12-2-2	6.00	12.00		3.76	28.27	2.0	11.00
SC-12-2.5-1	6.00	12.00		3.36	28.27	2.5	11.00
SC-12-2.5-2	6.00	12.00		3.36	28.27	2.5	11.00
SC-12-3-1	6.00	12.00		3.07	28.27	3.0	11.00
SC-12-3-2	6.00	12.00		3.07	28.27	3.0	11.00
SC-12-4-1	6.00	12.00		2.66	28.27	4.0	11.00
SC-12-4-2	6.00	12.00		2.66	28.27	4.0	11.00
SC-12-6-1	6.00	12.00		2.17	28.27	6.0	11.00
SC-12-6-2	6.00	12.00		2.17	28.27	6.0	11.00
RC-12-8-1	6.00	12.00	2.12		28.27	8.0	11.00
RC-12-8-2	6.00	12.00	2.12		28.27	8.0	11.00
RC-12-12-1	6.00	12.00	1.73		28.27	12.0	11.00
RC-12-12-2	6.00	12.00	1.73		28.27	12.0	11.00
RC-12-16-1	6.00	12.00	1.50		28.27	16.0	11.00
RC-12-16-2	6.00	12.00	1.50		28.27	16.0	11.00

Legend



In test series 7, the effect of the duct size was investigated in plain concrete cylinders. Test specimens consisted of 6 in. by 12 in. cylinders with preformed concentric holes varying from 0.94 in. to 3.38 in. The holes were preformed using greased PVC pipes that were knocked out of the specimens when the concrete reached 4,000 psi. A total of 12 specimens were tested, 10 with holes and two solid ones for comparison of results. The concrete consisted of an 8,000 psi nominal strength mix with a maximum aggregate size of 0.75 in. The characteristic concrete strength at testing was 6,790 psi. All specimens were tested with a 4.5 in. in diameter A-36 steel plate that provided a constant  $A/A_b$  ratio of 1.78. (See Table 3.6)

Table 3.6 Matrix of Test Series 7

Specimen	Block Size		Plate Size	Block Area (in <sup>2</sup> )	R $A/A_b$	Duct Size (in.)	$f'_c$ target (ksi)
	Cylinder		Round				
	h (in)	L (in)	b (in)				
1	6.00	12.00	4.50	28.27	1.78	0.00	7.00
2	6.00	12.00	4.50	28.27	1.78	0.00	7.00
3	6.00	12.00	4.50	28.27	1.78	0.94	7.00
4	6.00	12.00	4.50	28.27	1.78	0.94	7.00
5	6.00	12.00	4.50	28.27	1.78	1.44	7.00
6	6.00	12.00	4.50	28.27	1.78	1.44	7.00
7	6.00	12.00	4.50	28.27	1.78	2.00	7.00
8	6.00	12.00	4.50	28.27	1.78	2.00	7.00
9	6.00	12.00	4.50	28.27	1.78	2.38	7.00
10	6.00	12.00	4.50	28.27	1.78	2.38	7.00
11	6.00	12.00	4.50	28.27	1.78	3.38	7.00
12	6.00	12.00	4.50	28.27	1.78	3.38	7.00

### 3.3 Reinforced Concrete Specimens

Forty-two reinforced square prisms were tested in this series. The types of lateral reinforcement consisted of spirals, ties and a combination of spirals and ties. The primary objective of these tests was the evaluation of the effect of the lateral reinforcement ratio on the ultimate bearing strength. Figs. 3.2 and 3.3 show typical reinforced specimens ready for concrete placement.



Fig. 3.2 Specimen Reinforced with Spiral and Ties



Fig. 3.3 Specimens Reinforced with Ties

Since the tests by Suzuki and Nakatsuka (1982) suggested a relationship between the mechanical reinforcing ratio ( $\omega=2q_b$ ) and the ultimate bearing strength, it was proposed that the specimens were tested at different compressive strengths. The mechanical reinforcing ratio was varied between 0.13 and 0.66. In the case of blocks reinforced with ties only half of the mechanical reinforcement ratio was considered as effective for confinement.

The spiral reinforcement consisted of Grade 60, No. 3 bars that were machine bent. The actual yield strength of the rebar was taken from the certified mill test report. The typical diameter for the spirals (center to center of bars) in spirals-only specimens was 6.75 in. For specimens with spirals and ties, the diameter of the spiral was 6 in. Spiral pitch varied from 1.125 in. to 2.5 in. for the spirals-only specimens. A constant pitch of 2 in. was used in the case of the specimens with spiral and ties. The square ties had an exterior width of 7 in. this allowed  $\frac{1}{2}$  in. concrete cover on all sides.

The concrete used was an 8,000 psi nominal strength mix with a maximum aggregate size of  $\frac{3}{4}$  in. The bearing plate for the first 6 tests consisted in a 0.5 in. x 4.625 in. x 4.625 in. A-36 steel plate for an  $A/A_b$  ratio of 3. The other 36 specimens were tested with a 0.5 in. x 4 in. x 4 in. plate for an  $A/A_b$  ratio of 4. Table 3.7 presents the details of the test specimens.

The specimens were cast upside down. After the forms were stripped, a thin layer of epoxy was applied to the bottom of the specimens to level the surface that was in contact with the steel platform. After the specimens reached the desired strength, they were placed in the compression machine, aligned and loaded at a rate of 25,000 lbs/min to failure.

Table 3.7 Matrix of Reinforced Specimens Test Series

Specimen	Type of Reinforc.	Plate (b, in.)	Block (h, in.)	A/A <sub>b</sub> ratio	A <sub>s</sub> Spiral (in <sup>2</sup> )	A <sub>s</sub> Ties (in <sup>2</sup> )	Spiral Diam.(in)	Spiral Pitch (in)	Tie Width (in)	Tie Spacing (in)
AR-1	spiral	4.00	8.00	4.00	0.11		6.75	2.50		
DL-4	spiral	4.00	8.00	4.00	0.11		6.75	2.50		
AR-2	spiral	4.00	8.00	4.00	0.11		6.75	2.50		
DR-4	spiral	4.00	8.00	4.00	0.11		6.75	2.50		
DL-3	spiral	4.00	8.00	4.00	0.11		6.75	2.00		
DL-3	spiral	4.00	8.00	4.00	0.11		6.75	2.00		
AR-4	spiral	4.00	8.00	4.00	0.11		6.75	1.88		
AR-3	spiral	4.00	8.00	4.00	0.11		6.75	2.00		
DR-3	spiral	4.00	8.00	4.00	0.11		6.75	2.00		
AL-3	spiral	4.00	8.00	4.00	0.11		6.75	1.44		
AL-1	spiral	4.00	8.00	4.00	0.11		6.75	1.50		
DR-2	spiral	4.00	8.00	4.00	0.11		6.75	1.50		
AL-4	spiral	4.00	8.00	4.00	0.11		6.75	1.38		
DR-1	spiral	4.00	8.00	4.00	0.11		6.75	1.25		
AL-2	spiral	4.625	8.00	3.00	0.11		6.75	1.13		
DL-1	spiral	4.625	8.00	3.00	0.11		6.75	1.13		
CL-2	ties	4.00	8.00	4.00		0.11			6.63	3.50
BL-2	ties	4.00	8.00	4.00		0.11			6.63	3.25
BL-3	ties	4.00	8.00	4.00		0.11			6.63	2.50
CL-3	ties	4.00	8.00	4.00		0.11			6.63	2.50
CR-3	ties	4.00	8.00	4.00		0.11			6.63	2.00
CL-4	ties	4.00	8.00	4.00		0.11			6.63	2.00
CR-2	ties	4.00	8.00	4.00		0.11			6.63	2.00
EL-4	ties	4.00	8.00	4.00		0.11			6.63	2.00
ER-6	ties	4.00	8.00	4.00		0.11			6.63	2.00
CR-1	ties	4.00	8.00	4.00		0.11			6.63	1.50
EL-2	ties	4.00	8.00	4.00		0.11			6.63	1.50
BL-4	ties	4.00	8.00	4.00		0.11			6.63	1.50
CL-1	ties	4.00	8.00	4.00		0.11			6.63	1.50
EL-3	ties	4.00	8.00	4.00		0.11			6.63	1.50
BL-1	ties	4.63	8.00	3.00		0.11			6.63	1.13
EL-1	ties	4.63	8.00	3.00		0.11			6.63	1.13
CR-4	spiral + ties	4.00	8.00	4.00	0.11	0.11	6.00	2.00	6.63	4.00
ER-1	spiral + ties	4.00	8.00	4.00	0.11	0.11	6.00	2.00	6.63	3.50
BR-4	spiral + ties	4.00	8.00	4.00	0.11	0.11	6.00	2.00	6.63	3.00
ER-4	spiral + ties	4.00	8.00	4.00	0.11	0.11	6.00	2.00	6.63	2.50
EL-6	spiral + ties	4.00	8.00	4.00	0.11	0.11	6.00	2.00	6.63	3.00
BR-1	spiral + ties	4.00	8.00	4.00	0.11	0.11	6.00	2.00	6.63	2.50
BR-3	spiral + ties	4.00	8.00	4.00	0.11	0.11	6.00	2.00	6.63	2.00
ER-3	spiral + ties	4.00	8.00	4.00	0.11	0.11	6.00	2.00	6.63	1.50
BR-2	spiral + ties	4.63	8.00	3.00	0.11	0.11	6.00	2.00	6.63	1.50
ER-2	spiral + ties	4.63	8.00	3.00	0.11	0.11	6.00	2.00	6.63	1.50

Chapter 5 presents a detailed report of the results from the bearing tests of plain and reinforced concrete specimens.

## Chapter 4. Analysis Procedures

### 4.1 Mohr Failure Criterion

As explained in Chapter 1, the Mohr failure criterion seems to fit very well the experimental results for bearing tests on plain concrete specimens. This criterion is one of the most widely accepted approaches to model the behavior of brittle materials such as rock and concrete, because of its relative simplicity.

The Mohr failure criterion is also known as the internal-friction theory and it considers two basic types of failures. The first one is the sliding failure. In this type of failure a fracture surface develops inclined to the direction of the maximum compressive stress and the movement of the resulting failure planes is parallel with respect to each other. This is the most likely to happen in a typical bearing test, when a cone or pyramid is developed under the bearing plate at failure. The second type is the splitting failure. The fracture plane now is generated normal to the axis of the tensile stress and the planes tend to separate in opposite directions.

According to Mohr if a material is tested to failure in its three pure states of stress, compression ( $\sigma'_c$ ), tension ( $\sigma'_t$ ) and shear ( $\sigma'_v$ ) and then we draw three Mohr circles, describing each of these limiting states (Fig.4.1), the tangent to these circles is a failure envelope for the material. If this material is now subjected to an arbitrary state of stress with  $\sigma_1$  and  $\sigma_3$  as the extreme principal stresses and the Mohr circle for the new condition lies within the envelope, the material is safe from failure.

In the Mohr criterion only the extreme principal stresses  $\sigma_1$  and  $\sigma_3$  are used. When the pure shear test is omitted, the resulting envelope always consists of a straight line and in this case the theory is called the modified Mohr's theory. In the case of plain concrete if we consider the ultimate compressive stress  $f'_c$  and the ultimate tensile stress  $f'_t$ , then the failure occurs when:

$$\frac{\sigma_1}{f'_t} - \frac{\sigma_3}{f'_c} \geq 1 \quad (\text{Eq. 4.1})$$

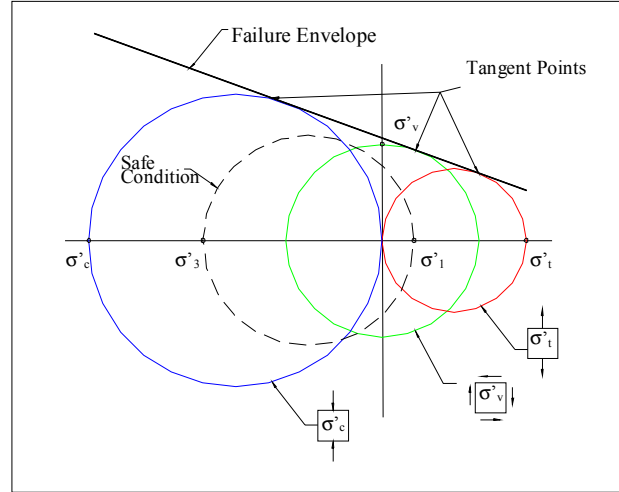


Fig. 4.1 Mohr Failure Criterion

In equation 4.1  $\sigma_1$  and  $\sigma_3$  are signed quantities but  $f'_c$  and  $f'_t$  are positive magnitudes of the failure strengths. Multiplying both sides of the equation by  $f'_c$  and considering now a point located on the failure envelope, we have:

$$\left( \frac{f'_c}{f'_t} \right) \sigma_1 - \sigma_3 = f'_c \quad (\text{Eq. 4.2})$$

If we define the ratio  $m = \frac{f'_c}{f'_t}$ , the final simplified expression for the failure surface is:

$$m\sigma_1 - \sigma_3 = f'_c \quad (\text{Eq. 4.3})$$

#### 4.2 Linear Elastic Finite Element Analysis of the Bearing Problem in a Square Prism

In order to develop an expression for the UBS of concrete blocks concentrically loaded based on the Mohr failure criterion it is necessary to know the magnitude and distribution of the principal stresses  $\sigma_1$  and  $\sigma_3$ . The classical solutions to the bearing problem were reviewed. The analysis of previous investigators such as Guyon (1951) and Yettram and Robbins (1969) were considered as a starting point.

Guyon provided a solution for the two-dimensional bearing problem (one way bearing). In one way bearing, bursting stresses develop primarily in one direction. The thickness of the block is considerably less than its width. One way bearing occurs when a strip load is applied

to a rectangular prism (Fig. 4.2). In this case, the plate covers the full thickness of the prism and only one dimension of the plate is varied to obtain the principal stresses for the different plate width ( $b$ ) to block width ( $h$ ) ratios (see Fig. 4.2).

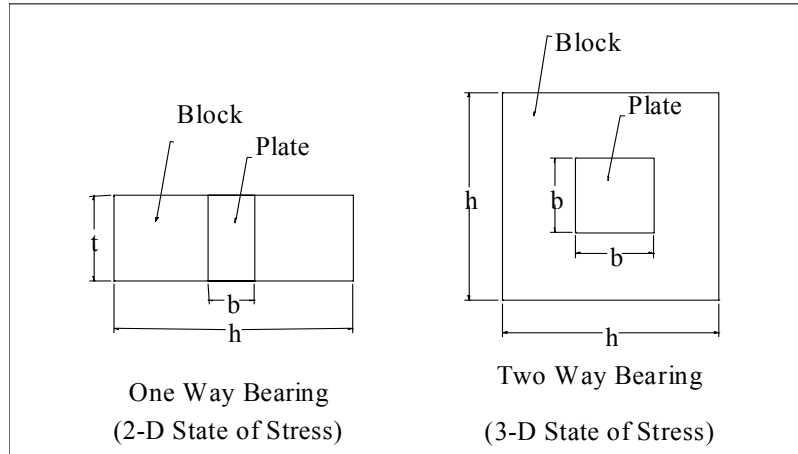


Fig. 4.2 Two and Three Dimensional Bearing Problems  
(Top view, load applied into plane of paper)

In the case of square prisms loaded through square plates, bursting stresses are generated in two orthogonal directions (Fig. 4.2). A different behavior is expected for these blocks. To develop an understanding of two-way bearing behavior a linear elastic finite element analysis (FEA) was performed. A typical square block 8 in. x 8 in. x 16 in. was modeled using 0.25 in. cube elements. The Poisson ratio was assumed to be 0.20 and the concrete modulus of elasticity was 3,600 ksi. The  $b/h$  ratio was varied from 0.125 to 0.875 in 0.125 increments. The block width,  $h$  was kept constant (8 in.) and the plate width,  $b$  varied from 1 in. to 7 in. A constant load of 100 kips was used in each case.

The analysis focused on the stresses developed in the plane of symmetry, parallel to the face of the block shown in Fig. 4.3. For each  $b/h$  ratio, the following variables were investigated: the magnitude and distribution along the centroidal axis of the principal stresses,  $\sigma_1$  (tensile-bursting) and  $\sigma_3$  (compressive) and the location of the maximum tensile stress ( $y$ ).

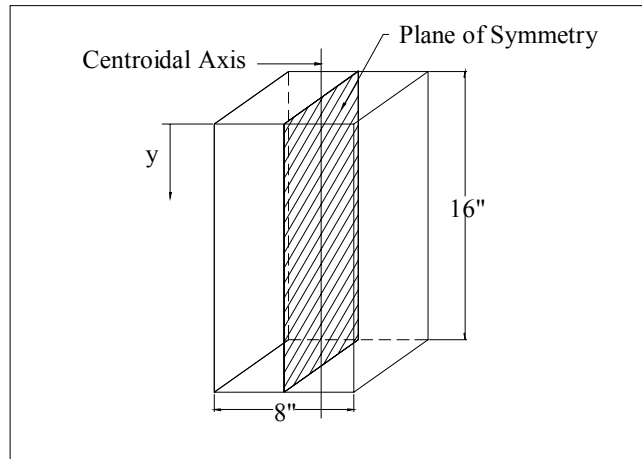


Fig. 4.3 Selected Plane for Principal Stress Investigation

The results for each case were tabulated in a spreadsheet and the variables of main importance plotted against the  $b/h$  ratio. For convenience, stresses were normalized to the average compressive stress ( $P/A$ ), where  $P$  was the load used for analysis (100 kips) and  $A$  is the area of the block (64 sq. in.). Therefore,  $P/A$  was taken as 1.5625 ksi. Figure 4.4 presents the distribution of the normalized maximum tensile stresses ( $\sigma_1 = f_t \text{ max}$ ) along the axis of symmetry. In a same manner Figure 4.5 presents the distribution of normalized maximum compressive stresses ( $\sigma_3$ ). In this case the results are in very good agreement with Saint-Venant's theory. The stress at the point  $y=h$  is equal to the uniform stress ( $P/A$ ).

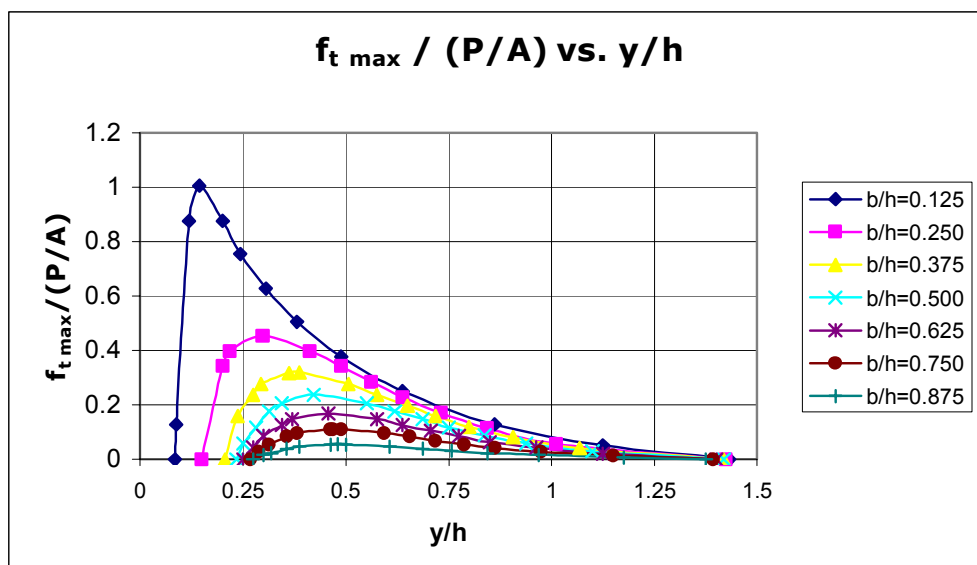


Fig. 4.4 Normalized Maximum Tensile Stresses along Longitudinal Axis.

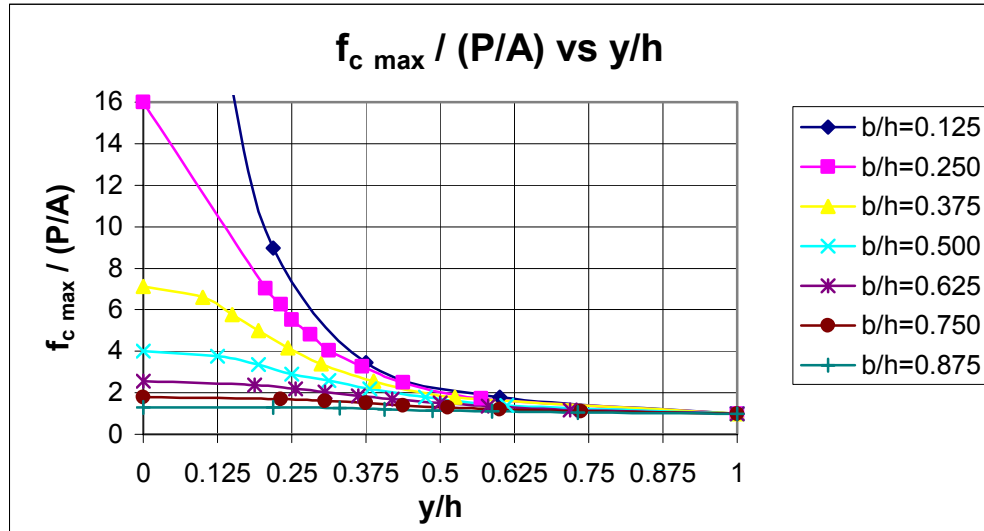


Fig. 4.5 Normalized Maximum Compressive Stresses along Longitudinal Axis.

It is also important to know the variation of  $f_{t \max}$  with the  $b/h$  ratio and the variation in the position of  $f_{t \max}$ , with a variation of  $b/h$ . This is shown in Figures 4.6 and 4.7 respectively. In Fig. 4.6, a new variable  $\beta$  is introduced for future use.  $\beta$  is the normalized ratio  $f_{t \max}$  over the average stress ( $P/A$ ). The results of this analysis are compared to Guyon's solution and to a tri-dimensional solution presented by Yettram and Robbins (1969).

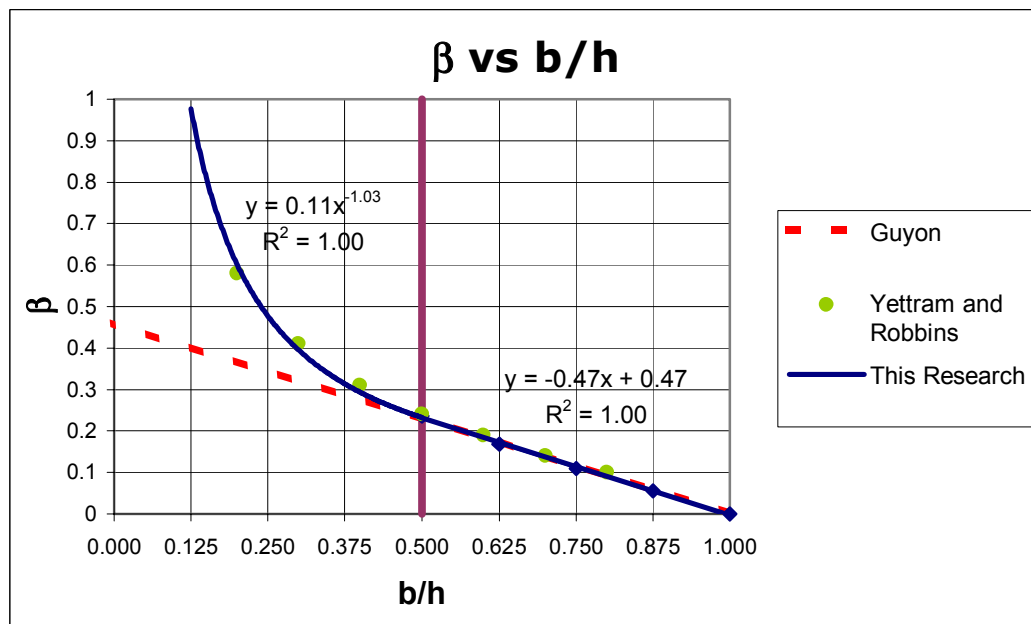


Fig. 4.6 Normalized Maximum Tensile Stresses  $\beta$  versus  $b/h$ .

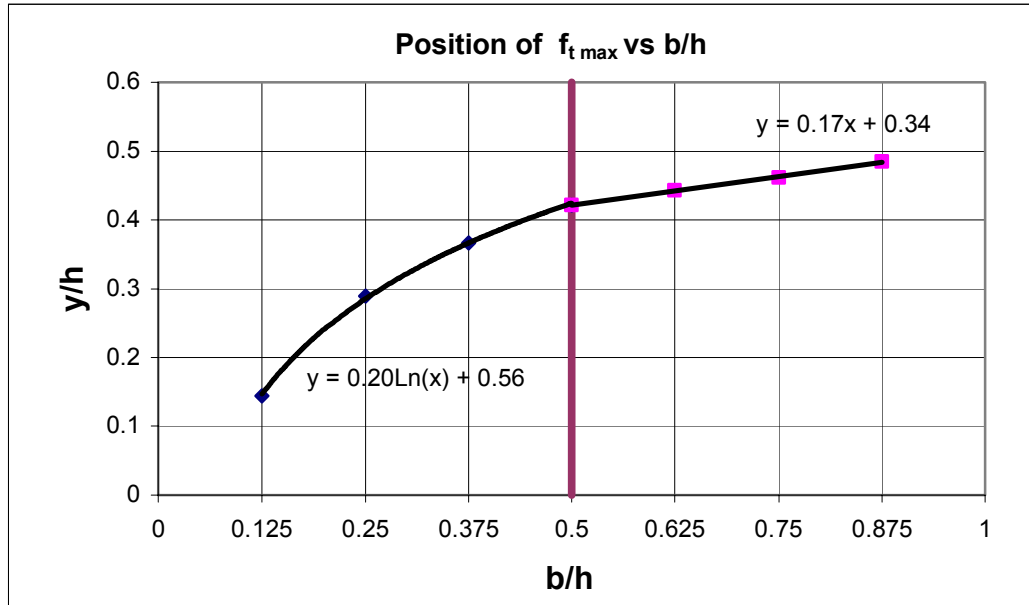


Fig. 4.7 Position of  $f_{tmax}$  versus  $b/h$ .

### 4.3 Development of Equation for Plain Concrete Specimens

Several assumptions were made to simplify the development of the equation for the ultimate bearing strength (UBS) of plain concrete prisms. The Mohr criterion explained in Section 4.1 is the theoretical base of the formulation. The general assumptions made are:

- 1) Failure is mainly controlled by the maximum tensile stress ( $\sigma_1 = f_{tmax}$ ) and initiates in a plane located at the position of maximum stress, ( $y$ ).
- 2) Behavior of plain concrete in tension is linear up to the point of failure. The ultimate tensile strength of concrete ( $f'_t$ ) is assumed to be equal to the split cylinder test strength.
- 3) The principal compressive stress ( $\sigma_3 = f_{cmax}$ ) is taken as an average stress at point  $y$ , assuming spreading of compressive stresses at a 45-degree angle from the top surface of the block. This average stress acts on an area described by the intersection points of a horizontal plane and the 45-degree angle projection lines.
- 4) The Aspect Ratio of the concrete element ( $L/h$ ) is  $\geq 1.5$ . This condition ensures that no significant effects on the UBS are going to take place due to the boundary condition at the bottom of the prism. (See Section 2.1) and (Niyogi 1974).

A graphical description of the above assumptions and variables involved is presented in Fig. 4.8. In the figure,  $P$  is the ultimate load,  $b$  is the width of the square plate,  $y$  is the position of the maximum tensile stress  $f_{t \max}$ ,  $A_y$  is the area subjected to the assumed uniform compressive state of stress ( $f_{c \max}$ ) at distance  $y$ ,  $A$ ,  $h$  and  $L$  are the area, width and length of the prism, respectively.

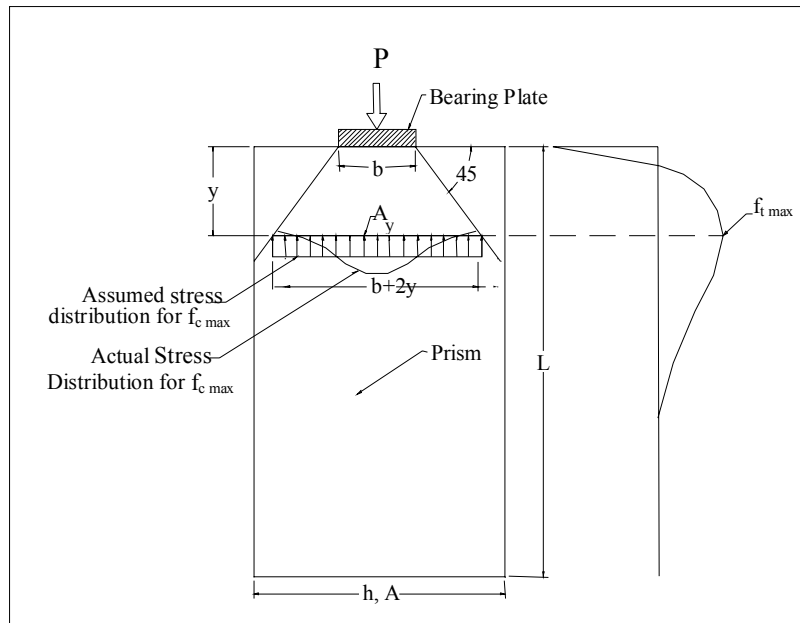


Fig. 4.8 Variables Description.

Taking equation 4.3 as the base expression, and redefining  $\sigma_1 = f_{t \max}$  in terms of  $\beta$  and the average stress ( $P/A$ ):

$$\sigma_1 = \beta \left( \frac{P}{A} \right) \quad (\text{Eq. 4.4})$$

Introducing a new variable,  $\alpha = \frac{A}{A_y}$ , with  $A_y = (b + 2y)^2$  and expressing  $\sigma_3 = f_{c \max}$  in terms of

$\alpha$  and  $P/A$  yields:

$$\sigma_3 = -\alpha \left( \frac{P}{A} \right) \quad (\text{Eq. 4.5})$$

Substituting  $\sigma_1$  and  $\sigma_3$  values obtained in Eqs.4.4 and 4.5 in Eq. 4.3 and introducing the minus sign corresponding to  $\sigma_3$  (compression):

$$m\beta\left(\frac{P}{A}\right) + \alpha\left(\frac{P}{A}\right) = f'_c \quad (\text{Eq. 4.6})$$

Rearranging the equation as a function of the ultimate load P, we have:

$$P = \frac{Af'_c}{m\beta + \alpha} \quad (\text{Eq. 4.7})$$

Where m is equal to the  $f'_c/f'_t$  ratio and the materials properties  $f'_c$  and  $f'_t$  are both determined experimentally. The parameter  $\beta$  is determined as follows (see Fig.4.6):

$$\beta = \frac{0.114}{\left(\frac{b}{h}\right)^{1.03}} \text{ for } \frac{b}{h} < 0.5 \quad (\text{Eq. 4.8a})$$

$$\beta = 0.466 + 0.469\left(\frac{b}{h}\right) \text{ for } \frac{b}{h} \geq 0.5 \quad (\text{Eq. 4.8b})$$

The parameter  $\alpha$  depends on the point where the maximum tensile stress (y) occurs and y is a function of the b/h ratio (see Fig. 4.7). The expressions governing these relationships are:

$$\alpha = 1.0, \text{ for } y \geq \frac{h-b}{2} \quad (\text{Eq. 4.8c})$$

$$\alpha = \frac{A}{A_y} = \frac{A}{(b+2y)^2}, \text{ for } y < \frac{h-b}{2} \quad (\text{Eq. 4.8d})$$

$$y = 0.20 \ln\left(\frac{b}{h}\right) + 0.56, \text{ for } \frac{b}{h} < 0.5 \quad (\text{Eq. 4.9a})$$

$$y = 0.17\left(\frac{b}{h}\right) + 0.34, \text{ for } \frac{b}{h} \geq 0.5 \text{ and } \quad (\text{Eq. 4.9b})$$

$$A_y = (b+2y)^2, \text{ for square blocks loaded through square plates}$$

$$A_y = \left(\frac{\pi}{4}\right)(b+2y)^2, \text{ for cylinder blocks loaded through round plates}$$

Equation 4.7 is the general expression for the UBS of plain concrete blocks of regular section, concentrically loaded and subject to the assumptions and limitations explained

previously. The formula applies to square blocks loaded through square plates and cylinders loaded through circular plates. In the case that other types of plates are used an equivalent square area (in the case of a square prism) or circular area (in the case of cylinders) has to be calculated to obtain accurate results.

#### **4.4 Development of Equation for Reinforced Concrete Specimens using Curve Fitting.**

Using the data from 36 reinforced specimens tested in this research, an expression was developed for the UBS of reinforced specimens based on a factor  $k$ , which modifies the plain concrete ultimate bearing strength. This factor  $k$  is determined by curve fitting of the plotted points of the ratio UBS reinforced over the UBS of plain concrete versus the mechanical reinforcing ratio ( $\omega$ ). Therefore the expression for the UBS of reinforced specimens based on curve fitting takes the form:

$$P_r = k \left( \frac{A f'_c}{m \beta + \alpha} \right) \quad (\text{Eq. 4.10})$$

The determination of factor  $k$  is presented in Chapter 5. According to the available test data a limit value of  $0.85 f'_c A$ , is recommended when using Eq. 4.10.

#### **4.5 Development of Equation for Reinforced Concrete Specimens using Mohr's failure criterion.**

In the case of reinforced concrete blocks, the concrete material properties have to be modified and substituted by an equivalent material with enhanced tensile strength ( $f'_{tr}$ ). The total reinforced tensile strength  $f'_{tr}$  is the summation of the split cylinder strength ( $f'_t$ ) plus the passive confining pressure provided by the lateral reinforcing ( $f_{lat}$ ). Since the confining reinforcement also enhances the ultimate compressive strength, a factor of 1.25 is suggested to modify the cylinder strength in the right side of equation 4.7. This calibration factor was obtained from the experiments performed on reinforced blocks. If we now define a new variable  $m_r$  as:

$$m_r = \frac{f'_c}{f'_t + f_{lat}} \quad (\text{Eq. 4.11})$$

Therefore the ultimate bearing strength of reinforced concrete blocks can be expressed as:

$$P_r = \frac{1.25Af'_c}{m_r\beta + \alpha} \quad (\text{Eq. 4.12})$$

A comparison of the results for the different approaches and the performance of the derived equations for plain and reinforced concrete blocks against experimental data is presented in detail in Chapter 5.

## Chapter 5. Tests results and Discussion

In this chapter test results from the experiments on plain and reinforced concrete prisms are presented in tabulated form and charts. A description of the characteristic failure mode of each test series is described at the beginning of each section. This description includes pictures of the different specimens at failure. In Section 5.1, results from the investigation of the ultimate bearing strength of plain concrete specimens are presented. Results are shown in the same sequence order as in Chapter 3. Each aspect or variable studied is presented in a different sub-section.

At the end of section 5.1 the results obtained from the actual tests are compared against the equation proposed for the prediction of the UBS of plain concrete specimens (Eq. 4.7). The performance of equation 4.7 is compared against the ACI equation and the ones proposed by Niyogi (1973) and Hawkins (1968) in tables 5.9 to 5.11. A histogram showing the average of the ratio  $P_{test}/P_{pred}$  and the coefficient of variation obtained using equation 4.7 from 131 tests is presented in Fig.5.23.

Section 5.2 presents the results from 36 bearing tests on reinforced specimens. At the end of the section, the performance of the two different equations (4.10 and 4.12) proposed for the prediction of the ultimate strength of reinforced specimens is evaluated against the experimental data of many previous AASHTO load transfer tests and others performed in Europe on VSL special anchorage devices and the ones from the NCHRP 356 study. The performance of these equations is measured by the average of the ratio  $P_{test}/P_{pred}$  and the coefficient of variation of this ratio. The performance of equation 4.12 is also evaluated against test results from this research and the ones obtained by Wurm and Daschner (1977).

### 5.1 Plain concrete Specimens

#### 5.1.1 Test Series 1

The objectives of this series were to understand the effect of varying the  $A/A_b$  ratio and the plate shape on the ultimate bearing strength. As presented in Chapter 3 specimens included square prisms and cylinders each loaded through both square and round bearing plates.

A typical square block specimen failure is shown in Fig. 5.1. The formation of a concrete cone or pyramid prior to general failure was the common case. After formation of first visible cracks the failure of the specimens was imminent. For the square blocks the typical failure consisted of splitting of the block into two or three parts with or without the formation of a failure cone. In the case of the cylinder blocks, a characteristic failure occurred with the splitting of the specimen into almost three identical parts (Fig. 5.2).

Table 5.1 shows the results from square and cylindrical blocks, tested to failure and loaded with square and round plates. The  $A/A_b$  ratio was varied from 2 to 16. The ultimate loads shown in each case are the average of at least two similar tests. The ultimate bearing stress ( $f'_b$ ) is normalized to the cylinder strength  $f'_c$ , in the last column.

The values of  $f'_b/f'_c$  obtained in Table 5.1 are plotted against the  $A/A_b$  ratios in Figs. 5.3 and 5.4. These figures given also show a comparison of the results with the ACI 318-02 recommendations for bearing and the limit established by the Code.



Fig. 5.1 Failure of Square Block Loaded with Round Plate,  $A/A_b=16$ .



Fig. 5.2 Failure of Cylinder Prism Loaded with Square Plate,  $A/A_b=4$ .

Table 5.1 Results from Test Series 1

Specimens	A (in <sup>2</sup> )	A <sub>b</sub> (in <sup>2</sup> )	A/A <sub>b</sub>	P <sub>u</sub> (lbs)	f <sub>b</sub> (psi)	f <sub>c</sub> (psi)	f <sub>b</sub> /f <sub>c</sub>
SS-4-2A, B	64.00	32.00	2	142,500	4,450	4,050	1.10
SS-4-4A, B	64.00	16.00	4	93,250	5,830	4,050	1.44
SS-4-6A, B	64.00	10.66	6	73,750	6,920	4,050	1.71
SS-4-8A, B	64.00	8.00	8	65,000	8,125	4,360	1.87
SS-4-12A, B	64.00	5.33	12	56,000	10,510	4,360	2.41
SS-4-16A, B	64.00	4.00	16	49,500	12,375	4,360	2.84
RS-4-2A, B	64.00	32.00	2	136,250	4,260	4,360	0.98
RS-4-4A, B	64.00	16.00	4	101,250	6,330	4,360	1.45
RS-4-6A, B	64.00	10.66	6	77,500	7,270	4,360	1.67
RS-4-8A, B	64.00	8.00	8	64,250	8,030	4,360	1.84
RS-4-12A, B	64.00	5.33	12	60,000	11,260	4,360	2.58
RS-4-16A, B	64.00	4.00	16	53,000	13,250	4,360	3.04
RC-4-2A, B	28.27	14.14	2	54,000	3,820	4,210	0.91
RC-4-4A, B	28.27	7.07	4	41,750	5,910	4,210	1.40
RC-4-6A, B, C	28.27	4.71	6	36,333	7,710	4,210	1.83
RC-4-8A, B	28.27	3.53	8	34,000	9,620	4,210	2.29
RC-4-12A, B, C	28.27	2.36	12	26,333	11,180	4,210	2.66
RC-4-16A, B	28.27	1.77	16	27,550	15,595	4,210	3.70
SC-4-2A, B	28.27	14.14	2	58,500	4,140	4,210	0.98
SC-4-4A, B	28.27	7.07	4	47,500	6,720	4,210	1.60
SC-4-6A, B	28.27	4.71	6	39,500	8,385	4,210	1.99
SC-4-8A, B	28.27	3.53	8	34,500	9,765	4,210	2.32
SC-4-12A, B	28.27	2.36	12	28,000	11,885	4,210	2.82
SC-4-16A, B	28.27	1.77	16	26,000	14,715	4,210	3.50

Legend

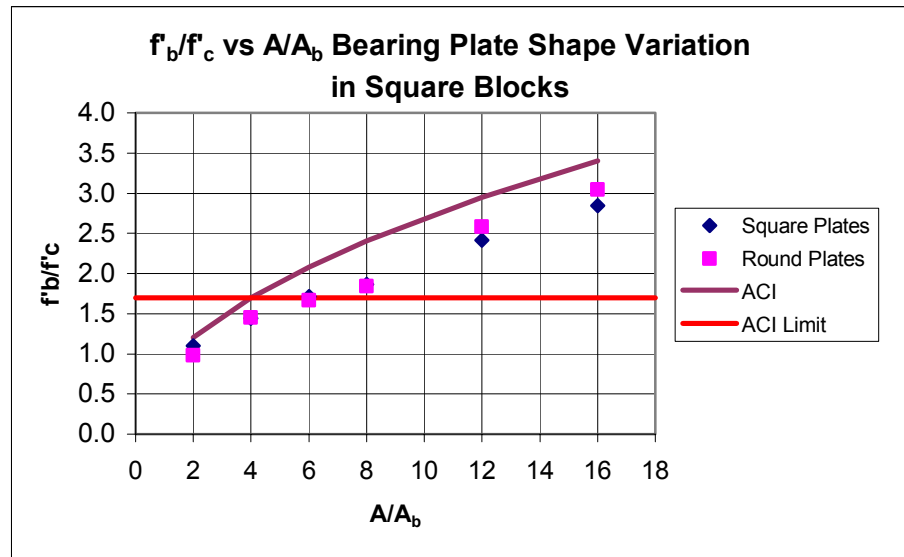
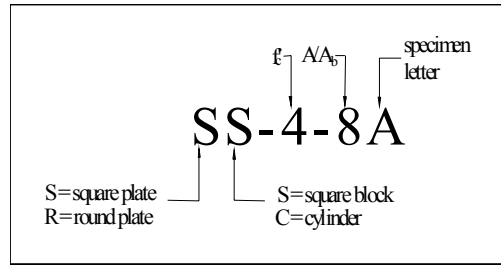


Fig. 5.3 Plot of  $f'_b/f'_c$  vs.  $A/A_b$  Ratio for Square Blocks (Series 1).

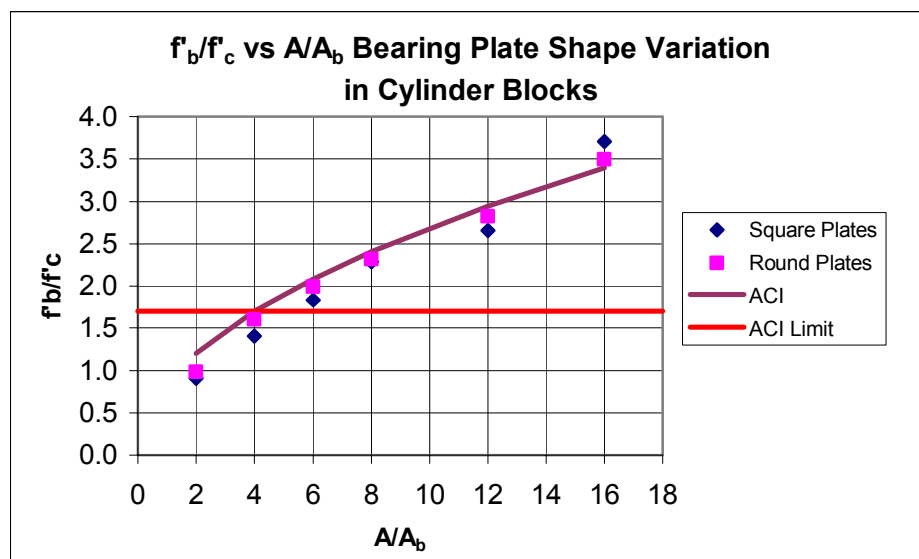


Fig. 5.4 Plot of  $f'_b/f'_c$  vs.  $A/A_b$  Ratio for Cylinder Blocks (Series 1).

Fig. 5.3 indicates that the ACI equation for bearing overestimates the UBS for the square specimens. Also the limit established by the Code ( $f'_b/f'_c = 1.7$ ) is very conservative for  $A/A_b$  ratios greater than 4. However, the results obtained for cylinder blocks have good agreement with the ACI equation. This is understandable since the ACI equation was derived from the results of tests on cylinder blocks loaded through circular plates (see Middendorf, 1960).

A very slight difference is observed in the results obtained with the use of square and round plates. From the results shown in Figs. 5.3 and 5.4, it can be inferred that the behavior of these specimens is insensitive to the plates' shape for the same  $A/A_b$  ratios.

### 5.1.2 Test Series 2

These tests focused on  $A/A_b$  ratios from 1.5 to 6. The objective of these tests was to give a better understanding of the UBS of plain specimens in the range in which most of the AASHTO specimens are tested. Failure modes were very similar to Test Series 1. However, for  $A/A_b$  ratios less than 4, general crushing of the contact area (Fig. 5.5) and a more profuse cracking on the face of the specimens was observed (Fig. 5.6). This is in very good agreement with the tensile stress distribution for the same  $A/A_b$  ratios in the finite element analysis where high tensile stresses develop at the faces of the block. Table 5.2 shows the results from square and cylindrical blocks, tested to failure and loaded only thru square plates. For practical reasons a hexagonal plate was used for  $A/A_b=1.5$ , in the tests of cylinder blocks. Figures 5.7 and 5.8 show the failure mode of this particular set.



Fig. 5.5 Cylinder Block at Failure  $A/A_b=2$



Fig. 5.6 Square Block at Failure  $A/A_b=3$



Fig. 5.7 Failure of Cylinder Block with  $A/A_b=1.5$  (Hexagonal Plate).



Fig.5.8 Typical Failure Pyramid from Cylinder in Fig. 5.7.

Table 5.2 Results for Test Series 2.

Specimens	A (in <sup>2</sup> )	A <sub>b</sub> (in <sup>2</sup> )	A/A <sub>b</sub>	P <sub>u</sub> (lbs)	f <sub>b</sub> (psi)	f <sub>c</sub> (psi)	f <sub>b</sub> /f <sub>c</sub>
SS-1.5-1,2	64.00	42.67	1.5	163,670	3,840	4,500	0.85
SS-2-1,2,3	64.00	32.00	2.0	161,500	5,050	4,500	1.12
SS-2.5-1,2	64.00	25.60	2.5	135,000	5,270	4,500	1.17
SS-3-1,2	64.00	21.33	3.0	119,500	5,600	4,500	1.25
SS-4-1,2	64.00	16.00	4.0	104,750	6,550	4,500	1.46
SS-6-1,2	64.00	10.67	6.0	84,500	7,920	4,500	1.76
SC-1.5-1,2	28.27	18.85	1.5	82,100	4,360	4,650	0.94
SC-2-1,2,3	28.27	14.14	2.0	67,740	4,790	4,650	1.03
SC-2.5-1,2	28.27	11.31	2.5	65,050	5,750	4,650	1.24
SC-3-1,2	28.27	9.42	3.0	51,900	5,510	4,650	1.18
SC-4-1,2	28.27	7.07	4.0	48,750	6,900	4,650	1.48
SC-6-1,2	28.27	4.71	6.0	40,420	8,580	4,650	1.84

The values of  $f'_b/f'_c$  presented in Table 5.2 are plotted against the  $A/A_b$  ratios in Fig. 5.9. This figure also shows a comparison of the results with the ACI 318-02 recommendations for bearing and the limit established by the Code.

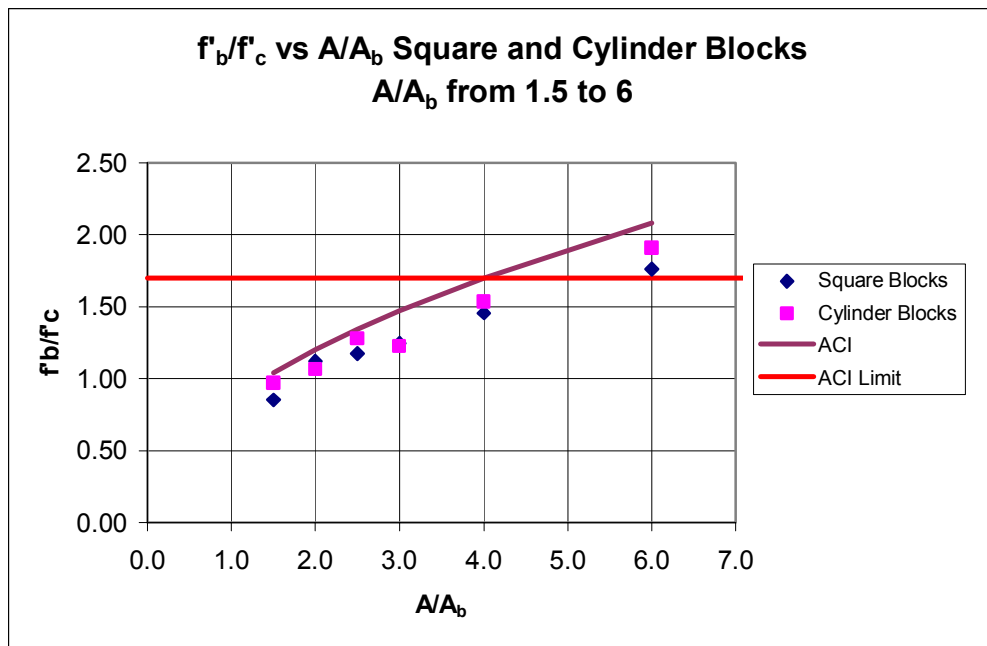


Fig. 5.9 Plot of  $f'_b/f'_c$  vs.  $A/A_b$  Test Series 2.

The results obtained for square and cylinder blocks are very similar for a variation of the  $A/A_b$  ratio between 1.5 and 6. As shown in Fig. 5.9, the ACI equation overestimates the ultimate bearing strength for these specimens and therefore is considered to be unconservative.

### 5.1.3 Test Series 3

This series focused on the investigation of the influence of the aspect ratio (length/width), on the UBS. All the specimens tested were 6 in. by 12 in. cylinders. A constant  $A/A_b=3$  was used in all the tests. Figures 5.10 and 5.11 show failure modes for aspect ratios of 3 and 1 respectively. Table 5.3 shows the results of all the tests in this series. A plot of the normalized bearing strength  $f'_b/f'_c$  vs. the aspect ratio ( $AR$ ) is shown in Fig. 5.12.



Fig. 5.10 Failure of Cylinder Block with Aspect Ratio = 3.



Fig. 5.11 Failure of cylinder block with aspect ratio = 1.

Table 5.3 Results from Test Series 3 (Aspect Ratio)

Specimen	Height (in.)	Width (in.)	Aspect Ratio (L/h)	$P_u$ (kips)	$f_b$ (ksi)	$f_c$ (ksi)	$f_b/f_c$
AR-0.5-1	3.00	6.00	0.50	16,310	1,730	4,140	0.42
AR-0.5-2	3.00	6.00	0.50	18,540	1,970	4,140	0.48
AR-0.66-1	4.00	6.00	0.66	38,390	4,070	4,140	0.98
AR-0.66-2	4.00	6.00	0.66	40,030	4,250	4,140	1.03
AR-1-1	6.00	6.00	1.00	38,680	4,100	4,140	0.99
AR-1-2	6.00	6.00	1.00	43,660	4,630	4,140	1.12
AR-1.33-1	8.00	6.00	1.33	47,280	5,020	4,140	1.21
AR-1.33-2	8.00	6.00	1.33	48,970	5,200	4,140	1.26
AR-1.5-1	9.00	6.00	1.50	49,750	5,280	4,140	1.28
AR-1.5-2	9.00	6.00	1.50	48,790	5,180	4,140	1.25
AR-2-1	12.00	6.00	2.00	47,790	5,070	4,140	1.23
AR-2-2	12.00	6.00	2.00	49,090	5,210	4,140	1.26
AR-3-1	18.00	6.00	3.00	52,140	5,530	4,140	1.34
AR-3-2	18.00	6.00	3.00	50,480	5,360	4,140	1.29

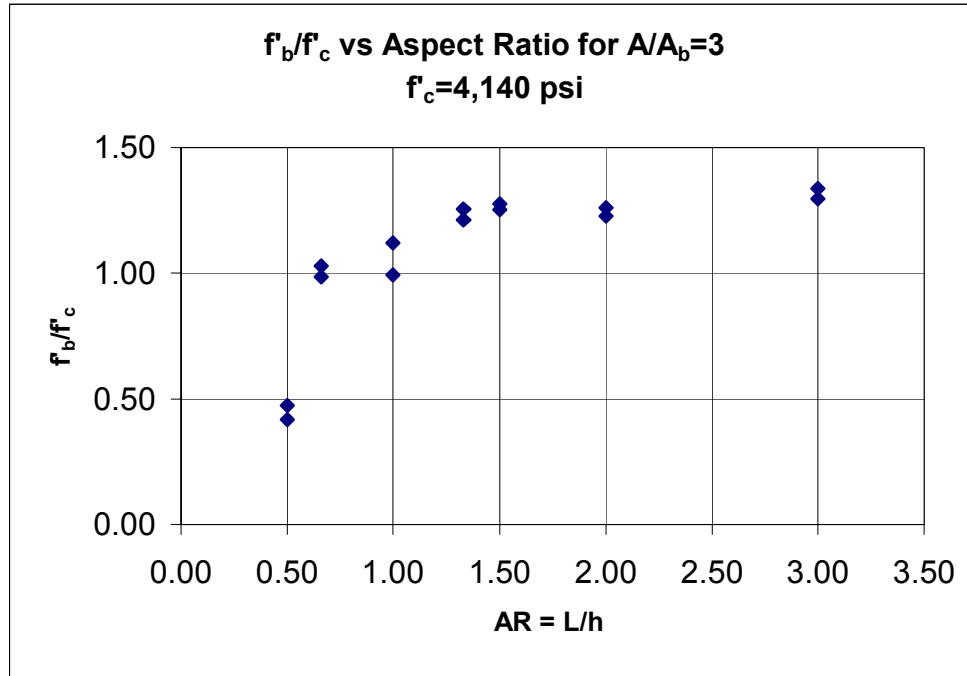


Fig. 5.12. Plot of  $f'_b/f'_c$  vs.  $AR$  for  $A/A_b=3$ , Cylinder Blocks.

Observing Fig. 5.12, it can be stated that for aspect ratios equal to or greater than 1.5 the UBS remains almost constant. Results for  $AR$  values less than 1.5 showed a reduction of the UBS as the aspect ratio decreases. Results obtained in experiments by Niyogi (1973) show a high variability of the results in the region  $AR < 1.5$ , depending mostly on the  $A/A_b$  ratio. However, the same results are obtained for  $AR > 1.5$ . In our case the support condition of the bottom of the specimen, resting on a thick compressible bearing pad could allow some bending of the specimen for  $AR < 1$ . In view of these results the use of an aspect ratio of 2 in the regular AASHTO load transfer test is highly justified.

#### 5.1.4 Test Series 4

In this test series lightweight concrete 6 in. by 12 in. cylinders were tested in the  $A/A_b$  range from 1.5 to 16. Various plate types were used, a hexagonal plate for  $A/A_b=1.5$ , square plates from 2 to 6 and round plates from 8 to 16. Lightweight specimens' modes of failure were quite similar to those of the normal weight concrete. For  $A/A_b > 4$  the failure was characterized by the formation of the typical cone under the bearing plate and the splitting of the cylinder into three similar portions (Fig. 5.13). It is likely to happen that if the specimen is capable to

fail in this mode the ultimate load reached is higher than the one obtained when the specimen fails with a different failure plane configuration. On the other hand, for small ratios ( $<4$ ), the crushing of the concrete in the contact area and a more erratic splitting of the specimen was the most likely to occur (Fig. 5.14). Table 5.4 shows the results for this test series. The normalized  $f'_b/f'_c$  is the average of at least two similar tests. A plot of the normalized bearing strength  $f'_b/f'_c$  vs. the  $A/A_b$  ratios is shown in Fig. 5.15.

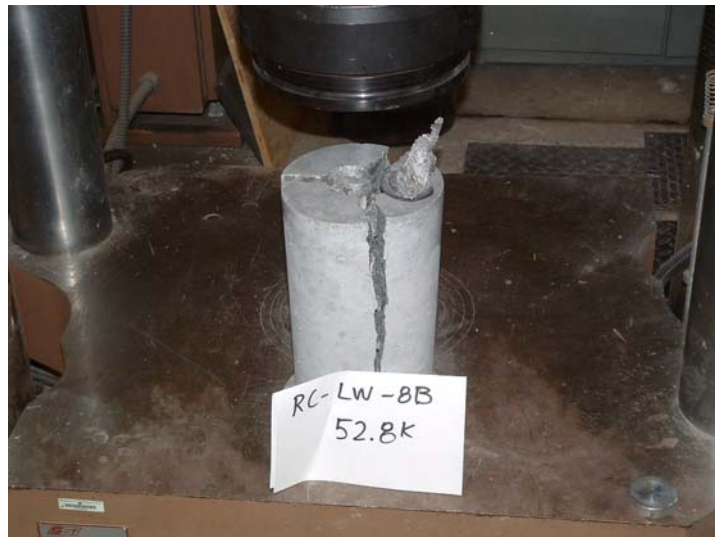


Fig. 5.13 Failure of Cylinder Block with  $A/A_b = 8$  (Round Plate).



Fig. 5.14 Failure of Cylinder Block with  $A/A_b = 2$  (Square Plate).

Table 5.4 Lightweight Concrete Cylinder Blocks (Series 4)

Specimens	A (in <sup>2</sup> )	A <sub>b</sub> (in <sup>2</sup> )	A/A <sub>b</sub>	P <sub>u</sub> (lbs)	f <sub>b</sub> (psi)	f <sub>c</sub> (psi)	f <sub>b</sub> /f <sub>c</sub>
SC-LW-1.5-1, 2	28.27	18.85	1.5	116,640	6,190	7,760	0.80
SC-LW-2-1, 2	28.27	14.14	2.0	97,230	6,880	7,760	0.89
SC-LW-2.5-1, 2,3	28.27	11.31	2.5	75,680	6,690	7,760	0.86
SC-LW-3-1, 2,3	28.27	9.42	3.0	66,530	7,060	7,760	0.91
SC-LW-4-1, 2	28.27	7.07	4.0	65,550	9,280	7,760	1.20
SC-LW-6-1, 2	28.27	4.71	6.0	57,840	12,280	7,760	1.58
RC-LW-8-1, 2	28.27	3.53	8.0	51,760	14,650	7,760	1.89
RC-LW-12-1, 2	28.27	2.36	12.0	40,260	17,090	7,760	2.20
RC-LW-16-1, 2	28.27	1.77	16.0	37,050	20,970	7,760	2.70

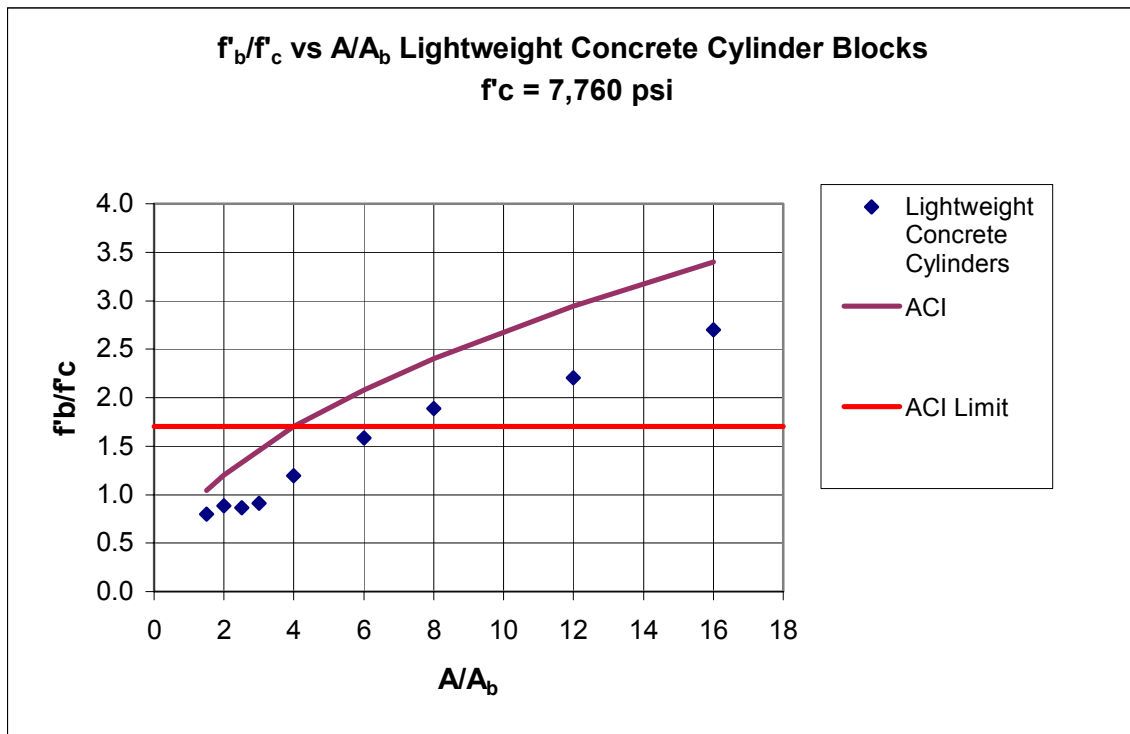


Fig. 5.15 Plot of  $f_b/f_c$  vs.  $A/A_b$  Lightweight Concrete Specimens (Test Series 4).

Figure 5.15 shows a high discrepancy between the UBS obtained by the ACI equation and the UBS reached in the tests of lightweight concrete specimens. This difference is evident even for very small  $A/A_b$  ratios (less than 4), where the tests on normal weight concrete showed a better agreement.

### 5.1.5 Test Series 5 and 6

The objective of this series was to evaluate the UBS in high strength concrete specimens. All specimens were 6 in. by 12 in. cylinders loaded with various plate shapes and a range of  $A/A_b$  ratios between 1.5 and 16. The plate shapes used were a hexagonal plate for  $A/A_b=1.5$ , square plates from 2 to 6 and round plates from 8 to 16.

Failure modes for all specimens in this series were very similar to those previously discussed for tests series 1 to 4. Typical failures for concrete strengths of 7,710 psi and 10,950 psi are shown in Figs. 5.16 and 5.17 respectively. Table 5.5 shows the results obtained in Series 5 and 6. The normalized  $f'_b/f'_c$  is the average of at least two similar tests, except for the  $A/A_b=2.5$  set in Series 6 ( $f'_c=10,950$  psi). A plot of the normalized bearing strength  $f'_b/f'_c$  vs. the  $A/A_b$  ratios is shown in Fig. 5.18.



Fig. 5.16 Failure of Cylinder Block with  $A/A_b=16$  (Round Plate).



Fig. 5.17 Failure of Cylinder Block with  $A/A_b = 1.5$  (Hex Plate).

Table 5.5 High Strength Concrete Cylinder Blocks (Series 5 and 6).

Specimens	A (in <sup>2</sup> )	A <sub>b</sub> (in <sup>2</sup> )	A/A <sub>b</sub>	P <sub>u</sub> (lbs)	f <sub>b</sub> (psi)	f <sub>c</sub> (psi)	f <sub>b</sub> /f <sub>c</sub>
SC-8-1.5A, B	28.27	18.85	1.5	117,000	6,208	7,710	0.81
SC-8-2A, B	28.27	14.14	2.0	109,500	7,747	7,710	1.00
SC-8-2.5A, B	28.27	11.31	2.5	92,750	8,202	7,710	1.06
SC-8-3A, B	28.27	9.42	3.0	84,500	8,967	7,710	1.16
SC-8-4A, B	28.27	7.07	4.0	64,000	9,056	7,710	1.17
SC-8-6A, B	28.27	4.71	6.0	58,500	12,416	7,710	1.61
RC-8-8A, B	28.27	3.53	8.0	47,250	13,371	7,710	1.73
RC-8-12A, B	28.27	2.36	12.0	41,750	17,722	7,710	2.30
RC-8-16A, B	28.27	1.77	16.0	38,250	21,648	7,710	2.81
HEXC-12-1.5A, B	28.27	18.85	1.5	160,505	8,516	10,948	0.78
SC-12-2A, B	28.27	14.14	2.0	125,475	8,877	10,948	0.81
SC-12-2.5A, B	28.27	11.31	2.5	110,050	9,732	10,948	0.89
SC-12-3A, B	28.27	9.42	3.0	103,980	11,034	10,948	1.01
SC-12-4A, B	28.27	7.07	4.0	87,587	12,393	10,948	1.13
SC-12-6A, B	28.27	4.71	6.0	81,514	17,300	10,948	1.58
RC-12-8A, B	28.27	3.53	8.0	68,918	19,503	10,948	1.78
RC-12-16A, B	28.27	1.77	16.0	43,218	24,460	10,948	2.23

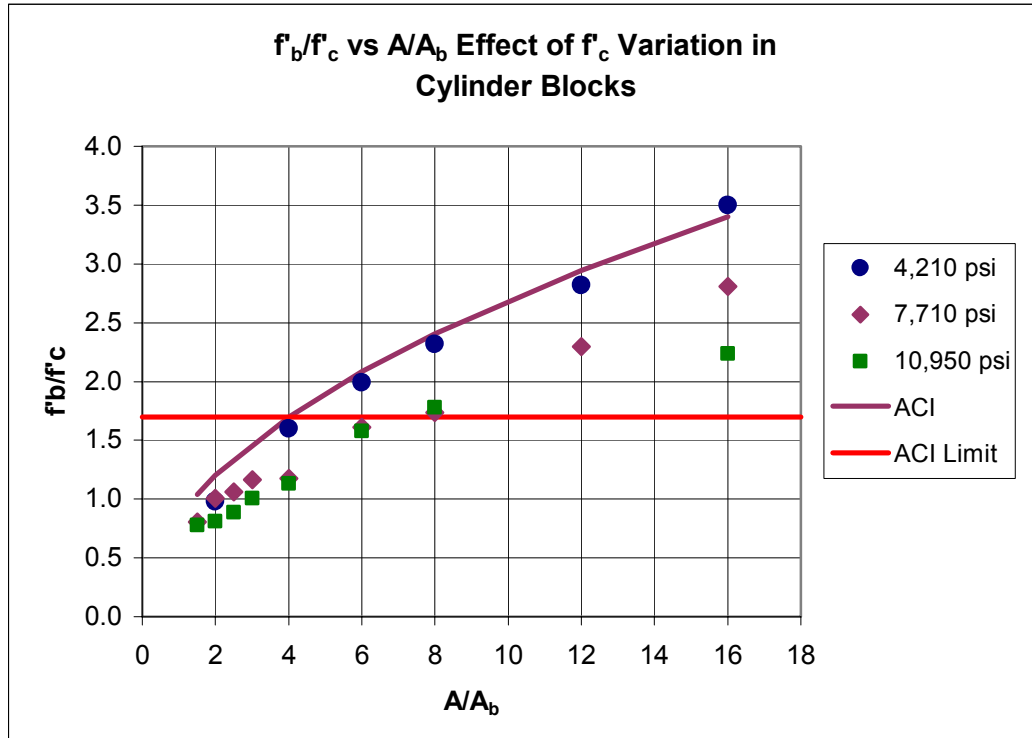


Fig. 5.18 Plot of  $f'_b/f'_c$  vs.  $A/A_b$  High Strength Concrete Specimens (Test Series 5 and 6).

In Fig. 5.18, test data from Series 1 is combined with Series 5 and 6 to illustrate the effect of a variation on the ultimate compressive stress ( $f'_c$ ) on the ultimate bearing stress. According to these results, an increase in  $f'_c$  produces a decrease in the normalized ultimate bearing stress  $f'_b/f'_c$ . The reduction of the normalized UBS is greater for  $A/A_b$  ratios  $> 6$ . This reduction is very accentuated between the 4,210 psi and 7,710 psi strengths, but milder between 7,710 psi and 10,950 psi. In the latter case the reduction was very slight up to an  $A/A_b$  ratio of 8. All these findings are in good agreement with the investigation by Niyogi (1973). Also in Fig. 5.18 it can be seen that the ACI equation overestimates the UBS for the high strength concrete specimens.

### 5.1.6 Test series 7

The objective of these tests was to understand the change in the UBS with a change in the duct size. The tests were performed on 6 in. by 12 in. cylinders and the duct size varied from 0 to 3.375 in. A constant plate size of 4.5 in. in diameter was used. For the majority of the

specimens the failure consisted of the spalling of the concrete all around the cylinder while the center of the specimen, within the perimeter of the duct remained almost intact (Fig. 5.19). The exceptions to this failure mode were the specimens with the greatest duct size ( $d=3.375$  in.). The failure of these occurred with the splitting of the specimens into three almost identical parts (Fig. 5.20).



Fig. 5.19 Failure of Cylinder Block with Duct Size of 2.375 in.

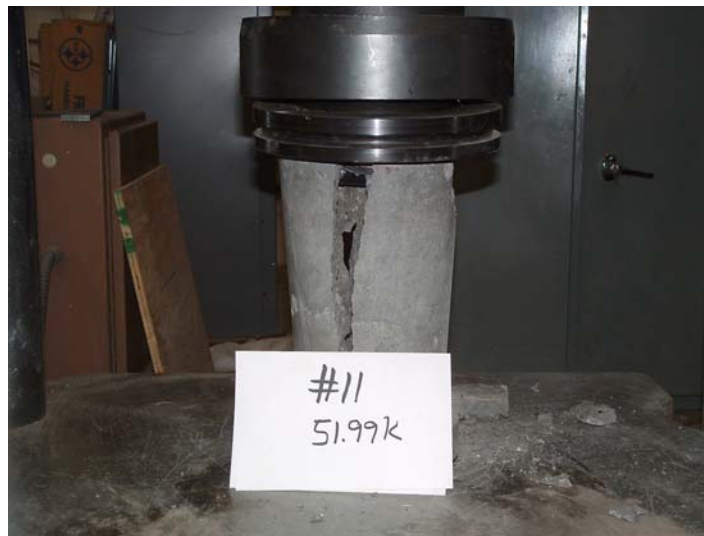


Fig. 5.20 Failure of Cylinder Block with Duct Size of 3.375 in.

Table 5.6 shows the results for the different duct sizes used in this series. Two tests on specimens without ducts were performed to provide a reference point for the rest of the

series. The normalized ultimate bearing stress  $f'_b/f'_c$  is shown in the last column. The net bearing area  $A_{bnet}$  was used to compute  $f'_b$ . Figure 5.21 shows the plot of  $f'_b/f'_c$  against the ratio  $A_{bnet}/A_b$ .

The development of Equation 4.7 was based on the average compressive stress at failure ( $P/A$ ), this is a uniform stress distribution at the base of the specimens, The value of the average compressive stress at failure for the specimens without ducts ( $f_{co} = P/A$ ) is very useful to normalize the average compressive stress of the specimens with ducts ( $f_c = P/A_{net}$ ) and check the validity of Equation 4.7 for these specimens. For this purpose, the values of the normalized average compressive stress  $f_c/f_{co}$  are tabulated in Table 5.7 and plotted against the ratio of the net area over the gross area ( $A_{net}/A$ ) in Fig. 5.22.

Table 5.6 Effect of Duct Size in Plain Concrete Specimens (Series 7).

Specimens	$A_b$ (in <sup>2</sup> )	Duct Size (in.)	$A_{bnet}$ (in <sup>2</sup> )	$A_b/A_{bnet}$	$P_u$ (lbs)	$f'_b$ (psi)	$f'_c$ (psi)	$f'_b/f'_c$
1	15.90	0.00	15.90	1.00	112,770	7,090	6,720	1.06
2	15.90	0.00	15.90	1.00	107,560	6,770	6,720	1.01
3	15.90	0.94	15.21	0.96	88,030	5,790	6,720	0.86
4	15.90	0.94	15.21	0.96	99,620	6,550	6,720	0.98
5	15.90	1.44	14.27	0.90	83,620	5,860	6,720	0.87
6	15.90	1.44	14.27	0.90	98,440	6,900	6,720	1.03
7	15.90	2.00	12.76	0.80	82,010	6,430	6,720	0.96
8	15.90	2.00	12.76	0.80	105,800	8,290	6,720	1.24
9	15.90	2.38	11.47	0.72	67,560	5,890	6,720	0.88
10	15.90	2.38	11.47	0.72	78,460	6,840	6,720	1.02
11	15.90	3.38	6.95	0.44	51,990	7,480	6,720	1.11
12	15.90	3.38	6.95	0.44	37,920	5,450	6,720	0.81

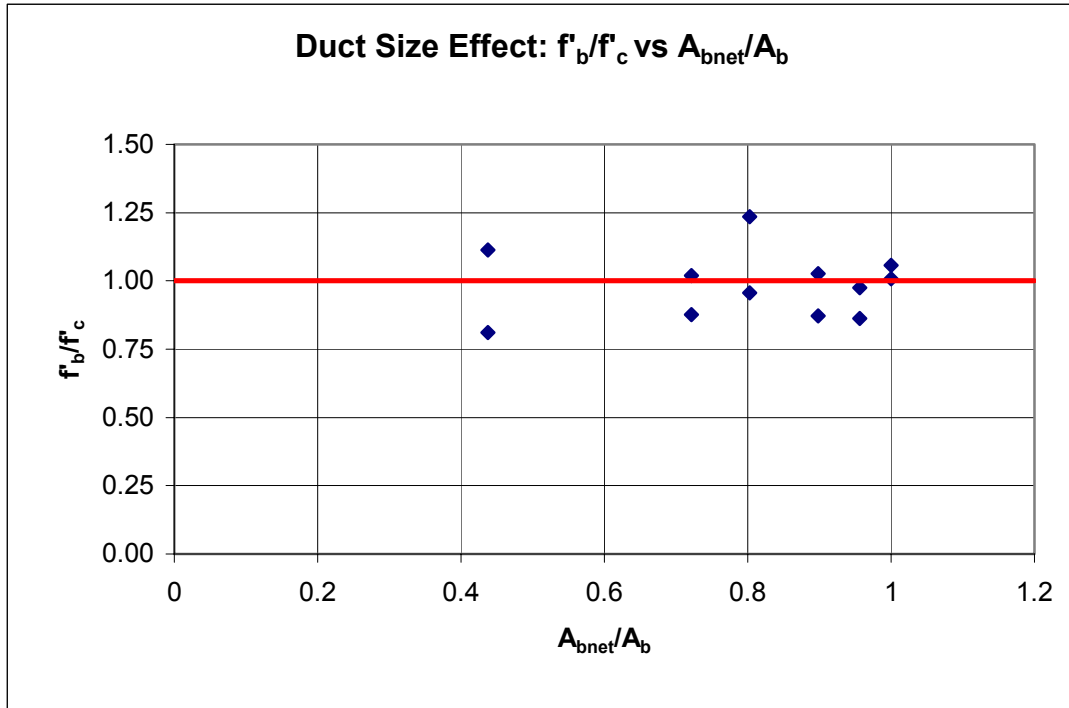


Fig. 5.21 Effect of the Duct Size on the Ultimate Bearing Stress.

Table 5.7 Effect of Duct Size on the Average Compressive Stress.

Specimens	A (in <sup>2</sup> )	Duct Size (in.)	A <sub>net</sub> (in <sup>2</sup> )	A/A <sub>net</sub>	P <sub>u</sub> (lbs)	f <sub>c</sub> (psi)	f <sub>co</sub> (psi)	f <sub>c</sub> /f <sub>co</sub>
1	28.27	0.00	28.27	1.00	112,770	3,990	3,900	1.02
2	28.27	0.00	28.27	1.00	107,560	3,810	3,900	0.98
3	28.27	0.94	27.58	0.98	88,030	3,190	3,900	0.82
4	28.27	0.94	27.58	0.98	99,620	3,610	3,900	0.93
5	28.27	1.44	26.65	0.94	83,620	3,140	3,900	0.81
6	28.27	1.44	26.65	0.94	98,440	3,690	3,900	0.95
7	28.27	2.00	25.13	0.89	82,010	3,260	3,900	0.84
8	28.27	2.00	25.13	0.89	105,800	4,210	3,900	1.08
9	28.27	2.38	23.84	0.84	67,560	2,830	3,900	0.73
10	28.27	2.38	23.84	0.84	78,460	3,290	3,900	0.84
11	28.27	3.38	19.33	0.68	51,990	2,690	3,900	0.69
12	28.27	3.38	19.33	0.68	37,920	1,960	3,900	0.50

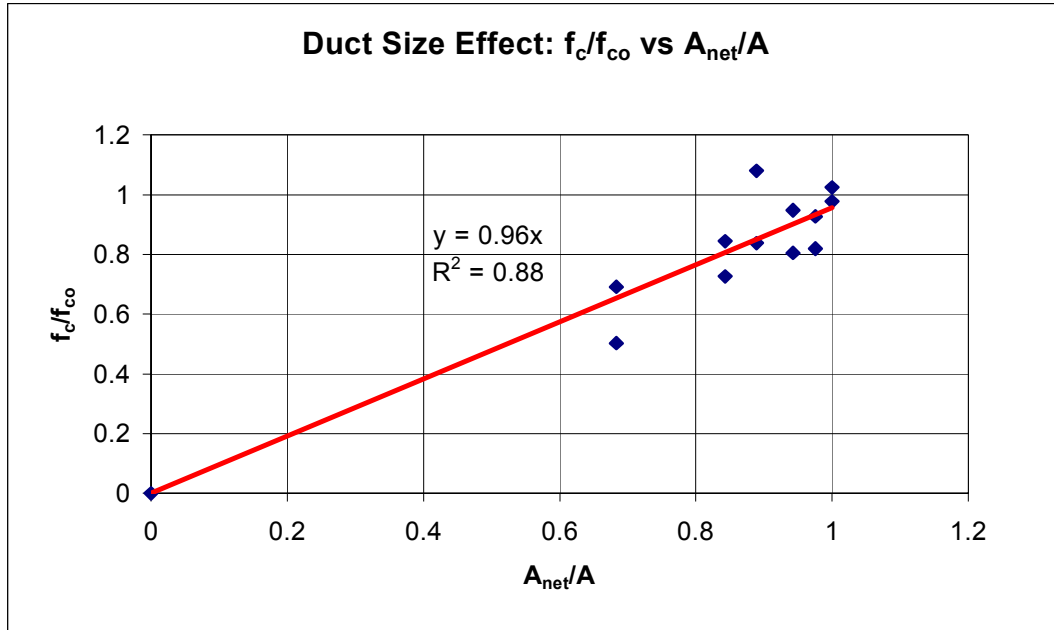


Fig. 5.22. Effect of the Duct Size on the Average Compressive Stress.

According to the values plotted in Fig. 5.21, the ultimate bearing stress of the specimens seems to be unaffected by the duct size. These results are in good agreement with the findings of Zielinski and Rowe (1960) in square prism specimens. A reasonable linear correlation exists between the ratios  $f_c/f_{co}$  and  $A_{net}/A$ . Under ideal conditions the slope of the line in Fig. 5.22 equals 1. Therefore, when determining the ultimate bearing stress in specimens with ducts, using Equation 4.7, the net area ( $A_{net}$ ) must be use in lieu of the gross area ( $A$ ).

### 5.1.7 Prediction of the UBS of Plain Concrete Specimens Using Equation Based on the Mohr Criterion (Equation 4.7)

Equation 4.7 (see below) is evaluated using the data from the specimens in Test Series 1, 2, 4, 5 and 6. Table 5.8 shows a typical worksheet for calculating the ultimate bearing strength. The table contains test values for the square blocks loaded with square plates in Series 1. In the last column of the table, the ratio of the failure load obtained in the actual test ( $P_{test}$ ) over the predicted failure load ( $P_{pred}$ ) is presented to show the performance of the equation.

$$P = \frac{A f_c}{m\beta + \alpha} \quad (\text{See Chapter 4 for } m, \beta \text{ and } \alpha \text{ values}) \quad (\text{Eq. 4.7})$$

Table 5.8. Prediction of UBS using Equation 4.7 (SS-Specimens, Series 1).

Plate (b, in.)	Block (h, in.)	$f_c$ (psi)	$f_t$ (psi)	A (in <sup>2</sup> )	b/h	$\beta$	y	(h-b)/2	$\alpha$	$P_{test}$ (lbs.)	$P_{pred}$ (lbs.)	$P_{test}/P_{pred}$
5.66	8.00	4,080	483	64	0.71	0.14	3.72	1.17	1.00	145,000	120,858	1.20
5.66	8.00	4,080	483	64	0.71	0.14	3.72	1.17	1.00	140,000	120,858	1.16
4.00	8.00	4,080	483	64	0.50	0.24	3.55	2.00	1.00	96,500	87,496	1.10
4.00	8.00	4,080	483	64	0.50	0.24	3.55	2.00	1.00	90,000	87,496	1.03
3.27	8.00	4,080	483	64	0.41	0.29	3.25	2.37	1.00	77,500	76,367	1.01
3.27	8.00	4,080	483	64	0.41	0.29	3.25	2.37	1.00	70,000	76,367	0.92
2.83	8.00	4,360	503	64	0.35	0.33	3.03	2.59	1.00	65,000	71,867	0.90
2.83	8.00	4,360	503	64	0.35	0.33	3.03	2.59	1.00	65,000	71,867	0.90
2.31	8.00	4,360	503	64	0.29	0.41	2.72	2.85	1.06	57,000	60,447	0.94
2.31	8.00	4,360	503	64	0.29	0.41	2.72	2.85	1.06	55,000	60,447	0.91
2.00	8.00	4,360	503	64	0.25	0.48	2.51	3.00	1.30	48,000	51,457	0.93
2.00	8.00	4,360	503	64	0.25	0.48	2.51	3.00	1.30	51,000	51,457	0.99
											Avg	1.00
											Sdev	0.10
											Coev	0.10

For this particular data set the average  $P_{test}/P_{pred}$  is 1.00 and the standard deviation 0.10 for a coefficient of variation of 0.10. For all the plain concrete specimens the average  $P_{test}/P_{pred}$  is 1.05 and the coefficient of variation is 0.09 (Fig 5.23).

Tables 5.9, 5.10 and 5.11 present a comparison of the prediction of the failure load for the bearing tests in series 1, 4 and 6 using equation 4.7, the ACI equation and the proposed expressions by Niyogi (1973) and Hawkins (1968) (see Chapter 2).

Table 5.9 Comparison of Equation 4.7 for Normal Weight Concrete

Normal Weight Concrete		Predicted Failure Loads				$P_{test}/P_{pred}$				
Specimen	Failure Load	Niyogi	Hawkins	ACI	Equation 4.7	Niyogi	Hawkins	ACI	Equation 4.7	
SS-4-2A	145,000	125,074	173,004	157,059	122,434	1.16	0.84	0.92	1.18	
SS-4-2B	140,000	125,074	173,004	157,059	122,434	1.12	0.81	0.89	1.14	
SS-4-4A	96,500	94,726	116,447	111,058	88,372	1.02	0.83	0.87	1.09	
SS-4-4B	90,000	94,726	116,447	111,058	88,372	0.95	0.77	0.81	1.02	
SS-4-6A	77,500	79,435	92,917	90,650	76,126	0.98	0.83	0.85	1.02	
SS-4-6B	70,000	79,435	92,917	90,650	76,126	0.88	0.75	0.77	0.92	
SS-4-8A	65,000	74,734	83,118	83,780	71,590	0.87	0.78	0.78	0.91	
SS-4-8B	65,000	74,734	83,118	83,780	71,590	0.87	0.78	0.78	0.91	
SS-4-12A	57,000	62,241	66,600	68,406	60,158	0.92	0.86	0.83	0.95	
SS-4-12B	55,000	62,241	66,600	68,406	60,158	0.88	0.83	0.80	0.91	
SS-4-16A	48,000	54,537	57,024	59,242	51,186	0.88	0.84	0.81	0.94	
SS-4-16B	51,000	54,537	57,024	59,242	51,186	0.94	0.89	0.86	1.00	
RS-4-2A	137,500	133,529	183,133	167,561	128,851	1.03	0.75	0.82	1.07	
RS-4-2B	135,000	133,529	183,133	167,561	128,851	1.01	0.74	0.81	1.05	
RS-4-4A	105,000	101,059	122,496	118,483	92,780	1.04	0.86	0.89	1.13	
RS-4-4B	97,500	101,059	122,496	118,483	92,780	0.96	0.80	0.82	1.05	
RS-4-6A	74,000	84,893	97,452	96,711	79,742	0.87	0.76	0.77	0.93	
RS-4-6B	81,000	84,893	97,452	96,711	79,742	0.95	0.83	0.84	1.02	
RS-4-8A	61,000	74,780	83,118	83,780	71,559	0.82	0.73	0.73	0.85	
RS-4-8B	67,500	74,780	83,118	83,780	71,559	0.90	0.81	0.81	0.94	
RS-4-12A	59,000	62,258	66,600	68,406	60,978	0.95	0.89	0.86	0.97	
RS-4-12B	61,000	62,258	66,600	68,406	60,978	0.98	0.92	0.89	1.00	
RS-4-16B	49,000	54,537	57,024	59,242	52,053	0.90	0.86	0.83	0.94	
RS-4-16B	57,000	54,537	57,024	59,242	52,053	1.05	1.00	0.96	1.10	
						Avg	0.95	0.82	0.83	1.00
						Sdev	0.08	0.06	0.05	0.09
						Coev	0.09	0.08	0.06	0.09

Table 5.10 Comparison of Equation 4.7 for Lightweight Concrete

Lightweight Concrete		Predicted Failure Loads				$P_{test}/P_{pred}$			
Specimens	Failure Load	Niyogi	Hawkins	ACI	Equation 4.7	Niyogi	Hawkins	ACI	Equation 4.7
SC-LW-1.5-1	114,730	116,707	164,851	152,197	111,914	0.98	0.70	0.75	1.03
SC-LW-1.5-2	118,540	116,707	164,851	152,197	111,914	1.02	0.72	0.78	1.06
SC-LW-2-1	103,340	104,973	135,432	131,806	85,872	0.98	0.76	0.78	1.20
SC-LW-2-2	91,123	104,973	135,432	131,806	85,872	0.87	0.67	0.69	1.06
SC-LW-2.5-1	78,141	96,272	116,658	117,891	74,104	0.81	0.67	0.66	1.05
SC-LW-2.5-2	67,789	96,272	116,658	117,891	74,104	0.70	0.58	0.58	0.91
SC-LW-2.5-3	81,123	96,272	116,658	117,891	74,104	0.84	0.70	0.69	1.09
SC-LW-3-1	69,458	89,489	103,478	107,619	67,296	0.78	0.67	0.65	1.03
SC-LW-3-2	72,998	89,489	103,478	107,619	67,296	0.82	0.71	0.68	1.08
SC-LW-3-3	57,142	89,489	103,478	107,619	67,296	0.64	0.55	0.53	0.85
SC-LW-4-1	62,446	79,450	85,948	93,201	59,609	0.79	0.73	0.67	1.05
SC-LW-4-2	68,655	79,450	85,948	93,201	59,609	0.86	0.80	0.74	1.15
SC-LW-6-1	55,558	66,760	66,625	76,098	50,771	0.83	0.83	0.73	1.09
SC-LW-6-2	60,122	66,760	66,625	76,098	50,771	0.90	0.90	0.79	1.18
SC-LW-8-1	52,843	58,823	55,866	65,903	45,203	0.90	0.95	0.80	1.17
SC-LW-8-2	50,672	58,823	55,866	65,903	45,203	0.86	0.91	0.77	1.12
SC-LW-12-1	39,271	48,973	43,839	53,810	37,858	0.80	0.90	0.73	1.04
SC-LW-12-2	41,238	48,973	43,839	53,810	37,858	0.84	0.94	0.77	1.09
SC-LW-16-1	35,763	42,900	37,049	46,601	32,546	0.83	0.97	0.77	1.10
SC-LW-16-2	38,321	42,900	37,049	46,601	32,546	0.89	1.03	0.82	1.18
Avg						0.85	0.78	0.72	1.08
Sdev						0.09	0.14	0.08	0.09
Coev						0.11	0.17	0.11	0.08

Table 5.11 Comparison of Equation 4.7 for High Strength Concrete

High Strength Concrete		Predicted Failure Loads				P <sub>test</sub> /P <sub>pred</sub>			
Specimens	Failure Load	Niyogi	Hawkins	ACI	Equation 4.7	Niyogi	Hawkins	ACI	Equation 4.7
HEXC-12-1.5-1	159,240	164,717	228,499	214,806	155,638	0.97	0.70	0.74	1.02
HEXC-12-1.5-2	161,770	164,717	228,499	214,806	155,638	0.98	0.71	0.75	1.04
SC-12-2-1	122,800	148,156	185,386	186,027	119,985	0.83	0.66	0.66	1.02
SC-12-2-2	128,150	148,156	185,386	186,027	119,985	0.86	0.69	0.69	1.07
SC-12-2.5-1	110,050	135,875	158,184	166,388	103,764	0.81	0.70	0.66	1.06
SC-12-3-1	106,040	126,302	139,260	151,891	94,348	0.84	0.76	0.70	1.12
SC-12-3-2	101,920	126,302	139,260	151,891	94,348	0.81	0.73	0.67	1.08
SC-12-4-1	91,169	112,134	114,353	131,541	84,267	0.81	0.80	0.69	1.08
SC-12-4-2	84,004	112,134	114,353	131,541	84,267	0.75	0.73	0.64	1.00
SC-12-6-1	82,130	94,223	87,315	107,403	72,085	0.87	0.94	0.76	1.14
SC-12-6-2	80,898	94,223	87,315	107,403	72,085	0.86	0.93	0.75	1.12
RC-12-8-1	67,200	83,021	72,492	93,014	64,193	0.81	0.93	0.72	1.05
RC-12-8-2	70,636	83,021	72,492	93,014	64,193	0.85	0.97	0.76	1.10
RC-12-16-1	48,114	60,548	47,076	65,771	46,226	0.79	1.02	0.73	1.04
RC-12-16-2	38,321	60,548	47,076	65,771	46,226	0.63	0.81	0.58	0.83
Avg						0.83	0.81	0.70	1.05
Sdev						0.08	0.12	0.05	0.07
Coev						0.10	0.15	0.07	0.07

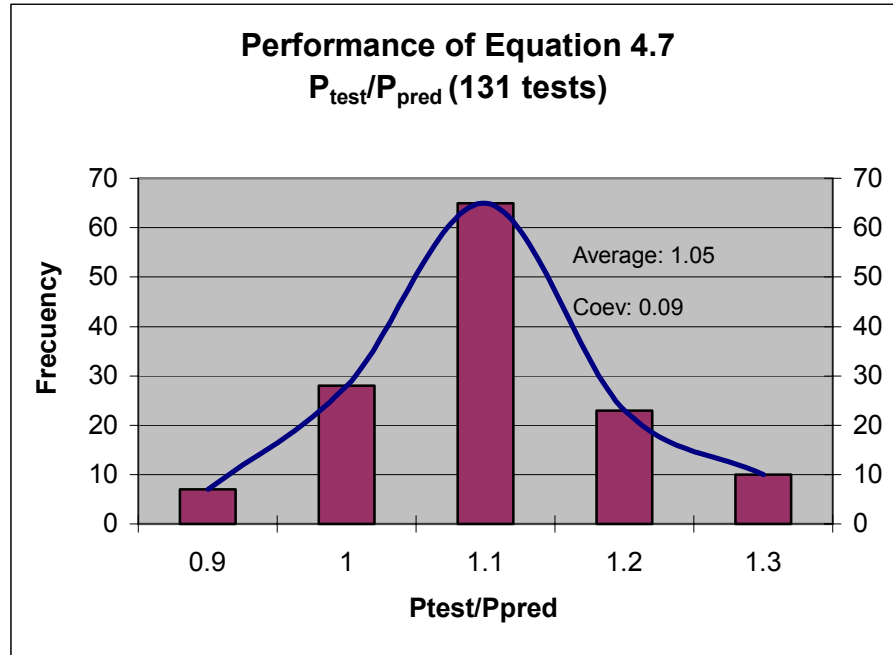


Fig. 5.23 Performance of Equation 4.7.

The comparisons in Tables 5.9, 5.10 and 5.11 show that the ACI, Niyogi and Hawkins expressions in general overestimate the ultimate bearing strength for this data set. In the particular case of lightweight specimens these expressions give more inaccurate predictions. On the other hand, Equation 4.7 gives, for all tests series,  $P_{test}/P_{pred}$  values very close to 1.0 or higher. This means it gives accurate predictions for all types of mixes and is on the conservative side. Additionally, the low coefficient of variation (9 percent) and the quasi-normal distribution shown in Fig. 5.23 indicates a very low dispersion in the results obtained using this formula.

## 5.2 Reinforced Specimens

The objective of this series was to evaluate the enhancement in the bearing strength produced by the confining steel. The reinforcing ratio was varied in specimens reinforced with spirals, ties and a combination of spirals and ties. Forty- two specimens were tested to failure; the first six specimens were discarded from the data because of premature failure caused by uneven support at the bottom surface of the prisms. After these unacceptable failures, a thin layer of epoxy was applied to all the specimens. A square plate 4 in. wide, for a constant  $A/A_b=4$ , was used for the remaining 36 specimens tested.

In general two types of failures modes were observed. The first type and more common failure consisted of a total degradation of the general zone where the maximum bursting stresses occurred. In most cases spalling of the concrete and bulging of the specimen in that location were observed (Figs. 5.24 and 5.25). A permanent deformation (1/16 in. to 1/8 in.) of the concrete beneath the plate was also observed along with compatibility cracks caused by the concrete deformation surrounding the plate.

The second failure mode occurred below mid height of the prism; cracking and crushing of the concrete in the bottom of the specimens was the norm in this case while the general zone remained almost intact (Fig. 5.26). In one of the specimens (Fig. 5.27), after removing the loose concrete, a failure cone was found in the base of the specimen while the upper part of the specimen was almost intact. In another case a concrete pyramid was formed in the base of the prism. These failures indicate that the limit state of pure compression also has to be considered when designing the prisms for the AASHTO load transfer test.



Fig. 5.24 Typical Failure in the General Zone.



Fig. 5.25 Typical Failure in the General Zone Showing Plate Indentation.



Fig. 5.26 Failure in the Base of the Prism



Fig. 5.27 Failure Cone in Specimen Failed in the Base.

The results from the tests on reinforced specimens are presented in Tables 5.12a and 5.12b. In the last column of Table 5.12b the ratio between the ultimate load of the reinforced specimens ( $P_r$ ) obtained in the actual tests and the plain concrete ultimate load ( $P$ ) calculated by Equation 4.7 is presented to obtain a plot of the mechanical reinforcement ratio ( $\omega$ ) versus  $P_r/P$  (Fig.5.28).

Table 5.12a Data of Reinforced Specimens.

Specimen	Type of Reinforc.	Plate (b, in.)	Block (h, in.)	$f'_c$ (psi)	$f'_t$ (psi)	$f_y$ (psi)	$A_s$ Spiral (in <sup>2</sup> )	$A_s$ Ties (in <sup>2</sup> )	Spiral Diam.(in)	Spiral Pitch (in)	Tie Width (in)	Tie Spacing (in)
AR-1	spiral	4.00	8.00	6,350	701	69,800	0.11	0.00	6.75	2.50	6.63	0.00
DL-4	spiral	4.00	8.00	6,350	701	69,800	0.11	0.00	6.75	2.50	6.63	0.00
AR-2	spiral	4.00	8.00	6,150	678	69,800	0.11	0.00	6.75	2.50	6.63	0.00
DR-4	spiral	4.00	8.00	6,150	678	69,800	0.11	0.00	6.75	2.50	6.63	0.00
DL-3	spiral	4.00	8.00	6,460	713	69,800	0.11	0.00	6.75	2.00	6.63	0.00
DL-3	spiral	4.00	8.00	6,150	678	69,800	0.11	0.00	6.75	2.00	6.63	0.00
AR-4	spiral	4.00	8.00	6,460	713	69,800	0.11	0.00	6.75	1.88	6.63	0.00
AR-3	spiral	4.00	8.00	5,870	656	69,800	0.11	0.00	6.75	2.00	6.63	0.00
DR-3	spiral	4.00	8.00	5,870	656	69,800	0.11	0.00	6.75	2.00	6.63	0.00
AL-3	spiral	4.00	8.00	6,150	678	69,800	0.11	0.00	6.75	1.44	6.63	0.00
AL-1	spiral	4.00	8.00	5,870	656	69,800	0.11	0.00	6.75	1.50	6.63	0.00
DR-2	spiral	4.00	8.00	5,870	656	69,800	0.11	0.00	6.75	1.50	6.63	0.00
AL-4	spiral	4.00	8.00	6,150	678	69,800	0.11	0.00	6.75	1.38	6.63	0.00
DR-1	spiral	4.00	8.00	6,150	678	69,800	0.11	0.00	6.75	1.25	6.63	0.00
CL-2	ties	4.00	8.00	6,350	701	89,650	0.00	0.11	6.75	0.00	6.63	3.50
BL-2	ties	4.00	8.00	6,350	701	89,650	0.00	0.11	6.75	0.00	6.63	3.25
BL-3	ties	4.00	8.00	6,350	701	89,650	0.00	0.11	6.75	0.00	6.63	2.50
CL-3	ties	4.00	8.00	6,350	701	89,650	0.00	0.11	6.75	0.00	6.63	2.50
CR-3	ties	4.00	8.00	6,460	713	89,650	0.00	0.11	6.75	0.00	6.63	2.00
CL-4	ties	4.00	8.00	6,460	713	89,650	0.00	0.11	6.75	0.00	6.63	2.00
CR-2	ties	4.00	8.00	6,150	701	89,650	0.00	0.11	6.75	0.00	6.63	2.00
EL-4	ties	4.00	8.00	6,350	701	89,650	0.00	0.11	6.75	0.00	6.63	2.00
ER-6	ties	4.00	8.00	5,870	656	89,650	0.00	0.11	6.75	0.00	6.63	2.00
CR-1	ties	4.00	8.00	6,350	701	89,650	0.00	0.11	6.75	0.00	6.63	1.50
EL-2	ties	4.00	8.00	6,350	701	89,650	0.00	0.11	6.75	0.00	6.63	1.50
BL-4	ties	4.00	8.00	6,150	678	89,650	0.00	0.11	6.75	0.00	6.63	1.50
CL-1	ties	4.00	8.00	6,150	678	89,650	0.00	0.11	6.75	0.00	6.63	1.50
EL-3	ties	4.00	8.00	6,150	678	89,650	0.00	0.11	6.75	0.00	6.63	1.50
CR-4	spiral + ties	4.00	8.00	6,150	678	68,900	0.11	0.11	6.75	2.00	6.63	4.00
ER-1	spiral + ties	4.00	8.00	6,150	678	68,900	0.11	0.11	6.75	2.00	6.63	3.50
BR-4	spiral + ties	4.00	8.00	6,150	678	68,900	0.11	0.11	6.75	2.00	6.63	3.00
ER-4	spiral + ties	4.00	8.00	6,150	678	68,900	0.11	0.11	6.75	2.00	6.63	2.50
EL-6	spiral + ties	4.00	8.00	5,870	656	68,900	0.11	0.11	6.00	2.00	6.63	3.00
BR-1	spiral + ties	4.00	8.00	5,870	656	68,900	0.11	0.11	6.00	2.00	6.63	2.50
BR-3	spiral + ties	4.00	8.00	5,870	656	68,900	0.11	0.11	6.00	2.00	6.63	2.00
ER-3	spiral + ties	4.00	8.00	6,150	678	68,900	0.11	0.11	6.75	2.00	6.63	1.50

Table 5.12b Test Results of Reinforced Specimens

Specimen	Type of Reinforc.	$\omega$ (spiral)	$\omega$ (ties)	$\omega$ (total)	$P_r$ (reinf) (kips)	P(plain) (kips)	$P_r/P$
AR-1	spiral	0.29	0.00	0.29	262	131	2.00
DL-4	spiral	0.29	0.00	0.29	277	131	2.11
AR-2	spiral	0.30	0.00	0.30	243	127	1.91
DR-4	spiral	0.30	0.00	0.30	273	127	2.15
DL-3	spiral	0.35	0.00	0.35	287	134	2.15
DL-3	spiral	0.37	0.00	0.37	287	127	2.26
AR-4	spiral	0.38	0.00	0.38	257	134	1.93
AR-3	spiral	0.39	0.00	0.39	245	122	2.00
DR-3	spiral	0.39	0.00	0.39	325	122	2.66
AL-3	spiral	0.51	0.00	0.51	282	127	2.22
AL-1	spiral	0.52	0.00	0.52	298	122	2.44
DR-2	spiral	0.52	0.00	0.52	293	122	2.39
AL-4	spiral	0.54	0.00	0.54	308	127	2.43
DR-1	spiral	0.59	0.00	0.59	304	127	2.39
CL-2	ties	0.00	0.13	0.13	230	131	1.75
BL-2	ties	0.00	0.14	0.14	220	131	1.68
BL-3	ties	0.00	0.19	0.19	238	131	1.81
CL-3	ties	0.00	0.19	0.19	252	131	1.92
CR-3	ties	0.00	0.23	0.23	274	134	2.05
CL-4	ties	0.00	0.23	0.23	293	134	2.19
CR-2	ties	0.00	0.23	0.23	256	131	1.95
EL-4	ties	0.00	0.23	0.23	278	131	2.12
ER-6	ties	0.00	0.25	0.25	255	122	2.08
CR-1	ties	0.00	0.31	0.31	296	131	2.25
EL-2	ties	0.00	0.31	0.31	305	131	2.32
BL-4	ties	0.00	0.32	0.32	230	127	1.81
CL-1	ties	0.00	0.32	0.32	280	127	2.21
EL-3	ties	0.00	0.32	0.32	275	127	2.17
CR-4	spiral + ties	0.41	0.09	0.50	307	127	2.42
ER-1	spiral + ties	0.41	0.11	0.52	357	127	2.81
BR-4	spiral + ties	0.41	0.12	0.54	280	127	2.21
ER-4	spiral + ties	0.41	0.15	0.56	294	127	2.31
EL-6	spiral + ties	0.43	0.13	0.56	285	122	2.33
BR-1	spiral + ties	0.43	0.16	0.59	307	122	2.51
BR-3	spiral + ties	0.43	0.19	0.63	274	122	2.24
ER-3	spiral + ties	0.41	0.25	0.66	303	127	2.38

$$\omega = 2q_b = \rho \left( \frac{f_y}{f'_c} \right) = \frac{4A_s f_y}{sDf'_c} = \frac{2f_{lat}}{f'_c}$$

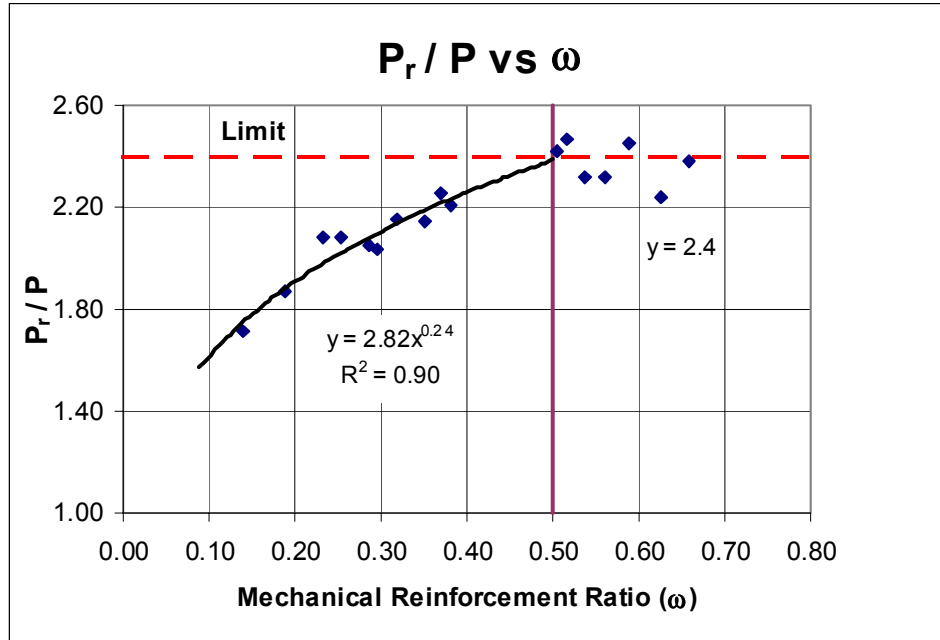


Fig. 5.28 Enhancement of the Ultimate Bearing Strength by Steel Reinforcement

The values plotted in Fig. 5.28 are average values from specimens with the same mechanical reinforcement ratio. In the case of blocks reinforced with ties only half of the mechanic reinforcement ratio was considered as effective for confinement (see Wollmann and Roberts-Wollmann 2000).

According to these results an increase of  $\omega$ , produces an increase in the ultimate load up to a point where no further benefit is achieved with an extra increase in the reinforcement ratio. Therefore the values of  $k$  suggested for use when evaluating Equation 4.10 (see below) are  $k = 2.82\omega^{0.24}$ , for  $\omega < 0.50$  and a limit value of  $k=2.4$  for  $\omega > 0.50$ .

$$P_r = k \left( \frac{Af'_c}{m\beta + \alpha} \right) \quad (\text{Eq. 4.10})$$

Another limit state apart from bearing has also to be considered. Re-examining the failure modes shown in Figs. 5.26 and 5.27 and others during this tests series, it is likely that some of the specimens failed in pure compression on the unreinforced base of the specimen. The ultimate bearing strength of the upper part of those specimens was substantially higher than

the ultimate load in pure compression of the lower part of the prism, which was, if not reinforced at all, more lightly reinforced. In view of these facts the limit state of  $0.85 f_c$  times the gross area ( $A$ ) has to be considered as a limit state when designing the specimens.

### **5.3 Comparison of Curve Fit Equation 4.10 with Previous Local Zone Tests**

Table 5.13 shows the specimens' data and failure loads from the existing database of Local Zone Tests for Special Anchorage devices. As mentioned at the beginning of this Chapter the database is a record of many previous AASHTO load transfer tests and others performed in Europe on VSL anchorage devices plus other tests performed in the NCHRP 356 study (Breen et al. 1994), since 1990.

The performance of the derived equation for reinforced specimens using curve fitting (Equation 4.10) is evaluated against this actual data. The ratio  $P_{test}/P_{pred}$  in table 5.14 is the parameter used to compare how well the equation predicts the actual test result. The table also shows the performance of the equation with the limit of  $0.85 f_c A$ .

Table 5.13. Special Anchorage Device Test Data

Test Name	Block Dimensions		Plate Designation	Plate Type	Plate Dimensions			Plate Hole Diam.	Duct Diam.	Concrete Strength (psi)	Bar Area (in <sup>2</sup> )	Ties		fy (ksi)	Failure Load (kips)
	a (in)	b (in)			Diameter (in)	c (in)	d (in)					Side Length (in)	Spacing (in)		
1	20.67	20.67	22-0.6	Multi	12.60		6.57	4.68	3,424	0.31	19.76	2.00	80.00	1,395	
2	20.67	20.67	22-0.6	Multi	12.60		6.57	4.68	3,536	0.31	19.76	2.00	80.00	1,432	
3	20.67	20.67	22-0.6	Multi	12.60		6.57	4.68	3,504	0.31	19.76	2.00	72.50	1,452	
4	20.67	20.67	22-0.6	Multi	12.60		6.57	4.68	3,552	0.31	19.76	2.00	72.50	1,389	
5	13.19	13.19	12-0.5	Multi	8.74		4.05	2.83	3,536	0.20	12.40	2.00	72.50	586	
6	13.19	13.19	12-0.5	Multi	8.74		4.05	2.83	3,656	0.20	12.40	2.00	72.50	600	
7	20.67	20.67	22-0.6	Multi	12.60		6.57	4.68	3,608	0.31	19.76	2.00	72.50	1,482	
8	20.67	20.67	22-0.6	Multi	12.60		6.57	4.68	3,576	0.31	19.76	2.00	72.50	1,547	
9	16.73	16.73	22-0.6	Multi	12.60		6.57	4.68	4,760	0.20	15.94	2.00	72.50	1,307	
10	26.97	26.97	37-0.6	Multi	16.54		9.61	6.00	3,304	0.44	26.18	2.36	72.50	2,267	
11	21.85	21.85	37-0.6	Multi	16.54		9.61	6.00	5,536	0.39	21.06	2.36	72.50	2,244	
12	17.12	18.90	22-0.6	Multi	12.60		6.57	4.68	5,418	0.31	17.22	2.16	72.50	1,479	
13	21.00	21.00	31-0.5	Multi	12.60		6.57	4.68	3,990	0.31	18.50	2.00	60.00	1,153	
14	21.00	21.00	31-0.5	Multi	12.60		6.57	4.68	4,130	0.31	18.50	2.00	60.00	896	
15	21.00	21.00	31-0.5	Multi	12.60		6.57	4.68	4,090	0.31	18.50	2.00	60.00	1,114	
16	21.00	21.00	31-0.5	Multi	12.60		6.57	4.68	4,070	0.31	18.50	2.00	60.00	1,089	
17	21.00	21.00	31-0.5	Multi	12.60		6.57	4.68	3,620	0.31	18.50	2.00	67.50	1,250	
18	21.00	21.00	31-0.5	Multi	12.60		6.57	4.68	3,700	0.31	18.50	2.00	67.50	1,251	
19	21.00	21.00	31-0.5	Multi	12.60		6.57	4.68	3,870	0.31	18.50	2.00	67.50	1,274	
20	18.00	18.00	19-0.5	Multi	10.16		5.39	3.25	3,451	0.31	16.00	2.00	60.00	1,030	
21	18.00	18.00	19-0.5	Multi	10.16		5.39	3.25	3,597	0.31	16.00	2.00	60.00	1,165	
22	18.00	18.00	19-0.5	Multi	10.16		5.39	3.25	3,490	0.31	16.00	2.00	60.00	1,143	
23	22.50	22.50	31-0.5	Multi	12.60		6.57	4.68	3,533	0.44	20.25	2.00	60.00	1,770	
24	22.50	22.50	31-0.5	Multi	12.60		6.57	4.68	3,473	0.44	20.25	2.00	60.00	1,966	
25	22.50	22.50	31-0.5	Multi	12.60		6.57	4.68	3,473	0.44	20.25	2.00	60.00	1,856	
26	29.00	29.00	37-0.6	Multi	16.53		9.61	6.00	3,596	0.44	27.00	2.00	60.00	2,774	
27	29.00	29.00	37-0.6	Multi	16.53		9.61	6.00	3,596	0.44	27.00	2.00	60.00	2,796	
28	29.00	29.00	37-0.6	Multi	16.53		9.61	6.00	3,596	0.44	27.00	2.00	60.00	2,804	
29	16.50	16.50	12-0.6	Multi	8.66		4.72	3.38	3,200	0.11	13.75	1.38	60.00	566	
30	16.50	16.50	12-0.6	Multi	8.66		4.72	3.38	3,200				60.00	440	
31	16.50	16.50	12-0.6	Multi	8.66		4.72	3.38	6,400				60.00	792	
32	16.50	16.50	12-0.6	Multi	8.66		4.72	3.38	6,400	0.20	14.50	4.50	60.00	914	

Table 5.13 (Cont.). Special Anchorage Device Test Data

Test Name	Block Dimensions			Plate Designation	Plate Type	Plate Dimensions			Plate Hole Diam. (in)	Duct Diam (in)	Concrete Strength (psi)	Spiral		Ties		fy (ksi)	Failure Load (kips)
	a (in)	b (in)				diameter (in)	c (in)	d (in)				Bar Area (in <sup>2</sup> )	Diam. (in)	Pitch (in)	Bar Area (in <sup>2</sup> )		
33	16.50	16.50		12-0.6	Multi	8.66			4.72	3.38	4,277	0.31	11.00	2.00		60.00	563
34	16.50	16.50		12-0.6	Multi	8.66			4.72	3.38	4,490	0.31	11.00	2.00	14.50	60.00	738
35	9.88	9.88		7-0.5	Multi		6.50	6.50	2.50	2.50	5,150	0.20	7.88	2.00		80.00	316
36	11.88	11.88		7-0.5	Multi		6.50	6.50	2.50	2.50	5,150	0.20	7.88	2.00		80.00	420
37	9.88	9.88		7-0.5	Multi		6.50	6.50	2.50	2.50	4,825	0.20	7.88	2.00	7.88	80.00	326
38	9.88	9.88		7-0.5	Multi		6.50	6.50	2.50	2.50	4,825	0.20	7.88	2.00	7.88	80.00	362
39	9.88	9.88		7-0.5	Multi		6.50	6.50	2.50	2.50	5,880						231
40	9.00	12.00		7-0.6	Multi		6.50	6.50	2.50	2.50	4,062	0.20	8.00	2.00		80.00	279
41	9.00	12.00		7-0.6	Multi		6.50	6.50	2.50	2.50	4,142	0.20	8.00	2.00		80.00	326
42	9.00	12.00		7-0.6	Multi		6.50	6.50	2.50	2.50	4,062	0.20	8.00	2.00		80.00	289
43	9.00	12.00		7-0.6	Multi		6.50	6.50	2.50	2.50	4,142	0.20	8.00	2.00		80.00	313
44	18.00	18.00		12-0.6	Multi		9.84	9.84	4.96	3.65	5,330	0.31	14.00	2.25	15.00	65.40	1,156
45	18.00	18.00		12-0.6	Multi		9.84	9.84	4.96	3.65	5,330	0.31	14.00	2.25	15.00	65.40	1,199
46	18.00	18.00		12-0.6	Multi		9.84	9.84	4.96	3.65	5,330	0.31	14.00	2.25	15.00	65.40	1,156
47	21.00	21.00		31-0.6	Multi		14.96	14.96	7.95	5.20	5,700	0.44	17.00	2.25	18.00	65.40	2,173
48	21.00	21.00		31-0.6	Multi		14.96	14.96	7.95	5.20	5,700	0.44	17.00	2.25	18.00	65.40	2,089
49	21.00	21.00		31-0.6	Multi		14.96	14.96	7.95	5.20	6,030	0.44	17.00	2.25	18.00	65.40	2,257
50	12.40	12.40		7-0.6	Multi		6.35	6.35	3.54	2.87	4,756	0.20	10.23	2.00	11.42	72.50	621
51	12.40	12.40		7-0.6	Multi		6.35	6.35	3.54	2.87	4,327	0.20	10.23	2.00	11.42	72.50	648
52	20.47	20.47		19-0.6	Multi		10.16	10.16	5.90	4.56	4,060	0.31	17.91	2.95	19.49	72.50	1,281
53	20.47	20.47		19-0.6	Multi		10.16	10.16	5.90	4.56	4,060	0.31	17.91	2.36	19.49	72.50	1,397
54	19.00	19.00		19-0.6	Multi		11.04	11.04	5.90	5.16	5,489	0.31	15.00	2.00	17.00	62.00	1,655
55	19.00	19.00		19-0.6	Multi		11.04	11.04	5.90	5.16	5,489	0.31	15.00	2.00	17.00	62.00	1,677
56	19.00	19.00		19-0.6	Multi		11.04	11.04	5.90	5.16	5,489	0.31	15.00	2.00	17.00	62.00	1,655
57	21.00	21.00		19-0.6	Multi		11.04	11.04	5.90	5.16	3,381	0.31	17.00	2.00	19.00	62.00	1,447
58	21.00	21.00		19-0.6	Multi		11.04	11.04	5.90	5.16	3,381	0.31	17.00	2.00	19.00	62.00	1,488
59	21.00	21.00		19-0.6	Multi		11.04	11.04	5.90	5.16	3,381	0.31	17.00	2.00	19.00	62.00	1,455
60	17.00	17.00		12-0.6	Multi		9.90	9.90	4.60	3.70	5,650	0.31	13.00	3.00	14.00	64.20	1,250
61	17.00	17.00		12-0.6	Multi		9.90	9.90	4.60	3.70	5,650	0.31	13.00	3.00	14.00	64.20	1,268
62	17.00	17.00		12-0.6	Multi		9.90	9.90	4.60	3.70	5,650	0.31	13.00	3.00	14.00	64.20	1,208
63	17.00	17.00		12-0.6	Multi		9.90	9.90	4.60	3.70	6,067	0.31	13.00	3.00	14.00	78.50	1,165
64	17.00	17.00		12-0.6	Multi		9.90	9.90	4.60	3.70	6,067	0.31	13.00	3.00	14.00	78.50	1,127
65	17.00	17.00		12-0.6	Multi		9.90	9.90	4.60	3.70	6,067	0.31	13.00	3.00	14.00	78.50	1,107

Table 5.14 Performance of Equation 4.10 Against Actual Local Zone Tests.

Test	$P_{r\text{ test}}$	P	$P_{r\text{ pred}}$	$P_{r\text{ test}}/P_{r\text{ pred}}$	0.85 f'c A	$P_{r\text{ pred}}$ w/limit	$P_{r\text{ test}}/P_{r\text{ pred}}$
Name	(kips)	(kips)	(kips)		(kips)	(kips)	with limit
1	1,395	523	1,254	1.11	1,243	1,243	1.12
2	1,432	534	1,282	1.12	1,284	1,282	1.12
3	1,452	531	1,274	1.14	1,273	1,273	1.14
4	1,389	536	1,286	1.08	1,290	1,286	1.08
5	586	234	560	1.05	523	523	1.12
6	600	239	574	1.05	541	541	1.11
7	1,482	542	1,300	1.14	1,310	1,300	1.14
8	1,547	538	1,292	1.20	1,299	1,292	1.20
9	1,307	513	1,230	1.06	1,132	1,132	1.15
10	2,267	873	2,096	1.08	2,043	2,043	1.11
11	2,244	980	2,353	0.95	2,247	2,247	1.00
12	1,479	574	1,377	1.07	1,490	1,377	1.07
13	1,153	592	1,422	0.81	1,496	1,422	0.81
14	896	606	1,455	0.62	1,548	1,455	0.62
15	1,114	602	1,446	0.77	1,533	1,446	0.77
16	1,089	600	1,441	0.76	1,526	1,441	0.76
17	1,250	555	1,331	0.94	1,357	1,331	0.94
18	1,251	563	1,351	0.93	1,387	1,351	0.93
19	1,274	580	1,393	0.91	1,451	1,393	0.91
20	1,030	386	926	1.11	950	926	1.11
21	1,165	397	952	1.22	991	952	1.22
22	1,143	389	933	1.22	961	933	1.22
23	1,770	604	1,450	1.22	1,520	1,450	1.22
24	1,966	597	1,433	1.37	1,494	1,433	1.37
25	1,856	597	1,433	1.30	1,494	1,433	1.30
26	2,774	1,022	2,452	1.13	2,571	2,452	1.13
27	2,796	1,022	2,452	1.14	2,571	2,452	1.14
28	2,804	1,022	2,452	1.14	2,571	2,452	1.14
29	566	291	699	0.81	741	699	0.81
30	440	291	699	0.63	741	699	0.63
31	792	458	1,100	0.72	1,481	1,100	0.72
32	914	458	1,100	0.83	1,481	1,100	0.83
33	563	353	848	0.66	990	848	0.66
34	738	365	875	0.84	1,039	875	0.84
35	316	188	451	0.70	427	427	0.74
36	420	231	554	0.76	617	554	0.76
37	326	180	431	0.76	400	400	0.82
38	362	180	431	0.84	400	400	0.91
39	231	206	206	1.12	487	206	1.12
40	279	147	352	0.79	373	352	0.79
41	326	149	357	0.91	380	357	0.91
42	289	147	352	0.82	373	352	0.82

Table 5.14 (Cont.). Performance of Equation 4.10 against Actual Local Zone Tests.

Test Name	$P_{r\ test}$ (kips)	P (plain) (kips)	$P_{r\ pred}$ (kips)	$P_{r\ test}/ P_{r\ pred}$	0.85 $f_c A$ (kips)	$P_{r\ pred}$ w/limit (kips)	$P_{r\ test}/ P_{r\ pred}$ with limit
43	313	149	357	0.88	380	357	0.88
44	1,156	544	1,305	0.89	1,468	1,305	0.89
45	1,199	544	1,305	0.92	1,468	1,305	0.92
46	1,156	544	1,305	0.89	1,468	1,305	0.89
47	2,173	1,014	2,432	0.89	2,137	2,137	1.02
48	2,089	1,014	2,432	0.86	2,137	2,137	0.98
49	2,257	1,055	2,532	0.89	2,260	2,260	1.00
50	621	225	541	1.15	622	541	1.15
51	648	212	508	1.28	566	508	1.28
52	1,281	546	1,311	0.98	1,446	1,311	0.98
53	1,397	546	1,311	1.07	1,446	1,311	1.07
54	1,655	634	1,521	1.09	1,684	1,521	1.09
55	1,677	634	1,521	1.10	1,684	1,521	1.10
56	1,655	634	1,521	1.09	1,684	1,521	1.09
57	1,447	521	1,249	1.16	1,267	1,249	1.16
58	1,488	521	1,249	1.19	1,267	1,249	1.19
59	1,455	521	1,249	1.16	1,267	1,249	1.16
60	1,250	530	1,272	0.98	1,272	1,388	0.90
61	1,268	530	1,272	1.00	1,272	1,388	0.91
62	1,208	530	1,272	0.95	1,272	1,388	0.87
63	1,165	556	1,333	0.87	1,333	1,490	0.78
64	1,127	556	1,333	0.85	1,333	1,490	0.76
65	1,107	556	1,333	0.83	1,333	1,490	0.74
			Avg	0.99		Avg	1.00
			Sdev	0.18		Sdev	0.18
			Coev	0.18		Coev	0.18

Results from Table 5.14 show a fairly good correlation between the predicted values and the actual test results since the average  $P_{r\ test}/ P_{r\ pred}$  is 0.99 and the coefficient of variation is 18 percent. On the other hand, the average  $P_{r\ test}/ P_{r\ pred}$  with the compression failure limit is 1.00 with the same coefficient of variation. It is very interesting to note that  $k$  for all these tests is 2.4 since the mechanical reinforcing ratio ( $\omega$ ) for all the specimens is greater than 0.50. A comparison of the results obtained by this formula and the one proposed by the NCHRP 356 study is presented in the histogram of frequencies of Fig. 5.29.

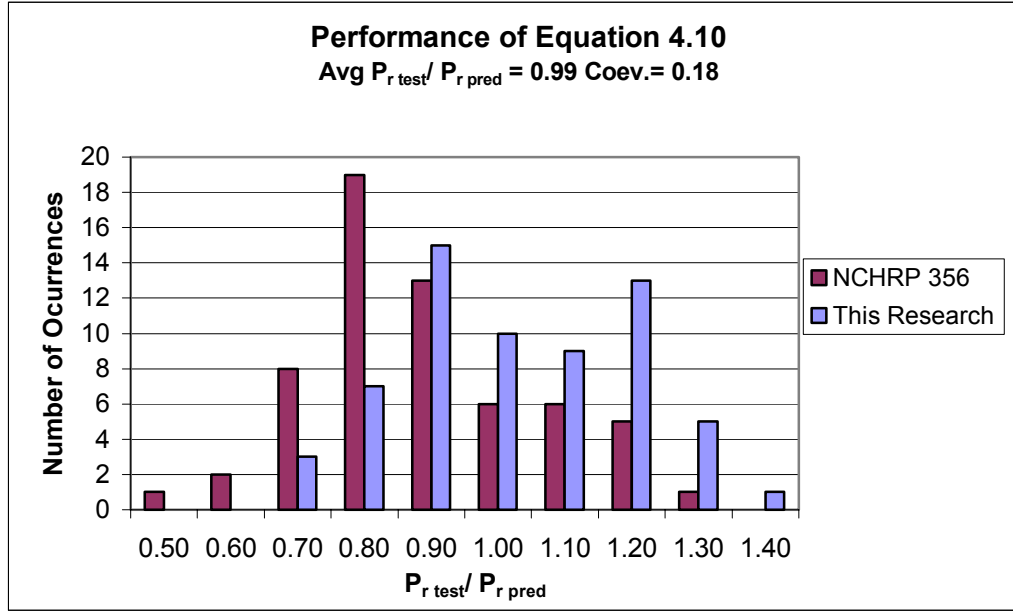


Fig. 5.29 Performance of Equation 4.10 and NCHRP 356 Equation  
Against Load Transfer Tests Database

#### 5.4 Prediction of the Ultimate Bearing Strength Using the Equivalent Material Approach and the Mohr Failure Criterion.

Using the same test data from Tables 5.12a and 5.12b, the values of  $P_{r\ test}/ P_{r\ pred}$  are now calculated using equation 4.12 (see below). The variables values, as well as the performance of the equation for the results of the experiments of this research are presented in table 5.15.

$$P_r = \frac{1.25 \cdot A \cdot f'_c}{m_r \cdot \beta + \alpha} \quad (\text{Eq. 4.12})$$

According to Table 5.15, equation 4.12 predicts the ultimate bearing strength of these specimens with an average  $P_{r\ test}/ P_{r\ pred}$  of 1.04 an a coefficient of variation of 8 percent. The factor of 1.25 used in equation 4.12 is a calibration factor obtained from the experiments and reflects the enhancement of the compression strength due to the confining steel.

The same equation is tested against the actual Load Transfer tests of Table 5.13 and against data from the experiments of Wurm and Daschner (1977). In the case of Special Anchorage Devices of round shape an equivalent square plate is use for the proper calculation of the  $b/h$  ratio. The results of these evaluations are presented in Tables 5.16 and 5.17 respectively.

Figs. 5.30 and 5.31 show the histogram of frequencies corresponding to each one of the evaluations. In the figures, a histogram of the NCHRP 356 equation is also included for comparison of results.

Table 5.15. Performance of Equation 4.12 against Experiments of this Research.

Specimen	Type of Reinforc.	Plate (b, in.)	Block (h, in.)	$f'_c$ (psi)	$f'_t$ (psi)	A (in <sup>2</sup> )	$f'_{lat}$ (psi)	$m_r$	$\beta$	$\alpha$	$P_{r\ test}$ (kips)	$P_{r\ pred}$ (kips)	$P_{r\ test}/P_{r\ pred}$
AR-1	spiral	4.00	8.00	6,350	701	64.00	910	3.94	0.23	1.00	262	266	0.99
DL-4	spiral	4.00	8.00	6,350	701	64.00	910	3.94	0.23	1.00	277	266	1.04
AR-2	spiral	4.00	8.00	6,150	678	64.00	910	3.87	0.23	1.00	243	259	0.94
DR-4	spiral	4.00	8.00	6,150	678	64.00	910	3.87	0.23	1.00	273	259	1.05
DL-3	spiral	4.00	8.00	6,460	713	64.00	1,137	3.49	0.23	1.00	287	286	1.00
DL-3	spiral	4.00	8.00	6,150	678	64.00	1,137	3.39	0.23	1.00	287	276	1.04
AR-4	spiral	4.00	8.00	6,460	713	64.00	1,213	3.36	0.23	1.00	257	291	0.88
AR-3	spiral	4.00	8.00	5,870	656	64.00	1,137	3.27	0.23	1.00	245	267	0.92
DR-3	spiral	4.00	8.00	5,870	656	64.00	1,137	3.27	0.23	1.00	325	267	1.22
AL-3	spiral	4.00	8.00	6,150	678	64.00	1,580	2.72	0.23	1.00	282	302	0.93
AL-1	spiral	4.00	8.00	5,870	656	64.00	1,517	2.70	0.23	1.00	298	289	1.03
DR-2	spiral	4.00	8.00	5,870	656	64.00	1,517	2.70	0.23	1.00	293	289	1.01
AL-4	spiral	4.00	8.00	6,150	678	64.00	1,655	2.63	0.23	1.00	308	305	1.01
DR-1	spiral	4.00	8.00	6,150	678	64.00	1,820	2.46	0.23	1.00	304	313	0.97
CL-2	ties	4.00	8.00	6,350	701	64.00	425	5.63	0.23	1.00	230	220	1.04
BL-2	ties	4.00	8.00	6,350	701	64.00	458	5.47	0.23	1.00	220	224	0.98
BL-3	ties	4.00	8.00	6,350	701	64.00	595	4.89	0.23	1.00	238	238	1.00
CL-3	ties	4.00	8.00	6,350	701	64.00	595	4.89	0.23	1.00	252	238	1.06
CR-3	ties	4.00	8.00	6,460	713	64.00	744	4.44	0.23	1.00	274	255	1.07
CL-4	ties	4.00	8.00	6,460	713	64.00	744	4.44	0.23	1.00	293	255	1.15
CR-2	ties	4.00	8.00	6,150	701	64.00	744	4.39	0.23	1.00	256	252	1.02
EL-4	ties	4.00	8.00	6,350	701	64.00	744	4.39	0.23	1.00	278	252	1.10
ER-6	ties	4.00	8.00	5,870	656	64.00	744	4.19	0.23	1.00	255	238	1.07
CR-1	ties	4.00	8.00	6,350	701	64.00	992	3.75	0.23	1.00	296	272	1.09
EL-2	ties	4.00	8.00	6,350	701	64.00	992	3.75	0.23	1.00	305	272	1.12
BL-4	ties	4.00	8.00	6,150	678	64.00	992	3.68	0.23	1.00	230	266	0.87
CL-1	ties	4.00	8.00	6,150	678	64.00	992	3.68	0.23	1.00	280	266	1.05
EL-3	ties	4.00	8.00	6,150	678	64.00	992	3.68	0.23	1.00	275	266	1.04
CR-4	spiral + ties	4.00	8.00	6,150	678	64.00	1,409	2.95	0.25	1.00	307	282	1.09
ER-1	spiral + ties	4.00	8.00	6,150	678	64.00	1,450	2.89	0.26	1.00	357	281	1.27
BR-4	spiral + ties	4.00	8.00	6,150	678	64.00	1,504	2.82	0.27	1.00	280	280	1.00
ER-4	spiral + ties	4.00	8.00	6,150	678	64.00	1,580	2.72	0.28	1.00	294	279	1.05
EL-6	spiral + ties	4.00	8.00	5,870	656	64.00	1,645	2.55	0.28	1.00	285	274	1.04
BR-1	spiral + ties	4.00	8.00	5,870	656	64.00	1,721	2.47	0.29	1.00	307	272	1.13
BR-3	spiral + ties	4.00	8.00	5,870	656	64.00	1,835	2.35	0.31	1.00	274	270	1.01
ER-3	spiral + ties	4.00	8.00	6,150	678	64.00	1,885	2.40	0.33	1.00	303	275	1.10
												Avg	1.04
												Sdev	0.08
												Coev	0.08

Table 5.16. Performance of Equation 4.12 against Load Transfer Tests Database.

Test Name	Dimensions		$f_c$ psi	$f_t$ calculated (psi)	$f_{lat}$ (total) (psi)	b/h	$\beta$	$\alpha$	$m_r$	Anet (in <sup>2</sup> )	$m_r$	$P_{r\ test}$ (kips)	$P_{r\ pred}$ (kips)	$P_{r\ test}/P_{r\ pred}$
	h, block (in)	b, plate (in)												
	1	20.67												
2	20.67	11.16	3,536	446	1,983	0.54	0.21	1.00	1.46	410.06	1.46	1,432	1,384	1.03
3	20.67	11.16	3,504	444	1,797	0.54	0.21	1.00	1.56	410.06	1.56	1,452	1,348	1.08
4	20.67	11.16	3,552	447	1,797	0.54	0.21	1.00	1.58	410.06	1.58	1,389	1,362	1.02
5	13.19	7.74	3,536	446	1,877	0.59	0.19	1.00	1.52	167.69	1.52	586	574	1.02
6	13.19	7.74	3,656	453	1,877	0.59	0.19	1.00	1.57	167.69	1.57	600	590	1.02
7	20.67	11.16	3,608	450	1,797	0.54	0.21	1.00	1.61	410.06	1.61	1,482	1,378	1.08
8	20.67	11.16	3,576	448	1,797	0.54	0.21	1.00	1.59	410.06	1.59	1,547	1,369	1.13
9	16.73	11.16	4,760	517	1,978	0.67	0.15	1.00	1.91	262.70	1.91	1,307	1,210	1.08
10	26.97	14.65	3,304	431	1,661	0.54	0.21	1.00	1.58	699.12	1.58	2,267	2,165	1.05
11	21.85	14.65	5,536	558	1,856	0.67	0.15	1.00	2.29	449.16	2.29	2,244	2,307	0.97
12	17.12	11.16	5,418	552	2,052	0.65	0.16	1.00	2.08	275.90	2.08	1,479	1,401	1.06
13	21.00	11.16	3,990	474	1,581	0.53	0.22	1.00	1.94	423.81	1.94	1,153	1,488	0.78
14	21.00	11.16	4,130	482	1,581	0.53	0.22	1.00	2.00	423.81	2.00	896	1,526	0.59
15	21.00	11.16	4,090	480	1,581	0.53	0.22	1.00	1.98	423.81	1.98	1,114	1,515	0.74
16	21.00	11.16	4,070	478	1,581	0.53	0.22	1.00	1.98	423.81	1.98	1,089	1,510	0.72
17	21.00	11.16	3,620	451	1,779	0.53	0.22	1.00	1.62	423.81	1.62	1,250	1,419	0.88
18	21.00	11.16	3,700	456	1,779	0.53	0.22	1.00	1.66	423.81	1.66	1,251	1,442	0.87
19	21.00	11.16	3,870	467	1,779	0.53	0.22	1.00	1.72	423.81	1.72	1,274	1,493	0.85
20	18.00	9.00	3,451	441	1,934	0.50	0.23	1.00	1.45	315.71	1.45	1,030	1,019	1.01
21	18.00	9.00	3,597	450	1,934	0.50	0.23	1.00	1.51	315.71	1.51	1,165	1,052	1.11
22	18.00	9.00	3,490	443	1,934	0.50	0.23	1.00	1.47	315.71	1.47	1,143	1,028	1.11
23	22.50	11.16	3,533	446	1,685	0.50	0.23	1.00	1.66	489.06	1.66	1,770	1,557	1.14
24	22.50	11.16	3,473	442	1,685	0.50	0.23	1.00	1.63	489.06	1.63	1,966	1,537	1.28
25	22.50	11.16	3,473	442	1,685	0.50	0.23	1.00	1.63	489.06	1.63	1,856	1,537	1.21
26	29.00	14.64	3,596	450	1,556	0.50	0.23	1.00	1.79	812.74	1.79	2,774	2,589	1.07
27	29.00	14.64	3,596	450	1,556	0.50	0.23	1.00	1.79	812.74	1.79	2,796	2,589	1.08
28	29.00	14.64	3,596	450	1,556	0.50	0.23	1.00	1.79	812.74	1.79	2,804	2,589	1.08
29	16.50	7.67	3,200	424	1,194	0.46	0.25	1.00	1.98	263.31	1.98	566	707	0.80
30	16.50	7.67	3,200	424	1,691	0.46	0.25	1.00	1.51	263.31	1.51	440	766	0.57
31	16.50	7.67	6,400	600	1,691	0.46	0.25	1.00	2.79	263.31	2.79	792	1,244	0.64
32	16.50	7.67	6,400	600	1,875	0.46	0.25	1.00	2.59	263.31	2.59	914	1,283	0.71
33	16.50	7.67	4,277	490	1,691	0.46	0.25	1.00	1.96	263.31	1.96	563	947	0.59
34	16.50	7.67	4,490	503	1,875	0.46	0.25	1.00	1.89	263.31	1.89	738	1,006	0.73
35	9.88	6.5	5,150	538	2,032	0.66	0.16	1.00	2.00	92.61	2.00	316	453	0.70

Table 5.16 (Cont.). Performance of Equation 4.12 against Load Transfer Tests Database.

Test Name	Dimensions		$f_c$ psi	$f_t$ calculated (psi)	$f_{lat}$ (total) (psi)	b/h	$\beta$	$\alpha$	$m_r$	Anet (in <sup>2</sup> )	$m_r$	$P_{r\ test}$ (kips)	$P_{r\ pred}$ (kips)	$P_{r\ test}/P_{r\ pred}$
	h, block	b, plate												
	(in)	(in)												
36	11.88	6.5	5,150	538	2,032	0.55	0.21	1.00	2.00	136.11	2.00	420	617	0.68
37	9.88	6.5	4,825	521	2,286	0.66	0.16	1.00	1.72	92.61	1.72	326	440	0.74
38	9.88	6.5	4,825	521	2,590	0.66	0.16	1.00	1.55	92.61	1.55	362	449	0.81
39	9.88	6.5	5,880	575	0	0.66	0.16	1.00	10.22	92.61	10.22	231	209	1.11
40	10.50	6.5	4,062	478	2,000	0.62	0.18	1.00	1.64	76.09	1.64	279	300	0.93
41	10.50	6.5	4,142	483	2,000	0.62	0.18	1.00	1.67	76.09	1.67	326	305	1.07
42	10.50	6.5	4,062	478	2,000	0.62	0.18	1.00	1.64	76.09	1.64	289	300	0.96
43	10.50	6.5	4,142	483	2,000	0.62	0.18	1.00	1.67	76.09	1.67	313	305	1.03
44	18.00	9.84	5,330	548	1,520	0.55	0.21	1.00	2.58	313.54	2.58	1,156	1,356	0.85
45	18.00	9.84	5,330	548	1,520	0.55	0.21	1.00	2.58	313.54	2.58	1,199	1,356	0.88
46	18.00	9.84	5,330	548	1,520	0.55	0.21	1.00	2.58	313.54	2.58	1,156	1,356	0.85
47	21.00	14.96	5,700	566	1,728	0.71	0.13	1.00	2.48	419.77	2.48	2,173	2,253	0.96
48	21.00	14.96	5,700	566	1,728	0.71	0.13	1.00	2.48	419.77	2.48	2,089	2,253	0.93
49	21.00	14.96	6,030	582	1,728	0.71	0.13	1.00	2.61	419.77	2.61	2,257	2,354	0.96
50	12.40	6.35	4,756	517	1,955	0.51	0.23	1.00	1.92	147.29	1.92	621	610	1.02
51	12.40	6.35	4,327	493	2,135	0.51	0.23	1.00	1.65	147.29	1.65	648	581	1.12
52	20.47	10.16	4,060	478	1,339	0.50	0.23	1.00	2.23	402.70	2.23	1,281	1,344	0.95
53	20.47	10.16	4,060	478	1,607	0.50	0.23	1.00	1.95	402.70	1.95	1,397	1,405	0.99
54	19.00	11.04	5,489	556	1,490	0.58	0.19	1.00	2.68	340.10	2.68	1,655	1,536	1.08
55	19.00	11.04	5,489	556	1,490	0.58	0.19	1.00	2.68	340.10	2.68	1,677	1,536	1.09
56	19.00	11.04	5,489	556	1,490	0.58	0.19	1.00	2.68	340.10	2.68	1,655	1,536	1.08
57	21.00	11.04	3,381	436	1,331	0.53	0.22	1.00	1.91	420.10	1.91	1,447	1,251	1.16
58	21.00	11.04	3,381	436	1,331	0.53	0.22	1.00	1.91	420.10	1.91	1,488	1,251	1.19
59	21.00	11.04	3,381	436	1,331	0.53	0.22	1.00	1.91	420.10	1.91	1,455	1,251	1.16
60	17.00	9.90	5,650	564	1,829	0.58	0.19	1.00	2.36	278.25	2.36	1,250	1,350	0.93
61	17.00	9.90	5,650	564	1,829	0.58	0.19	1.00	2.36	278.25	2.36	1,268	1,350	0.94
62	17.00	9.90	5,650	564	1,829	0.58	0.19	1.00	2.36	278.25	2.36	1,208	1,350	0.89
63	17.00	9.90	6,067	584	1,688	0.58	0.19	1.00	2.67	278.25	2.67	1,165	1,393	0.84
64	17.00	9.90	6,067	584	1,688	0.58	0.19	1.00	2.67	278.25	2.67	1,127	1,393	0.81
65	17.00	9.90	6,067	584	1,688	0.58	0.19	1.00	2.67	278.25	2.67	1,107	1,393	0.79
													Avg	0.96
													Sdev	0.17
													Coev	0.18

Table 5.17 Performance of Equation 4.12 against Wurm and Daschner Experiments

Test Name	Dimensions		$f_c$	$f_t$	$f_{lat}$	b/h	$\beta$	$\alpha$	Anet	$m_r$	$P_{r\ test}$	$P_{r\ pred}$	$P_{r\ test}/P_{r\ pred}$
	h, block	b, plate											
	(in)	(in)	psi	(psi)	(psi)				(in <sup>2</sup> )		(kips)	(kips)	
13	11.81	5.91	3,766	460	838	0.50	0.23	1.00	139.48	2.90	467	393	1.19
19	11.81	5.91	3,754	459	838	0.50	0.23	1.00	139.48	2.89	421	392	1.07
25	11.81	5.91	3,526	445	838	0.50	0.23	1.00	139.48	2.75	434	376	1.15
14	11.81	5.91	3,766	460	1,168	0.50	0.23	1.00	139.48	2.31	445	428	1.04
20	11.81	5.91	3,754	459	1,168	0.50	0.23	1.00	139.48	2.31	454	427	1.06
26	11.81	5.91	3,526	445	1,168	0.50	0.23	1.00	139.48	2.19	439	408	1.08
15	11.81	5.91	3,766	460	680	0.50	0.23	1.00	139.48	3.30	399	372	1.07
21	11.81	5.91	3,754	459	680	0.50	0.23	1.00	139.48	3.29	414	371	1.12
27	11.81	5.91	3,526	445	680	0.50	0.23	1.00	139.48	3.13	421	356	1.18
16	11.81	5.91	3,572	448	754	0.50	0.23	1.00	139.48	2.97	445	369	1.21
22	11.81	5.91	3,720	457	754	0.50	0.23	1.00	139.48	3.07	430	379	1.13
28	11.81	5.91	3,698	456	754	0.50	0.23	1.00	139.48	3.06	425	378	1.13
18	11.81	5.91	3,572	448	379	0.50	0.23	1.00	139.48	4.32	315	311	1.01
24	11.81	5.91	3,720	457	379	0.50	0.23	1.00	139.48	4.45	311	320	0.97
30	11.81	5.91	3,698	456	379	0.50	0.23	1.00	139.48	4.43	302	318	0.95
36	11.81	5.91	3,550	447	381	0.50	0.23	1.00	139.48	4.29	309	311	0.99
37	11.81	5.91	4,129	482	381	0.50	0.23	1.00	139.48	4.78	328	342	0.96
38	11.81	5.91	4,129	482	381	0.50	0.23	1.00	139.48	4.78	352	342	1.03
35	11.81	5.91	3,550	447	528	0.50	0.23	1.00	139.48	3.64	342	336	1.02
39	11.81	5.91	4,129	482	528	0.50	0.23	1.00	139.48	4.09	357	370	0.97
40	11.81	5.91	3,982	473	528	0.50	0.23	1.00	139.48	3.98	362	361	1.00
33	11.81	5.91	3,731	458	921	0.50	0.23	1.00	139.48	2.71	437	400	1.09
34	11.81	5.91	3,550	447	921	0.50	0.23	1.00	139.48	2.59	417	387	1.08
41	11.81	5.91	3,982	473	921	0.50	0.23	1.00	139.48	2.86	441	418	1.06
31	11.81	5.91	3,731	458	1,625	0.50	0.23	1.00	139.48	1.79	450	460	0.98
32	11.81	5.91	3,731	458	1,625	0.50	0.23	1.00	139.48	1.79	438	460	0.95
42	11.81	5.91	3,982	473	1,625	0.50	0.23	1.00	139.48	1.90	450	482	0.93
115	11.81	5.91	3,652	453	643	0.50	0.23	1.00	139.48	3.33	388	359	1.08
116	11.81	5.91	4,380	496	643	0.50	0.23	1.00	139.48	3.84	377	404	0.93
117	11.81	5.91	4,414	498	643	0.50	0.23	1.00	139.48	3.87	410	406	1.01
119	11.81	5.91	3,652	453	982	0.50	0.23	1.00	139.48	2.54	439	401	1.10
120	11.81	5.91	4,380	496	982	0.50	0.23	1.00	139.48	2.96	503	453	1.11
121	11.81	5.91	4,414	498	982	0.50	0.23	1.00	139.48	2.98	494	455	1.08
123	11.81	5.91	3,652	453	1,491	0.50	0.23	1.00	139.48	1.88	567	444	1.28
124	11.81	5.91	4,380	496	1,491	0.50	0.23	1.00	139.48	2.20	571	506	1.13
125	11.81	5.91	4,414	498	1,491	0.50	0.23	1.00	139.48	2.22	556	508	1.09
127	11.81	5.91	3,652	453	1,826	0.50	0.23	1.00	139.48	1.60	593	464	1.28
128	11.81	5.91	4,380	496	1,826	0.50	0.23	1.00	139.48	1.89	549	532	1.03
129	11.81	5.91	4,414	498	1,826	0.50	0.23	1.00	139.48	1.90	607	535	1.14
118	11.81	3.94	4,312	492	643	0.33	0.35	1.00	139.48	3.80	282	321	0.88
122	11.81	3.94	4,312	492	982	0.33	0.35	1.00	139.48	2.92	342	370	0.92
126	11.81	3.94	4,312	492	1,491	0.33	0.35	1.00	139.48	2.17	379	425	0.89
130	11.81	3.94	4,312	492	1,826	0.33	0.35	1.00	139.48	1.86	399	454	0.88
												Avg	1.05
												Sdev	0.10
												Coev	0.09

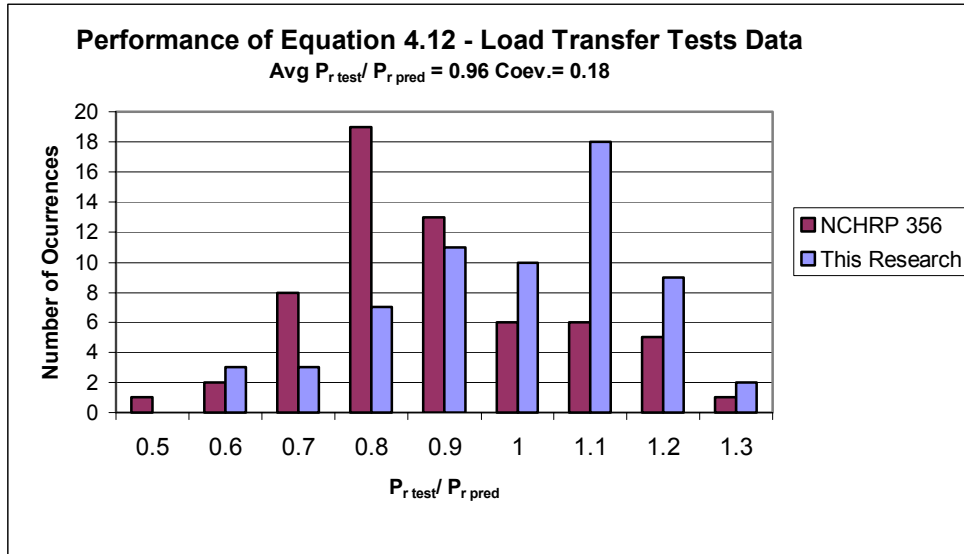


Fig. 5.30 Performance of Equation 4.12 Against Local Transfer Tests Database

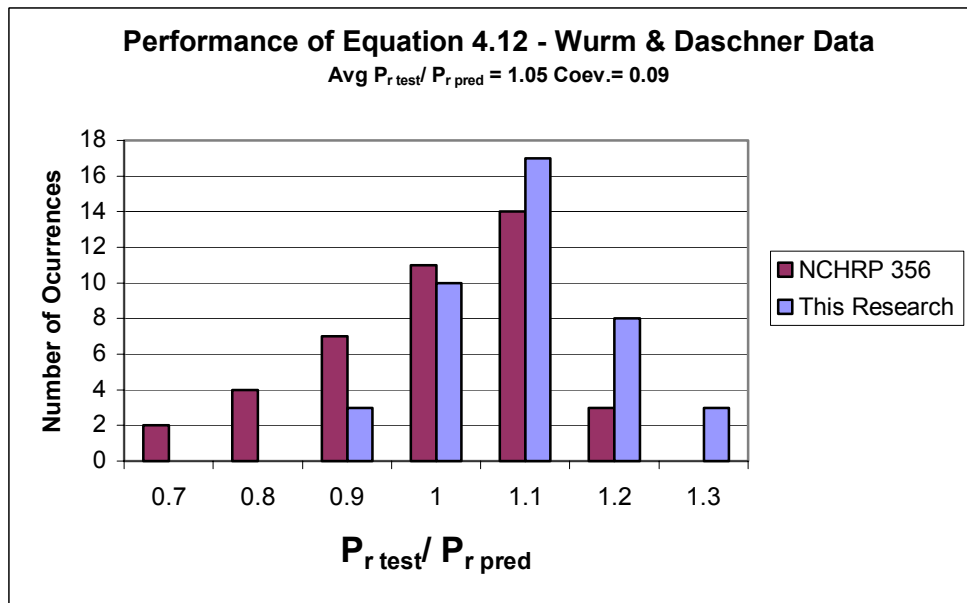


Fig. 5.31 Performance of Equation 4.12 Against Wurm and Daschner Data

Equation 4.12 also shows a good correlation with test data. For the experiments in this research and those in the experiments performed by Wurm and Daschner (1977), the coefficients of variation are remarkably good (8 percent and 9 percent respectively). However, when compared against the database of Load Transfer Tests it is moderately high (18 percent).

A reason for this discrepancy could be the fact that for most of the specimens, two crucial variables,  $f_{lat}$  and  $f'_t$  had to be estimated. In the case of  $f_{lat}$ , tensile tests or mill certifications of the rebar were missing. In the case of  $f'_t$ , actual values from split cylinder tests were also missing. When evaluating  $f_{lat}$  for the specimens, the nominal yield strength was used in lieu of the actual yield strength. For  $f'_t$ , the split cylinder strength was estimated as  $7.5\sqrt{f'_c}$ . However for the last 22 specimens of the database (Specimens 44 to 65),  $f_{lat}$  was known and therefore the average  $P_{r\ test}/P_{r\ pred}$  for these specimens was 0.98 and the coefficient of variation was 12 percent.

Finally, an overall comparison of the results obtained from Equation 4.12 and those obtained by the NCHRP 356 equation is performed using all the data from this research, the existing Load Transfer Tests data and the Wurm and Daschner data combined. The results are plotted in the histogram of Fig. 5.32.

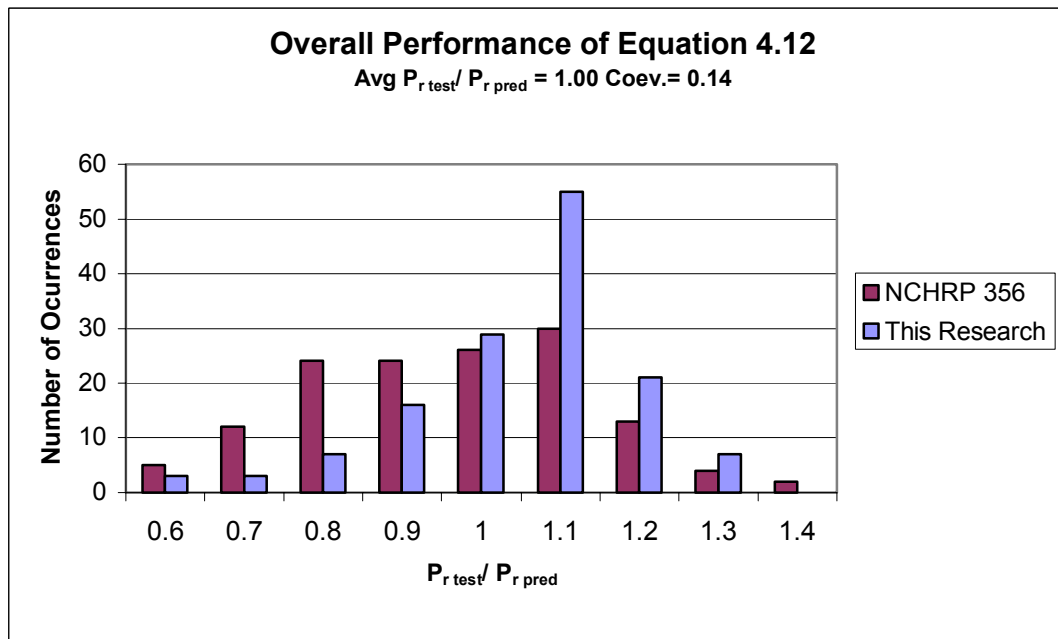


Fig. 5.32 Comparison of performance of Equation 4.12 against NCHRP 356 Equation (All available Data)

In general Equation 4.12 predicts the ultimate bearing strength of the local zone with an improved  $P_{r\ test}/P_{r\ pred}$  and a smaller coefficient of variation than the ones given by the NCHRP 356 equation. Overall average  $P_{r\ test}/P_{r\ pred}$  for Equation 4.12 is 1.00 and the coefficient of variation is 14 percent. This is an improvement over an overall average  $P_{r\ test}/P_{r\ pred}$  equal to 0.92 and a coefficient of variation of 21 percent for the NCHRP 356 equation.

## Chapter 6. Conclusions and Recommendations

### 6.1 Conclusions

The general objective of this work was to find an expression for the ultimate strength of the local zone for Load Transfer Tests specimens with an improved  $P_{test}/P_{pred}$  and a smaller coefficient of variation in comparison with those from the equation of the NCHRP 356 study (Eq. 1.1).

To obtain this improved equation the plain and reinforced concrete bearing strength was reviewed. A total of 199 bearing tests were performed on plain and reinforced concrete prisms to evaluate the variables involved in the bearing problem. A finite element analysis of a typical square block was performed to understand the nature and distribution of stresses in blocks under bearing stresses. Using the results from the finite element analysis and the Mohr failure criterion a new expression for the ultimate strength of the local zone was derived (Eq. 4.12).

The performance of this new equation was evaluated with the existing data of Load Transfer Tests, the data of the NCHRP 356 study, the results from the investigation of Wurm and Daschner and those obtained in this research. The outcome of this evaluation was that Eq. 4.12 predicts the ultimate strength of the local zone with an average  $P_{test}/P_{pred}$  of 1.00 and a coefficient of variation of 14 percent for the above-mentioned test data. This is equivalent to and improvement of 12 percent (from 0.89 to 1) in the prediction of the ultimate strength of the local zone in comparison with the NCHRP 356 study and an improvement of 33 percent in the coefficient of variation (from 0.21 to 0.14).

The study of the particular aspects of the UBS of plain concrete blocks and the results from 157 bearing tests performed led to the following conclusions:

- The ultimate bearing strength increases with an increase of the  $A/A_b$  ratio.
- The plate shape has negligible influence in the UBS in the  $A/A_b$  range between 2 and 16.

- The failure mode of plain concrete specimens is characterized by the formation of a failure cone or pyramid under the bearing plate, followed by the splitting of the block.
- For this data set, ACI equation, in general, overestimates the UBS of the specimens. A greater discrepancy existed for lightweight concrete specimens.
- The UBS remains constant for aspect ratios equal to or greater than 1.5.
- An increase in  $f'_c$  produces a decrease in the normalized ultimate bearing strength. In light of equation 4.7, this could be translated to the fact that the split cylinder strength does not increase at the same rate as the ultimate compressive strength.
- The duct size does not affect significantly the UBS. The net area can be used for all the calculations.
- The ultimate bearing strength of plain concrete blocks under concentric loading can be estimated accurately with Eq. 4.7. An evaluation of this equation against the results of 131 tests in normal and lightweight concrete resulted in an average  $P_{test}/P_{pred}$  of 1.05 and a coefficient of variation of 9 percent.

The study of the particular aspects of the UBS of reinforced concrete blocks and the results from 36 bearing tests performed led to the following conclusions:

- Two very distinct failure modes were observed in these specimens. One was characterized by the degradation of the local zone and was considered as a pure bearing failure. The other was characterized by the degradation of the base of the specimen and was assumed to be a compression failure.
- The ultimate bearing strength increases with an increase in the mechanical reinforcing ratio. However, results from this research suggest that for values of  $\omega > 0.50$ , no further benefit is achieved with additional increase of the reinforcing ratio.
- The ultimate bearing strength of reinforced concrete blocks under concentric loading can be estimated accurately with Eq. 4.12. An evaluation of this equation against the results of 36 tests in reinforced concrete specimens with mechanical reinforcing ratio varying from 0.13 to 0.66 gives an average  $P_{test}/P_{pred}$  of 1.04 and a coefficient of variation of 8 percent.

## 6.2 Recommendations

In the use of the derived equations for the prediction of the ultimate strength of plain and reinforced concrete blocks, the determination of the experimental values of the splitting strength  $f'_t$  in the case of plain concrete specimens and the lateral confining pressure  $f_{lat}$  and  $f'_t$  in the case of reinforced specimens, is crucial for accuracy of the results. Equations 4.8 and 4.10 are very sensitive to changes in these experimental values. For the determination of the splitting strength, the average of three consecutive split cylinder tests is suggested as the characteristic  $f'_t$  value. In the case of  $f_{lat}$ , the actual yield strength of the rebar ( $f_y$ ) has to be determined experimentally to obtain more accurate calculations of this value. However, the estimated value of  $f'_t = 7.5\sqrt{f'_c}$  and the nominal yield strength,  $f_y$  can be used for design of reinforced specimens, producing conservative results. The lateral confining pressure,  $f_{lat}$ , is usually 3 or 4 times greater than  $f'_t$  and therefore the variable of major weight when determining the parameter  $m_r$  of Eq. 4.12. The nominal yield strength is commonly smaller than the actual yield strength, therefore producing a smaller value of  $f_{lat}$ , a greater value of  $m_r$  and a more conservative value of the predicted ultimate load.

Several topics of further study are suggested to enrich the knowledge in this area:

- Evaluation of the behavior of the local zone for special anchorage devices using non-linear analysis. The interaction between the embedded plate and the surrounding concrete needs to be investigated.
- A more precise evaluation of the confining pressure ( $f_{lat}$ ) needs to be addressed by recording strains in the rebar and in the concrete core in actual Load Transfer Tests.
- The effect of cyclic and sustained loading on the UBS. The study of this effect can answer the question of why some specimens do not reach the expected ultimate loads.
- A study of the size effects on reinforced specimens.
- In terms of the cracking criteria, study the relationship between the reinforcing ratio and the cracks widths.

## References

1. American Association of State and Highway Transportation Officials (AASHTO), “Standard Specifications for Highway Bridges”, 17th Edition, 2002.
2. American Association of State and Highway Transportation Officials (AASHTO), “LRFD Specifications for Highway Bridges”, 3rd Edition, 2004.
3. ACI Committee 318, “Building Code Requirements for Structural Concrete and Commentary (ACI 318-02).” American Concrete Institute, Farmington Hills, Mich., 2002, pp. 137
4. Ahmed, T., Burley, E., Rigden, S., “Bearing Capacity of Plain and Reinforced Concrete loaded over a Limited Area”. ACI Structural Journal, May-June 1998, pp. 330-342.
5. Au, T., Baird D. L., “Bearing Capacity of Concrete Blocks”. Journal of the American Concrete Institute, Proceedings, Vol. 56 No. 9, March 1960, pp. 869-879.
6. Bauschinger, J., “*Versuche mit Quadern aus Natursteinen,*” (Tests with Blocks of Natural Stone Report), Mechanical and Technical Laboratory, Technical University of Munich, Vol.6, 1876, pp. 13.
7. Breen, J.E., Burdet, O., Roberts, C.L., Sanders, D.H., Wollmann, G.P., “Anchorage Zone Reinforcement for Post-tensioned Concrete Girders,” NCHRP Report 356, Transportation Research Board, Washington, D.C., 1994.
8. Cook, R. D., Young, W. C., Advanced Mechanics of Materials, 2<sup>nd</sup> Ed., Prentice Hall, New Jersey, 1999, pp. 53-54.

9. Cowan, H. J., "The Strength of Plain, Reinforced and Prestressed Concrete under the Action of Combined Stresses with Particular Reference to Combined Bending and Torsion of Rectangular Sections". Magazine of Concrete Research, Vol. 5, No. 14, Dec. 1953, pp. 75-86.
10. Guyon, Y., Prestressed Concrete, John Wiley and Sons, New York 1953, pp. 130-133.
11. Hawkins, N. M., "The Bearing Strength of Concrete Loaded through Rigid Plates," Magazine of Concrete Research, Vol. 20, No. 62, Mar. 1968, pp. 31-40.
12. Komendant, A. E., Prestressed Concrete Structures, 1<sup>st</sup> Ed. McGraw-Hill, New York, 1952, pp. 172-173.
13. Liu, Y., Guan, J., Wang, Q., "Bearing Strength of Concrete and its Failure Mechanism," China Civil Engineering Journal, Vol. 18, No. 2, May 1985, pp. 53-65.
14. Meyerhof, G. G., "The Bearing Capacity of Concrete and Rock," Magazine of Concrete Research, Vol. 4, No. 12, Apr. 1953, pp. 107-116.
15. Middendorf, K. H., "Practical Aspects of End Zone Bearing of Post-Tensioning Tendons," PCI Journal, Vol. 8, No. 4, Aug. 1963, pp. 57-62.
16. Niyogi, S. K., "Bearing Strength of Concrete - Geometric Variations," ASCE Structural Division Journal, Vol. 99, No. ST7, July 1973, pp. 1471-1490.
17. Niyogi, S. K., "Bearing Strength of Concrete – Support, Mix, Size Effect," ASCE Structural Division Journal, Vol. 100, No. ST8, Aug. 1974, pp. 1685-1702.
18. Niyogi, S. K., "Bearing Strength of Reinforced Concrete Blocks," ASCE Structural Division Journal, Vol. 105, No. ST5, May 1975, pp. 1125-1137.

19. Richart, F. E., Brandtzaeg, A., Brown, R. L., “ A Study of the Failure of Concrete Under Combined Compressive Stresses,” Bulletin No. 185, University of Illinois, Experimental Station, Nov. 1928.
20. Roberts-Wollmann, C. L., “Design and Test Specifications for Local Tendon Anchorage Zones,” ACI Structural Journal, Vol. 97 No. 6, Nov. 2000, pp. 867-875.
21. Suzuki, K., Nakatsuka, T. “Estimation of Bearing Strength of Reinforced Anchorage Zone in Post-Tensioned Prestressed Concrete Members,” technology Reports of the Osaka University, Vol. 32, No. 1680, Oct. 1982, pp. 419-428.
22. Vable, M., *Mechanic of Materials*, 1<sup>st</sup> Ed., Oxford University Press, New York, 2002, pp. 675-676.
23. Wollmann, G. P., Roberts-Wollmann, C. L. “Anchorage Zone Design,” Post-Tensioning Institute, Phoenix, AZ, 2000, pp. 1-16.
24. Wurm, P., Daschner, F., “*Versuche uber Teilflaechenbelastung von Normalbeton*,”(Test Results of Normal Weight Concrete Subjected to Partial Load), *Deutscher Ausschuss fur Stahlbeton* (German Committee for Reinforced Concrete), No. 286, Berlin, 1977, pp. 1-80.
25. Yettram, A. L., Robbins, K., “Anchorage Zone Stresses in Axially Post-Tensioned Members of Uniform Rectangular Section,” *Magazine of Concrete Research*, Vol. 21, No. 67, June 1969, pp. 103-112.
26. Zielinski, J., Rowe, R. E., “An Investigation of the Stress Distribution in the anchorage Zones of Pot-Tensioned Concrete Members,” *Cement and Concrete Association*, London, Research Report No. 9, Sept. 1960, pp. 1-32.

## **Vita**

Rodolfo Arturo Bonetti was born in Santo Domingo, Dominican Republic on October 5, 1968. He spent his childhood in Santiago, D. R., where he graduated from high school in 1986 at Instituto Evangelico. He studied Civil Engineering at Pontificia Universidad Catolica Madre y Maestra and during the junior and senior years his interests focused on Structural Engineering. He graduated from PUCMM in 1991 and moved back to Santo Domingo to work along his father in a family owned construction company. In 1996 he enrolled in the M.B.A. program at PUCMM - Santo Domingo, graduating in 1999. In 2003 enrolled at Virginia Tech to pursue his Masters Degree in Civil Engineering and performed research in the area of the bearing strength of plain and reinforced concrete.